Crystal Chemistry and Structure of Vesuvianite

By

Makio OHKAWA

With 9 Tables and 20 Text-figures

To be published in Journal of Science of the Hiroshima University,

Series C, Vol. 10, No. 1 (1994)

Abstract: The chemical variation of vesuvianite samples from 16 different localities, eleven in Japan, two in Norway, one in Canada, Pakistan, and Russia, have been examined using electron-microprobe analyses. For some of selected samples boron content was also examined. Results of analyses were reduced to formula unit on the basis of 50 cations excluding B.

The crystal structures of six high-symmetry (*P*4/*nnc*) vesuvianite from Japan and three low-symmetry (non-*P*4/*nnc*) vesuvianites from Japan, Pakistan and Norway were determined by single-crystal X-ray diffraction method. The nine crystals have the following cell parameters; a = 15.568(2), 15.559(3), 15.528(3), 15.472(2), 15.564(2), 15.559(3), 15.572(2), 15.759(1), 15.563(2); c = 11.790(1), 11.797(2), 11.755(2), 11.754(1), 11.841(1), 11.826(2), 11.833(2), 11.727(1), 11.818(1) Å, respectively. The structure refinements were carried out in the space group *P*4/*nnc*, *P*4/*n* and *P*4*nc*. The final R indices for 1821, 1493, 1357, 1415, 3024, 3743, 2053, 1745 and 1873 independent reflections are 0.038, 0.031, 0.040, 0.032, 0.063, 0.082, 0.038, 0.039 and 0.042, respectively. The EXAFS method was also used to investigate the local environment of the Cu and Mn ions in the crystal structure of vesuvianites from Norway and Japan.

The chemical analyses of low-symmetry vesuvianites indicate a very small amount of F and almost negligible Cl while high-symmetry one contains a considerable amount of F and Cl. The high-symmetry vesuvianite can contain Cl^- ions preferentially occupying the O(10) site which is split into two sites; one is occupied by Cl^- and the other by F^-. The chemical compositions of high-symmetry vesuvianites are more variable than those of low-symmetry vesuvianites.

The ordering of cation and vacancy in the two alternately and statistically occupied sites in a unit cell causes the lowering of the symmetry from the space group P4/nnc to *P*4/*n* or *P*4*nc*. The ordering scheme of *P*4*nc* structure is firstly confirmed in this paper. In the three low-symmetry vesuvianites, the refined site occupancy ratios for occupied

(B(a) and C(a)) and vacant sites (B(b) and C(b)) are 63:37, 62:38 and 92:8 (%), respectively, and the values suggest that the ordering in these crystals is not complete.

In low-symmetry vesuvianite, the satisfaction of the local charge balance on O(10) anions requires alternate occupancy of oxygen and hydroxyl with an associated hydrogen bond and ordering sequences of cations. In Cl- and F-bearing high-symmetry vesuvianite, on the other hand, occupying of Cl and F in O(10) sites interrupts the sequences of cations and vacancies along the fourfold rotation axes.

Boron-bearing vesuvianite from Russia contain more Mg and less Al than those of boron-free vesuvianite. Boron occupies the additional cation sites, tetrahedrally coordinated site at the 8*h* position and triangularly coordinated site at the 2*a* position. The excess of the scattering power at these sites derived from the measured amounts of boron indicates that some elements other than boron should occupy in boron positions.

CONTENTS

I. INTRODUCTION

Vesuvianite (idocrase) is a well-known rock-forming mineral with complex crystal chemistry and structure. Vesuvianite commonly occurs in metamorphic calc-silicate rocks mostly in skarn, rarely in rodingites and in veins associated with mafic rocks and serpentinites. The crystal structure of vesuvianite is related to grossular garnet. In fact, the two minerals often coexist intimately in nature (e.g. Deer et al., 1982). The general chemical formula of vesuvianite is represented as

$Ca_{19}(Mn, Fe)(F, OH)_2(Mg, Fe, Mn, Al, Ti)_8Al_4(OH, F, O)_8(SiO_4)_{10}(Si_2O_7)_4$

(Yoshiasa and Matsumoto, 1986).

The crystal structure of vesuvianite was first investigated by Warren and Modell (1931) on the basis of the structural similarities between the cubic grossular garnet and the tetragonal vesuvianite. The structure of vesuvianite around the fourfold inversion axis is closely related to that of grossular garnet; the *c* dimension of vesuvianite is approximately equal in length to the cube-edge of grossular. Warren and Modell (1931) compare the tetragonal vesuvianite with cubic garnet. They solved the structure by postulating the presence of garnet-like columns within the vesuvianite cell (Fig. 1). However, it has not been clarified why vesuvianite crystal should have an arrangement of assemblies of garnet-like columns.

Since Warren and Modell (1931), several chemical formulae were suggested (e.g. Machatschki, 1932; Barth, 1963). However, the formula and structure of vesuvianite are not get fully established.

Coda et al. (1970) revised the atom distribution along the fourfold rotation axis of the structural model proposed by Warren and Modell (1931) and their result was confirmed by Rucklidge et al. (1975). In the revised model, two oxygen and four statistically half-occupied cation sites are arranged along each fourfold rotation axis in a unit cell. The crystal structure of vesuvianite is characterized chiefly by the atomic arrangement along the fourfold rotation axis. Atoms arranged along this axis are not

connected directly to the grossular-like structure. Two anion and four cation positions are arranged along the fourfold rotation axis. Two fivefold and two eightfold coordinated cation positions are statistically half occupied by one Fe and one Ca ion, respectively (Coda et al., 1970 ; Rucklidge et al., 1975). These fivefold and eightfold sites are labeled B and C, respectively, in this paper according to Rucklidge et al. (1975). It should be emphasized that the adjacent B and C positions are not occupied together because of their close arrangement (i.e., only one of each is fully occupied). Furthermore, Coda et al. (1970) pointed out the close arrangement of the C sites. Consequently, it can be concluded that the site occupancy ratio of B : C is 1 : 1. However, this has not been confirmed experimentally.

These above structural models were successfully determined in the space group *P*4/*nnc*. However, before the crystal structure of vesuvianite have actually been solved by Warren and Modell (1931), it is so far known that the X-ray analyses of several vesuvianites show the presence of violating reflections for the space group *P*4/*nnc*, and some symmetry variations have also been recognized. Arem and Burnham (1969) reported that single crystal X-ray photographs of several vesuvianites show violations of glide-plane extinction criteria in the space group *P*4/*nnc*. They also reported the possible additional space groups. Coda et al. (1970) explained these violations supposing the ordering of their additional atoms along the fourfold rotation axes. The crystal structures of non-*P*4/*nnc* vesuvianite have been determined and the ordering of cations and vacancies along the fourfold rotation axis has been confirmed by many investigators e.g., Giuseppetti and Mazzi (1983), Allen and Burnham (1983), Allen (1985), Fitzgerald et al. (1986b, 1987). These authors determined the atomic arrangement with the space group *P*4/*n* (and $P\bar{4}$). However, the confirmed atomic arrangement is only one of the two possible ordered schemes. The other atomic arrangement with the space group *P*4*nc* have been remained to be solved. Giuseppetti and Mazzi (1983) tried to refine the arrangement in the *P*4*nc* symmetry. However, their refinement indicated negative temperature factors and large standard deviations.

Recently Allen and Burnham (1992) tried to clarify the difference between high and low-symmetry vesuvianite in detail. Although they obtained a comprehensive structure model for vesuvianite, it is still far from general solution of the problem, especially for local configurations and bond-valence satisfaction around the fourfold rotation axis. Groat et al. (1992a, b) stressed significance of the problem. Thus, the problem of local configurations and bond-valence satisfaction around the fourfold rotation axis together with the true symmetry are still remained to be solved.

The purpose of this study is to clarify the crystal chemistry and structure of vesuvianite. Structural and chemical differences between high and low vesuvianite are discussed in detail. Special attention is paid on the structural variation around the fourfold rotation axis, because the local charge balance on anions of both high- and low-symmetry vesuvianites are fundamental for the crystal chemistry of the mineral. For this purpose, specimens collected from sixteen localities were examined chemically, and nine selected specimens, six high and three low vesuvianites were analyzed by single crystal X-ray diffraction method. Two selected specimens were examined by EXAFS method.

Acknowledgments

The author wishes to express his sincerest gratitude to Professor Setsuo Takeno of the Hiroshima University for his constant and invaluable advice rendered during the course of the work as well as for his critical reading of the manuscript. The author is also indebted to Professors Ikuo Hara, Yuji Okimura, Satoru Honda and Yuji Sano of the same University for their guidance and advice. He also gratefully acknowledges his debt to Associate Professor Rhuji Kitagawa. Thanks are also due to Dr. Akira Yoshiasa for his helpful advice and encouragement. Thanks are also due to Mr. A. Minami, Engineer of the same University for his help in the chemical analysis by XMA.

The author gratefully acknowledges to Dr. Akira Kato of the National Science Museum, Tokyo for indicating a guiding principle to start this study and providing the

investigated Japanese samples. Special thanks are due to Dr. Chiyoko Henmi of Okayama University for providing the investigated Japanese samples.

Parts of X-ray experiments are performed at the Institute of Scientific and Industrial Research, Osaka University by courtesy of Prof. Fumikazu Kanamaru of the same Institute. The author thanks to Mr. Takanori Tanaka of the same Institute for help in the operation of the X-ray equipment. Parts of this work has performed under the approval of the Photon Factory Program Advisory Committee (Proposal No. 88-135).

II. Experimental

A. Specimens used in this study

Vesuvianites from eleven localities in Japan, two in Norway, one in Canada, Pakistan, and Russia, respectively, were investigated in this study. Most of the specimens were found in metamorphic calc-silicate rocks, and the rest were in rodingites and in veins associated with mafic rocks and serpentinites. Colors of these specimens are rather variable such as green, brown, black, blue and lilac. Foreign specimens are collected from noted localities. Localities and colors of these specimens are summarized in Table 1.

B. Electron-microprobe analysis

Chemical analyses were carried out for the all vesuvianites using a JCMA-733II electron microprobe analyzer. Synthetic crystal of NaCl was used for Cl standard. Several points of each sample were measured repeatedly at least five times. The averages of these values are listed in Table 1. Water content was calculated based on the obtained structural formula. Table 1 also shows the number of ions calculated from the analytical data normalized on 50 cations per formula unit. In the calculation, all Fe ions were assumed to be present in the divalent state (Iron content was obtained as total iron). For specimen 8 (Wilui River), values of B_2O_3 and H_2O contents were taken from Groat et al. (1992a).

C. Structural analyses

1. Single-crystal X-ray diffraction method

i. Collection of X-ray data

Single-crystal X-ray intensity data were collected on the nine specimens; five Japanese specimens (Obira mine in Oita prefecture, Sanpo mine in Okayama prefecture, Jinmu mine in Hiroshima prefecture, and Ogose and Chichibu mine in Saitama

prefecture), four foreign specimens (Sauland and Saueseter in Norway, Muslimbagh in Pakistan and Wilui River in Russia).

The specimens were ground into spheres (except the Jinmu vesuvianite) to minimize differential absorption. Jinmu vesuvianite was not ground because of its small crystal size. These samples were mounted on fine glass capillaries with epoxy. The intensity data were collected on a RIGAKU AFC-5 four-circle diffractometer with graphite-monochromatized MoKα radiation (50KV, 180-200mA) and were corrected for Lorentz and polarization factors. No absorption corrections were made because of small μr values for MoKα radiation (0.20 - 0.31 for the respective specimens). Cell parameters of these nine vesuvianites were refined from measured 2θ value of selected 25 reflections. Details of the data collection are summarized in Table 2.

ii. Refinement

The vesuvianites are classified into three types of space group of *P*4/*nnc*, *P*4/*n* and *P*4*nc* by examining the difference in intensities of pairs of *hkl*-*khl* reflections (space group *P*4/*n*), and the absence or presence of reflections violating glide plane extinction criteria for space group *P*4/*nnc*, i.e., a) *hk*0 reflections with *h*+*k* odd (*P*4*nc*), b) *h*0*l* reflections with *h*+*l* odd and c) *hhl* reflections with *l* odd (*P*4/*n*).

In the present study, the symmetries of vesuvianites were determined by precise analyses of the systematic absences of reflections using single-crystal X-ray diffractometer. Only reflections with intensities larger than 3σ (standard deviation of intensity) were taken into consideration from all measured reflections.

The systematic absences of vesuvianites except three low-symmetry vesuvianites were almost consistent with the space group *P*4/*nnc*, although a few fairly weak reflections violating glide plane extinction criteria for space group *P*4/*nnc* were exist. In this study, these weak reflections were ignored and refinement was executed in the space group *P*4/*nnc*.

Three low-symmetry vesuvianites showed the presence of relatively strong glide-violating reflections for $P4/nnc$. The Ogose vesuvianite showed strong $h0l$ ($h+l$ odd) and hhl (l odd) reflections and no $hk0$ ($h+k$ odd) reflections. The Muslimbagh vesuvianite showed strong $hk0$ ($h+k$ odd), and more strong $h0l$ ($h+l$ odd) and hhl (l odd) reflections. The Saueseter vesuvianite showed strong $hk0$ ($h+k$ odd) reflections and a few weak $h0l$ ($h+l$ odd) and hhl (l odd) reflections. The ratios of agreement for pairs of $F(hkl)$ and $F(khl)$ ($\sum|F(hkl)-F(khl)|/\sum F(hkl)+F(khl)$) were 0.02 (Obira), 0.02 (Sanpo), 0.03 (Jinmu), 0.02 (Sauland), 0.04 (Ogose), 0.08 (Muslimbagh) and 0.04 (Saueseter), 0.02 (Wilui River) and 0.03 (Chichibu), respectively.

These characteristics described above show that the symmetry of Ogose vesuvianite tends toward $P4/n$, that of Muslimbagh toward $P4$ (or $P\bar{4}$) and that of Saueseter toward $P4nc$. The final refinements were done in the space groups $P4/n$ (Ogose and Muslimbagh) and $P4nc$ (Saueseter).

In the refinements attempted in the space groups $P4/nnc$ and $P4nc$, averaged intensities of equivalent hkl and khl reflections were employed excluding the observed glide-violating reflections.

The refinements were made using the program RFINE 2 (Finger, 1969). Scattering factors of neutral atoms were taken from *International Tables for X-ray Crystallography* Vol. IV (Ibers and Hamilton, 1974). Anomalous dispersion corrections were made for all atoms. Site assignments and terminology were based on the model of Rucklidge et al. (1975). The refinement was initiated with the positional parameters reported by Yoshiasa and Matsumoto (1986), using the program RFINE 2 (Finger, 1969). Hydrogen atom positions were not included in the refinements.

[Note: Structural refinements of four vesuvianites (Sauland, Sanpo, Jinmu and Chichibu) are already appeared in Ohkawa et al. (1992). However, these vesuvianites were re-examined in this study using the same intensity data reported previously, especially on the site occupancy refinement of O(10) and O(11). Cell parameters of these

specimens were refined using re-collected 25 reflections in this study, thus these values are differ from those of Ohkawa et al. (1992).]

At first, total site occupancy factors are set to ideal occupancy ratio and site assignments are modified as to be occupied by suitable ions according to the chemical compositions. After several cycles of refinements, it is suggested that three Si (Si(1), Si(2) and Si(3)), four Ca (Ca(1), Ca(2), Ca(3) and C) and one Al (A) sites are almost occupied by the Si, Ca and Al ions, respectively. Consequently, the occupancy factors of these sites were constrained to the theoretical values in the final refinement.

In high-symmetry *P*4/*nnc* models, total occupancy factors of statistically half occupied B and C sites were constrained to 0.5 after several cycles of refinements. For the three low-symmetry vesuvianites (space group *P*4/*n* and *P*4*nc*), total site occupancy ratios are refined. The refined site occupancy ratios for B(a) and C(a) versus B(b) and C(b) of three vesuvianites are 63:37(1), 62:38(1) and 92:8(1) (%), respectively.

In the refinement of *P*4*nc* model for Saueseter vesuvianite, it is difficult to decide the exact thermal parameters of atoms in ideally unoccupied B(b) and C(b) sites because of the small site occupancy (approximately 8%). Therefore, these parameters were constrained to the same values as occupied B(a) and C(a) sites. The thermal parameter of B(b) site of Ogose vesuvianite were also constrained to that of B(a) site, because the site has significant positional disorder and indicates a negative anisotropic temperature factor.

The final *R*-values are 0.038, 0.031, 0.040, 0.032, 0.063, 0.082, 0.038, 0.042 and 0.039, respectively (Table 2). Refined occupancy factors for each site are shown in Table 3. The refined positional and thermal parameters are listed in Tables 4 and 5, respectively. The interatomic distances were calculated using UMBADTEA (Finger, 1968, University of Minnesota Program for Computing Bond Angles and Distances, and Thermal Ellipsoids with Error Analysis) and are given in Table 6. Table 7 shows the length of edges of polyhedra.

2. EXAFS method

The EXAFS method was used to probe the local structural environment and to obtain further information on the average structure determined by single-crystal X-ray diffraction. Sauland and Nakatatsu vesuvianites were analyzed to examine the local structure around Cu and Mn ions. The crystal structure of the latter was previously examined by Yoshiasa and Matsumoto (1986).

Both vesuvianites were ground into powder in an agate mortar, and pressed with powdered boron nitride into pellets of 10.0 mm diameter with suitable thickness. The X-ray absorption measurements near the Cu and Mn K-edge were made with synchrotron radiation at the Photon Factory facilities, Tsukuba. The EXAFS interference function was extracted from the measured absorption data using standard techniques (Maeda, 1987). The Fourier transform of the EXAFS interference function to real space yields a radial structure function. The high frequency noise and the small residual background in each spectrum were removed by a Fourier filtering technique. The Fourier filtered EXAFS data were fitted using the least-squares minimization technique with an analytical EXAFS formula. The back-scattering amplitude of photoelectrons and the phase shift function employed here were the theoretical curves tabulated by Teo and Lee (1979).

The structural parameters around the Cu and Mn ions obtained by the least-squares parameters fitting of a fivefold one shell model for Cu-vesuvianite and vesuvianite from Nakatatsu mine are listed in Table 8.

III. RESULT AND DISCUSSION

A. Chemistry

In the vesuvianite structure, substitutions are occurred with a wide range. Chemical formulae and normalization schemes for vesuvianite are proposed by many investigators (e.g. Warren and Modell, 1931; Machatschki, 1932; Barth, 1963; Ito and Arem, 1970; Coda et al., 1970; Rucklidge et al., 1975; Deer et al., 1982; Allen, 1985; Hoisch, 1985; Yoshiasa and Matsumoto, 1986; Groat et al., 1992a). However, it is difficult to determine an adequate general formula for vesuvianite because of the structural complexities. Hoisch (1985) described that chemical data should be normalized on the basis of 50 cations per formula unit. Allen (1985) suggested that analytical results should be recalculated on the basis of 50 cations and 78 anions per formula unit. Charge balance is maintained by adjusting the O^{2-}/OH^{-} ratio. Groat et al. (1992a) analyzed a large number of vesuvianite from a various localities and evaluated the possible formulae and normalization schemes, and examined the range of composition found in vesuvianite. They divided the chemical data into boron-free and boron-bearing sets, and described that formula-unit normalization is best done on the basis of 50 (X+Y+Z) cations for boron-free vesuvianite, and 19 X cations for boron-bearing vesuvianite. The chemical formulae proposed by Allen (1985) and Groat et al. (1992a) are as follows.

Allen (1985)

$X_{18}(C_i, B_j)A_4Y_8Z_{18}(O, OH, F)_{78}$ $0<i<1$, $j=2-i$

X = Ca, Na, K, Fe^{2+}, Mn

Y = Al, Mg, Fe^{2+}, Fe^{3+}, Ca, Ti, Cr, Mn, Cu, Zn

Z = Si, Al

B = Mg, Fe^{2+}, Fe^{3+}, Cu, Zn

C = Ca, Na, Fe^{2+}, Mn

Groat et al. (1992a)

$X_{19}Y_{13}Z_{18}T_{0-5}O_{68}W_{10}$

$X = Ca, Na, Ln^{3+}, Pb^{2+}, Sb^{3+}$

$Y = Al, Mg, Fe^{3+}, Fe^{2+}, Ti^{4+}, Mn, Cu, Zn$

$Z = Si$

$T = B$

$W = (OH, F, O)$

Allen (1985) allowed the occupancy fractions of the B and C sites implying that two B positions may possibly be occupied so long as the two adjacent C positions are vacant. Groat et al. (1992a) constrained these values to the ideal value. According to these studies, the author used the 50 cation normalization scheme for vesuvianites. For boron-bearing vesuvianite, formula unit was calculated based on 50 cations excluding B^{3+} (and H^{+}). H_2O was calculated by charge balance, assuming 78 anions per formula unit and all Fe as ferrous. Table 1 shows the number of atoms per 50 cations in the four vesuvianites.

[The number of Si and Ca atoms per formula unit is nearly 18 and 19, respectively. However, in some specimens, the number of Ca atoms per formula unit exceed the ideal value of 19. This exceeding should be considered as an experimental uncertainties.]

Anion contents is important for understanding the crystal chemistry and structure of vesuvianite. Fluorine and chlorine are important anions of minor or trace elements contained in rock forming minerals. In vesuvianite structure, the two elements are contained replacing hydroxyl ions. Cl in vesuvianite was first reported by Serdyuchenko et al. (1968). Groat et al. (1992a) found that vesuvianite from Long Lake mine in Ontario contains up to 1.18 wt.% Cl. They also indicated that almost all of the chlorine-bearing vesuvianites contain significant amounts of F.

In Cl-bearing vesuvianites examined in this study (Table 1), contents of Cl (and F) are rather variable. The contents of Cl (wt.%) are 0.38-0.94 (Nakatatsu), 0.48-0.72 (Sanpo), 0.17-0.58 (Jinmu) and 0.49-0.74 (Kiura) wt.%, respectively. Neither remarkable zonings nor correlations between F and Cl could not be perceived. The present Cl-bearing vesuvianites contain significant amounts of F like those examined by

Groat et al. (1992a). Figure 2 shows the relationship between F and Cl contents of examined vesuvianites. The remarkable correlation is recognized between F and Cl contents. However, Cu-bearing vesuvianite from Sauland contains significant amounts of F although Cl content is very low. Although Groat et al. (1992a) indicate that many of the S-bearing vesuvianites are rich in F, S-bearing Saueseter vesuvianite (No.4 in Table 1, SO_3 0.49 wt.%) is poor in F. Vesuvianites with lower-symmetry than *P*4/*nnc* such as Ogose, Saueseter and Muslimbagh vesuvianites examined in this study and that from Jeffrey mine are poor in F and very poor in Cl. At the present state, it can be concluded that low-symmetry vesuvianites are poor in F and Cl free, and high-symmetry vesuvianites are rich in both F and Cl.

B. Structure

1. General structure

The vesuvianite structure (Fig. 3) is composed of exquisitely alternate combination of decomposed pieces of columns parallel to the fourfold axis of garnet structure (Warren and Modell, 1931). The fundamental difference in arrangement of the column between garnet and vesuvianite structures is a direction of rotation of columns. Figure 1 is fundamentally founded on that of Warren and Modell (1931) (and also Allen and Burnham, 1992). However, it should be emphasized that columns are slightly interfered mutually in the vesuvianite structure (see Fig. 1). As a result, SiO_4 tetrahedra of each column are linked together and form Si_2O_7 double tetrahedra, and the *a* axis of vesuvianite (15.6 Å) is slightly shorter than a diagonal axis of garnet, i.e., $a_{\text{vesuvianite}} < \sqrt{2}\, a_{\text{grossular}}$ and $c_{\text{vesuvianite}} = a_{\text{grossular}}$. The different arrangement of the column from garnet structure yields a characteristic structure along the fourfold rotation axis in vesuvianite. Atoms arranged along the axis are not connected directly to the garnet-like column. Two O(10) and four cation sites are arranged along each fourfold rotation axis in a unit cell. Ideally, two adjacent O(10) positions are occupied by oxygen and hydroxyl with an associated hydrogen bond, and two 5-coordinated B sites and two 8-coordinated

C sites are statistically half occupied by Fe and Ca atoms, respectively. Adjacent B and C positions or two adjacent C positions are not simultaneously occupied by two atoms because of their close arrangement (Fig. 4; left). When both B positions are occupied or vacant, charge balance of oxygen atoms will be collapsed. In a case where only B sites are occupied, O(9) bonds only to Si(3). This atomic arrangement may be a sort of defect structure and should be unstable. Figure. 5 shows impossible atomic arrangements along the fourfold rotation axis in the crystal structure of vesuvianite. The polyhedra around the C sites cannot share a face because of the short distance between the Ca ions (Coda et al., 1970; Giuseppetti and Mazzi, 1983). Therefore, ideal distribution of cations to these sites is alternate occupation of both B and C positions (Fig. 4; right). This is an only possible arrangements along the fourfold rotation axis. Consequently, the ideal site occupancy ratio of B : C is limited as 1 : 1. However, this has not been proved completely by experiment. In such a crystal structure, the statistical distribution of half occupied B and C sites yields the forbidden reflections with respect to the space group *P*4/*nnc*.

The ordering of cations and vacancies at B and C sites reduce the symmetry of vesuvianite from *P*4/*nnc* to *P*4/*n* or *P*4*nc*. Two types of sequences are considered along each fourfold rotation axis in a unit cell. The combinations of the two ordered sequences make four possible ordered arrangements in the unit cell; two sequences in the unit of two of them are anti-parallel (*P*4/*n*) and those of other two are parallel (*P*4*nc*) with each other, respectively (Fig. 6).

The ordering scheme of non-*P*4/*nnc* vesuvianite was confirmed by Giuseppetti and Mazzi (1983), Allen and Burnham (1983) and Fitzgerald et al. (1986b, 1987) in the space group *P*4/*n* and Allen (1985) in $P\bar{4}$, and all of these researches confirmed the ordering of cation and vacant positions along the fourfold rotation axis. These studies, however, also revealed that the examined crystals possess incomplete ordered structure implying some sort of domain structure, and that violation of glide plane extinction criteria are yielded by the ordered domains and the intensities of the glide-violating reflections are proportioned

to the size of the domains. Veblen and Wiechmann (1991) observed fine-scale domains in dark-field and high-resolution TEM images.

Generally, high-symmetry vesuvianite is found in metamorphic calc-silicate rocks, and low-symmetry vesuvianite is found in rodingites and in veins associated with mafic rocks and serpentinites. According to Allen and Burnham (1992), high-symmetry vesuvianite forms at relatively high temperatures (400 - 800 °C), and low-symmetry vesuvianite forms at temperatures below 300 °C as a product of hydrothermal alteration or deposition. Allen and Burnham (1992) described that the essential difference between high and low vesuvianite is the presence of resolvable domains.

2. Symmetrical analysis

Previous studies on symmetry of vesuvianite (e.g. Veblen and Wiechmann, 1991; Allen and Burnham, 1992) indicated that the crystals show the evidence of small departures from the tetragonal symmetry. Veblen and Wiechmann (1991) suggested that low-symmetry vesuvianite is not tetragonal. Allen and Burnham (1992) described that some refinements of cell parameters show nontetragonal cell parameters.

In the present study, nontetragonal cell parameters are observed in some refinements of cell parameters. However, to detect a certain evidence of such difference of cell parameters is quite difficult. It may also be possible that the observed difference of cell parameters is ascribed to a effect of experimental uncertainty. The author consider that such minor deviations from tetragonal symmetry can be tolerated. Thus, this problem will not be further mentioned in this study. In the present study, the refinement of the crystal structure were execute in the tetragonal model.

According to the previous studies on symmetry of vesuvianite (Allen and Burnham, 1992), high-symmetry vesuvianite and low-symmetry vesuvianite are distinguished on the basis of the size of ordered domains. To simplify the discussion, attention will only be focused on the atomic configuration along the fourfold rotation axis. In a unit cell level, only two schemes of cation-vacancy ordering are possible and the two schemes

have respective opposite pattern with each other and are represented by the space groups $P4/n$ and $P4nc$.

The intensities of glide-violating reflections depend upon the size of the domains. As the size of the domains decreases, the general structure becomes gradually indistinguishable from perfect disordered structure with $P4/nnc$ symmetry. If a crystal contains equal volumes of oppositely ordered domains, the average structure exhibits $P4/nnc$ pseudo-symmetry. However, glide-violating reflections for space group $P4/nnc$ are manifested by the ordered domains.

As mentioned above section, in a unit cell level, the vesuvianites are classified into two types of space group of $P4/n$ and $P4nc$. If a crystal is consist of ordered domains of $P4/n$ and $P4nc$, the reflection characteristics indicate the $P4$ symmetry. It is emphasized that the symmetry represented by the space group $P4$ is never appeared in a unit cell level.

The Saueseter vesuvianite showed strong $hk0$ reflections. Allen (1985) has demonstrated that most, if not all, weak violating $hk0$ reflections are a consequence of multiple diffraction. However, those in Saueseter samples are too strong to ascribe multiple diffraction.

The reflection characteristics of Muslimbagh vesuvianite show that the symmetry tends toward $P4$. It is also possible that the crystal has indeed $P\bar{4}$ symmetry which has the same cation-vacancy ordering schemes to that of $P4/n$. Allen (1985) successfully carried out a refinement in the space group $P\bar{4}$. However, the space group $P\bar{4}$ was not used for Muslimbagh vesuvianite in this study, and the refinement were done in the space group $P4/n$. The reason is as follows: The structure model represented in the space group $P4$ indicates that the crystal is consist of assemblage of ordered domains with both $P4/n$ and $P4nc$ symmetry. That is, the $P4$ symmetry structure model never exhibits complete ordered structure. Therefore, the refinement in the space group $P4$ is not so different from that of $P4/nnc$. The space group $P\bar{4}$ has the same possible schemes of cation-vacancy ordering for the B and C positions to that of the space group $P4/n$. The two space groups are distinguished by the schemes of positional order around the B and

C sites. In $P4/n$, the B and C sites are located on the fourfold axis, whereas in $P\bar{4}$, on the twofold axis.

In the three low-symmetry vesuvianites, the values of refined site occupancy factor for B(a) and C(a) versus B(b) and C(b), (63:37(1), 62:38(1) and 92:8(1) % for respective three specimens), indicate that the ordering in these crystals is incomplete. It shows that these low-symmetry crystals are consist of the domains having ordered structure, although the Saueseter vesuvianite has nearly complete $P4nc$ ordering scheme. The ordering scheme represented in the space group $P4nc$ is successfully confirmed in this study. The author considered that the existence of $hk0$ ($h+k$ odd) reflections in Muslimbagh vesuvianite is caused by addition of domains having $P4nc$ structure rather than the fact that the crystal has $P\bar{4}$ symmetry.

Note: The most simplest way to distinguish high and low-symmetry of vesuvianite is to examine the absence or presence of glide-violating reflection for $P4/nnc$. However, even if a crystal were labeled as high-symmetry in this study, a few extremely weak glide-violating reflections are observed on the four-circle X-ray diffractometer records. These kind of weak glide-violating reflections for $P4/nnc$ are already mentioned by previous workers (e.g. Allen and Burnham, 1992, Groat et al., 1992b). Based only on the consideration of glide-violating reflection, it is difficult to give a clear qualification for the distinction between high-symmetry and low-symmetry of vesuvianite. In this study, a crystal was considered to be low-symmetry only when relatively strong and numerous glide-plane violations are observed and obvious improvement is appeared in R indices.

3. Representation of polyhedra

In the space group $P4/nnc$, the vesuvianite structure contain ten sets of crystallographically non-equivalent cation-sites; three distinct 4-coordinated sites (Si(1), Si(2), Si(3)), one 5-coordinated site (B), two distinct 6-coordinated sites (A, AlFe), three distinct 8-coordinated sites (C, Ca(1), Ca(2)), and one 9-coordinated site (Ca(3)), respectively. In the space groups $P4/nnc$ and $P4/n$, the Ca(1), C, B, A and Si(1) sites

are on the special positions and the other sites are on the general positions. In the space group *P4nc*, the A site is on the general position. Polyhedra in vesuvianite structure are partially shown in Fig. 7.

[Boron-bearing vesuvianite (Wilui River) is not mentioned in this section since effect of boron is considerable on the overall structure as well as composition of vesuvianite and will be discussed in latter section.]

Si(1), Si(2) and Si(3) tetrahedra

The Si(1) and Si(2) tetrahedra are isolated, and the Si(3) tetrahedra shares an oxygen apices with each other forming the double tetrahedra. The respective tetrahedron shares the vertices with A and AlFe octahedra (except O(11) vertex). The Si(1) and Si(2) tetrahedra are distorted. The mean Si-O bond length of Si(3) is slightly shorter than that of any other tetrahedron. Difference between shared and unshared edges of Si(3) tetrahedron is smaller than that of the other tetrahedra. Thus, the Si(3) tetrahedron shows the highest regularity among the tetrahedra.

A and AlFe octahedra

The A octahedron shares two edges O(4)-O(11) with the two AlFe octahedra, i.e. the A octahedron bridges the garnet-like columns. This edge is the shortest of all the edges of A and AlFe octahedra. Present refinements indicate that the A sites are almost occupied by Al in boron-free both high and low-symmetry vesuvianites. The AlFe site can contain several kinds of ions. For example, Mg content is not negligible in vesuvianite. However, as the scattering factors of Mg and Al atoms are nearly identical, their scattering powers could not easily distinguished. Therefore, decision of the site preference of Mg is rather difficult.

In the present refinement, the octahedral AlFe sites were modified so as to be occupied by Al and Fe. As the result, the AlFe sites of three low-symmetry vesuvianites are occupied mostly by Al ions, and the occupancy parameters are similar with each other in both non-equivalent AlFe sites.

Figure 8 shows the mean cation-anion interatomic distances of the tetrahedral (Si(1), Si(2) and Si(3)), pentahedral (B) and octahedral (A and AlFe) sites. Figure 9 shows several effective ionic radius (Shannon, 1976). The average cation-anion interatomic distances around the octahedral A sites of the respective specimens suggest that the A sites are fully occupied only by Al. The fact agrees well to the results obtained by Rucklidge et al. (1975), and can be concluded that the Al^{3+} ions preferentially occupy the A site rather than the AlFe site.

Cation-anion interatomic distances around AlFe site of Sauland vesuvianite are smaller than those of the others, because the site does not contain larger and heavier ions. This result imply that all larger and heavier ions occupy the B site in Sauland vesuvianite. Franklin Cu-vesuvianite (Fitzgerald et al., 1986a), on the other hand, contain Zn ions in the AlFe site resulting the average cation-anion interatomic distance as 1.954 Å.

Ca(1), Ca(2), Ca(3) and C polyhedra

The 8-coordinated polyhedra about the Ca(1) and Ca(2) cations can be described as a slightly distorted triangular dodecahedron and the 8-coordinated polyhedron about the C cation as a slightly distorted square antiprism. Considering the cation-anion interatomic distances, Ca(3) can be interpreted as 9-fold coordination rather than 8-fold. This coordination number was suggested by Giuseppetti and Mazzi (1983) and Yoshiasa and Matsumoto (1986). Therefore, the Ca(3) polyhedron shares the faces (O(6)-O(7)-O(10)) with other Ca(3) polyhedron. Other Ca polyhedra share the edges with each other. Only Ca(3) polyhedron has complex coordination. In the present nine vesuvianites, Ca sites are occupied by Ca ions. Three low-symmetry vesuvianites show that the size of occupied C site is larger than that of vacant C site.

In the Saueseter *P4nc* vesuvianite, the appreciable shifts from average positions of non-equivalent sites are recognized at O(10) and Ca(3) sites. The non-equivalent O(10) and Ca(3) ions are shifted 0.124 and 0.101 Å from their average positions, respectively.

The similar shift of non-equivalent O(10) and Ca(3) sites are also shown in vesuvianites having $P4/n$ symmetry (Giuseppetti and Mazzi, 1983 and Fitzgerald et al., 1986b).

The Ca(3) cation shifts toward O(10) when the O(10) is not bonded to B cation. The size of square formed by four Ca(3) differs in both non-equivalent positions. The Ca(3)-Ca(3) distances (the length of a square side) are (a) 3.511 and (b) 3.670 Å, respectively. The average interatomic distances of the coordinated anions of both non-equivalent Ca(3) sites are almost equal. The non-equivalent Si(3) and AlFe cations are shifted 0.062 and 0.042 Å from their average positions, respectively. The structural strain caused by the cation ordering can be released mostly by a flexibility of Ca(3) polyhedra.

B polyhedra

The 5-coordinated polyhedron about B cation is square pyramid. The polyhedron has an O(10) ion as an apex and the basal plane is formed by a square of four O(6) ions. The B site is nearly at the center of the basal plane. The sizes of the fivefold coordinated B sites are larger than those of the octahedral A and AlFe sites. In addition, variation of the size of the B sites in each specimen is greater than that of the other sites.

Inspection of the refined occupancy factors at the B site shows that the B sites of the examined specimens, except those of Sauland Cu-bearing vesuvianite, are almost occupied by Fe ion.

The Sauland vesuvianite is characterized by its chemical composition. That is, significant amounts of Cu is contained in the structure, and Fe content is poor. Franklin Cu-vesuvianite contains significant amounts of Zn (Fitzgerald et al., 1986a) whereas Sauland Cu-bearing vesuvianite contain no Zn. The refined occupancy factors (Table 3) suggest that Cu ion occupy the B site in Sauland vesuvianite. Whether the rest part of B site is allotted to Mg or Al is not clear. Valley et al. (1985) suggested that the B site is occupied by Mg in Fe-poor vesuvianite. The effective ionic radius of Mg^{2+} is almost same to that of Cu^{2+}. Thus, the Cu ion should able to occupy the B site.

Three high-symmetry vesuvianite (Obira, Sanpo and Jinmu) have nearly equal chemical composition and local configuration around B site is similar with each other. Therefore, these three specimens could be grouped together. However, slight difference is recognizable in anion content as will be mentioned in latter section. In this section, only the Obira vesuvianite is mentioned.

Refinement of occupancy factors of the B site in high-symmetry Obira vesuvianite indicates that the B site is fully occupied by Fe. The interatomic distances of B-O(6) and B-O(10)A are 2.098 and 1.874 Å, respectively. Although the B-O(10)A distance is relatively shorter, B-O(6) distance is slightly longer than those of low-symmetry vesuvianites. Based only on the interatomic distances, whether the state of iron is Fe^{2+} or Fe^{3+} can not be determined. The coordination environment around the B site of high-symmetry vesuvianite will be mentioned in latter section.

The refined occupancy factors of the three low-symmetry vesuvianites indicate that the B sites are almost occupied by Fe. In Saueseter *P4nc* vesuvianite, the mean interatomic distances around B sites are 1.964 (92% occupied site) and 2.131 Å (8% occupied site), respectively. The more occupied site is smaller than the less occupied site. The inter atomic distance around 92 % occupied B site indicate that the B site is mainly occupied by Fe^{3+}. Giuseppetti and Mazzi (1983) and Fitzgerald et al. (1986) also showed that the occupied site is smaller than the unoccupied site in low-symmetry *P4/n* vesuvianite. In the two *P4/n* vesuvianites, the mean interatomic distances around B sites are 2.044 (63% occupied site) and 2.081 Å (37% occupied site) in Ogose vesuvianite and 2.037 (62% occupied site) and 2.092 Å (38% occupied site) in Muslimbagh vesuvianite, respectively. These values are slightly large for Fe^{3+} (1.98 ($^{V}Fe^{3+}$) Å). However, the site occupancy factor of B and C sites of these vesuvianite suggest that these sites are not perfectly split into occupied and unoccupied site, i.e. the ordering is incomplete because of the domain structure. Thus, the refinements give the average cation-anion interatomic distances for both occupied and unoccupied B sites yielding apparently longer bond length than actual bond length. Therefore, B sites of the two *P4/n* vesuvianites are also

mainly occupied by Fe^{3+}. Fitzgerald et al. (1986) assigned Al^{3+} to the B site in a vesuvianite from Jeffrey mine. The present chemical analysis of vesuvianite from Jeffrey mine shows less Fe content than those of the three refined specimens (Table 1). Valley et al. (1985) showed that Mg occupied the B site in a low-symmetry vesuvianite from Georgetown, but their refinement was carried out in the space group *P4/nnc*.

4. Local structure determined by the EXAFS method

The Fourier transforms for the Cu and Mn K-edges are shown in Fig. 10, where no phase shift correction is made. Bond length around Cu ions in Sauland vesuvianite and Mn ions in the Nakatatsu vesuvianite are calculated with fivefold one shell model, and the results are shown in Table 8. The distance of first-shell O ions from Cu ion is 1.98(1) Å for Sauland vesuvianite. The distance of first shell O ions from Mn ion is 2.10(1) Å for Nakatatsu vesuvianite. Table 8 also shows the cation-anion interatomic distances around B sites determined by X-ray single crystal diffraction method together with the effective ionic radius (Shannon, 1976). Cu ion is probably divalent state, and as is evident in Table 8, the obtained distance more agrees with the effective ionic radius of fivefold coordinated Cu ion rather than that of sixfold coordinated Cu ion. Thus, it is concluded that Cu ion prefers to occupy the fivefold coordinated B site in the vesuvianite. The fact is essentially equivalent to those of the present refinements and Fitzgerald et al. (1986a). Mn ion is probably divalent state. Divalent state of Mn is too large to occupy the sixfold AlFe site, and Mn^{2+} can occupy the fivefold B site. The obtained distance of Mn atom is longer than that of Cu atom. Therefore, Mn ion is divalent state and occupies the B site in Nakatatsu vesuvianite.

5. Anions in the crystal structure of vesuvianite

In the vesuvianite structure, only O(10) and O(11) are not bonded to Si ions. Coda et al. (1970) suggested that the two sites are probably associated with hydrogens, which is supported by subsequent investigators. In non-*P4/nnc* vesuvianite structures, Giuseppetti and Mazzi (1983) and Fitzgerald et al. (1986b) suggested existence of

hydrogen bonds between O(10) and O(10), i.e., the B site cation is bonded to O2- and the C site cation to hydroxyl. Recently, Lager et al. (1989) determined the hydrogen atom positions by neutron diffraction methods.

Two O(10) along the fourfold axis favor a hydrogen bond. Yoshiasa and Matsumoto (1986) and Ohkawa et al. (1992) obtained relatively short O(10)-O(10) distance and significant large thermal parameter of O(10) in F-bearing high-symmetry vesuvianite. Ohkawa et al. (1992) concluded that these facts can be interpreted as an effect of the distribution of F ion. Groat et al. (1992b) found significant positional disorder at the O(10) position. They explained that the disorder is caused by the splitting of O(10) into two sites.

There are two hydrogen positions in the vesuvianite structure. In this paper, the two hydrogens are labeled H(10) and H(11) corresponding to H(2) and H(1) of Lager et al. (1989), respectively. H(11) is associated with the oxygen occupying the O(11) position and forms a weak hydrogen bond with O(7). H(10) is bonded to one O(10) atom and forms a symmetrical hydrogen bond with a second O(10) along the fourfold rotation axis. (Hydrogen bonging has an attractive interaction in which hydrogen atoms share oxygen.)

The valence sums for anions in vesuvianites are calculated according to the method of Brown (1981). The selected valence sums are listed in Table 9. The value of bond strengths of O(1) through O(9) except O(7) of the respective specimens are almost equal to 2.0 and the value indicates that these sites are occupied by oxygen ions. The values of bond-valence sums of O(11) are approximately 1.2 - 1.3, suggesting strongly that O(11) oxygen is accompanied with a hydrogen. The values of valence sums of O(7) are slightly small than the expected value of 2.0 for oxygen. These facts suggest the existence of hydrogen bond between O(7) and O(11) in order to satisfy the bond-valence requirements at O(7). The incident bond-valence sum of O(10) has two cases, one is occupied B site and the other is unoccupied. In both cases, the valence sums are far shorter than 2.0.

These results are equivalent to those of previous studies (Giuseppetti and Mazzi, 1983, Yoshiasa and Matsumoto, 1986, Groat et al., 1992b).

The F and Cl ions replace hydroxyl locally. Then, which site, O(10) or O(11), is occupied by these ions is important. In high F content vesuvianite, occupancy factors for O(11) site are refined using the atomic scattering factors of O and F, although the distinction of the two scattering factors is not clear because of the similarity. The refined occupancy factors for O(10) and O(11) sites are also listed in Table 3.

i. Distribution of O(11)

O(11) site is coordinated to cations at the Ca(3), A and AlFe sites. The O(11) site lie above a triangle formed by the three sites. H(11) is associated with the oxygen occupying the O(11) position forming a weak hydrogen bond with O(7).

If O(11) site is occupied by F, positional disorder of the anion at the O(11) position can possibility be expected. However, by inspecting the isotropic and anisotropic temperature factors, any discernible positional disorder of the anion at the O(11) position can not be found regardless of F and Cl contents. Substitution of F^- for OH^- at O(11) site may cause a removal of hydrogen bond from bond-valence at O(7). As a result of the F^- for OH^- substitution, any local adjustments must occur to satisfy the bond-valence at O(7). Groat et al. (1992b) mentioned this problem and discussed as follows. Since the positional disorder of the anions at the O(7) positions are indiscernible, the bond-valence deficiency at O(7) must be compensated by an increase in incident bond-valence from the coordinating cations. The O(7) anion is bonded to Si(2) and three Ca(3) cations. The O(7)-Si(2) bond lengths are almost constant, and there is no change in the anisotropic displacement parameters of Si(2) with changing F content. The O(7)-Ca(3) bond lengths have significant variation correlating with increased F^- for OH^- substitution. These opinion of Groat et al. (1992b) is entirely perceived in the present study. Almost constant O(7)-Si(2) bond lengths and variable O(7)-Ca(3) bond lengths are recognized (Fig. 11).

The shortening of mean O(7)-Ca(3) bond lengths correlated with increased F+Cl contents is recognized (Fig. 12).

In Saueseter *P4nc* vesuvianite, the interatomic distances from O(11a) to coordinated cations are shorter than those of O(11b). As a result, bond-valence sums of non-equivalent O(11) site in Saueseter *P4nc* vesuvianite are 1.46 and 1.29, and the values are slightly different with each other. In addition, the thermal parameters are also different in two non-equivalent O(11) sites. Although scattering powers at these sites are almost identical, the fact implies that contributions of hydrogen bond to respective non-equivalent O(11) oxygens are different, or some anion other than oxygen (F or S?) preferentially occupy the either site. The bond distances from O(11) to two O(7) are (a) 2.847 and 2.961 Å, and (b) 2.731 and 2.932 Å, respectively. The similar difference of interatomic distance between non-equivalent O(11) and O(7) were also shown in vesuvianites having *P*4/n symmetry (Giuseppetti and Mazzi, 1983 and Fitzgerald et al., 1986b). However, *P*4/*n* vesuvianites have nearly equal values of the bond-valence sums and of the thermal parameters of non-equivalent O(11) sites.

ii. Distribution of O(10)

If complete cation-vacancy disordering at B and C positions occurs, the sequence of B and C cations is not repeated along the fourfold rotation axis. In such disordered structure, there must be three possible local atomic arrangements around two adjacent O(10) anions (Fig. 13). However, another concept is suggested by Groat et al. (1992b) who showed that complete ordering along a specific fourfold axis exists and wide-range disorder is caused by disordering of polarity between individual fourfold axis.

The root-mean-square thermal displacements for the O(10) ion along the fourfold rotation axis is significantly greater than that of the others. Rucklidge et al. (1975) pointed out that the B cation is almost coplanar with the square formed by four O(6), and so can vibrate in the direction perpendicular to this plane. From this point of view, the

O(10) ion bonded to B site cation (apex of the square pyramid) is almost coplanar with a square formed by four Ca(3) cations.

In the vesuvianite structure, possible two adjacent O(10) pair are as follows; O-O, O-H-O, O-F, O-CL, F-H-O, F-F, F-CL, CL-H-O. Which pair is more conceivable? In the vesuvianite structure, whether the attractive interactions such as hydrogen bonds are present or not is not clear between chlorine and oxygen, chlorine and fluorine and two fluorine atoms. If two F ions make hydrogen bond, FHF^- bond is strong and generally in most cases is symmetric. In the FHF^- bond, interatomic distance between F ions is shorter than that of O ions.

Since the local distribution at two adjacent O(10) positions is significant, the problems should be discussed based on the anion contents of vesuvianites.

ii-1. High-symmetry vesuvianite

Figure. 14 shows electron density maps of the high-symmetry vesuvianites in the plane which passes the O(10) ions. The general shape of the electron density peaks for C and B ions is normal but that of O(10) ions is rather abnormal. All of the four high-symmetry vesuvianites contain significant amounts of F, but content of Cl is considerably different with each other (see Table 1).

Cl-bearing vesuvianite (Obira, Sanpo and Jinmu)

Obira, Sanpo and Jinmu vesuvianites contain significant amount of Cl ion. In the electron density map (Fig. 14), O(10) appears as pear-shaped. In addition, the position of O(10) does not coincide with the centroid of the electron density peak. The distance between the two O(10) peaks is too short for both O and F ions. In the difference Fourier map, some residual electron densities are recognized. The pear-shaped O(10) is characterized in Cl-bearing vesuvianite. In contrast to Obira and Sanpo vesuvianites, the O(10) positions in Jinmu vesuvianite coincide almost with the centroid of the electron density peak. The shape of O(10) in Jinmu vesuvianite is rather normal than those of

Obira and Sanpo vesuvianites suggesting that the peculiar shape of O(10) is proportioned to Cl content.

Obira vesuvianite contains the most Cl ion among the three specimens. In the Fourier map of Obira vesuvianite (Fig. 14), O(10) has two peaks indicating that the O(10) site is split into two sites, O(10)A and O(10)B. The Fourier map (Fig. 14) shows that the electron density peak of O(10)B is higher than that of O(10)A, and the volume of the O(10)A site is smaller than that of the O(10)B site. Thus, the O(10)A positions can not be occupied by Cl ion. The distance between two adjacent O(10)B sites is too small for Cl ion to occupy the both O(10) sites simultaneously. Therefore, it is concluded that Cl ion can occupy the one of these two O(10)B positions. The respective two adjacent O(10)A and O(10)B anions violate the local twofold rotational symmetry. The relatively longer cation-O(10)B distances of Obira vesuvianite is reasonably explained by this arrangement. Figure 15 shows the atomic arrangements along the fourfold rotation axis of Obira Cl-bearing vesuvianite.

In the present least-squares calculation, we assumed that the O(10)A and O(10)B sites are half occupied by F and Cl ions, respectively. Then, no significant electron density residuals around the two adjacent O(10)A and O(10)B positions are recognized in the difference Fourier map.

The interatomic distances of Ca(3)-O(10)A and B-O(10)A are 2.616 and 1.881 Å, respectively. Although the previous studies showed that O(10) anion is not bonded to C cation, the interatomic distance C-O(10)A is 2.680 Å implying the bonding of O(10)A anion to the C cation. The C-O(9) distance of Obira vesuvianite is longer than that of the three low-symmetry vesuvianites, whereas the C-O(6) is shorter than that of the three low-symmetry vesuvianites, i.e., the C cation is shifted towards O(10).

Since the atomic scattering factor of O is similar to that of F , distinction between O and F in the O(10)A site is rather difficult. To clarify this problem, bond-valence calculations (Brown, 1981) will be useful but the calculation is not effective in this case.

The refinement in the space group *P*4/*nnc* give the average cation-anion interatomic distances for both occupied and unoccupied B sites. Then, the positional disorder is represented by high temperature factors. Therefore, the actual interatomic distance around occupied or unoccupied sites is probably shorter or longer than that of calculated value with *P*4/*nnc* structural model. The positional disorders of B, C and Ca(3) sites have significant large thermal vibrations. Therefore calculated bond-valences are not represent the actual bond-valence exactly. When the B site is occupied by Fe^{3+}, the bond-valence sum of F ion in O(10)A site is 1.13 and that of O ion is 1.47. When the B site is vacant, then O(10)A anion is bonded to Ca in the C site, those of F and O ions are 0.69 and 0.89, respectively. In the difference Fourier map, detection of the electron density residuals for the hydrogen atom between two O(10) positions is rather difficult. Therefore, F ion may occupy the O(10)A site accompanying no hydrogen bond between two O(10) anions. According to the ionic radii of F and Cl by Shannon (1976), the O(10)A-O(10)B distance of 2.754 Å is too short for F-Cl distance. The following two facts can explain the situation; 1) the chemical analysis data show that Cl content is not so high as to fill one of the two O(10) position, and/or 2) displacements of the positions of the O(10) anions probably occur judging from the significantly larger thermal parameters along the c axis of these sites than those of others.

Sanpo and Jinmu vesuvianites contain less Cl ion than that of Obira vesuvianite. In Sanpo and Jinmu vesuvianites, Cl and F ions in O(10) site probably distribute along the *c*-axis similarly as in the case of Obira vesuvianite. However, because two split prominent peaks are not recognized in O(10) position in the Fourier maps, it is difficult to distinguish the Cl and F positions. Therefore, the structural refinement with split positions in O(10) does not apply for the Sanpo and Jinmu vesuvianites. The site occupancy refinement of O(10) positions are performed assuming that the two positions are identical. The least-squares refinements indicate that site occupancies of Cl are 0.31 and 0.18 in O(10) for Sanpo and Jinmu vesuvianites, respectively. These occupancy

factors suggest that all Cl ions occupy the O(10) site. The refined occupancy factor is concordant with chemical analyses data.

The pear shaped O(10) sites in the electron density maps of Cl-bearing vesuvianites are reasonably interpreted by the effect of Cl ion distribution. The average distribution of O(10) ions produce a pear-shaped appearance on electron density maps, which can be related to the difference between the two vibration ellipsoids. In the crystal structure of Cl- and F-bearing vesuvianite, the O(10) site cannot be interpreted by a harmonic oscillation model. Cl ions prefer to occupy the O(10) site rather than the O(11) site. Presumably, Cl ion does not occupy the O(11) site and the fact suggests that the limit of Cl contents is 1 atom per formula unit. In fact, in all studied vesuvianites, Cl content is less than 1 atom per formula unit. In some F-rich vesuvianites, the content of F ion exceeds the limit allowed for O(10) site, 2 atom per formula unit. Thus, O(11) site can be occupied by F ion.

The Cl-bearing vesuvianites have large size of square formed by four Ca(3) cation. The lengths of edges of squares (Ca(3)-Ca(3) distances) are 3.685, 3.685 and 3.632, Å for the Cl-bearing three specimens, respectively. The Ca(3)-O(10) bond strength is rather small because of the large size of Ca(3) square.

Note: In the previous paper, it is proved that the O(10) site is almost fully occupied by F in the refined structure model on the vesuvianites from Sanpo and Jinmu mines (Ohkawa et al., 1992). Ohkawa et al. (1992) also indicated that the pear-shaped O(10) in the electron density maps of Sanpo and Jinmu vesuvianites are interpreted as an effect of the distribution of F ion. Effect of Cl ion was remained to be solved. However, the present chemical analyses show that these vesuvianites contain significant amount of Cl. Therefore, these vesuvianites were re-examined using the same intensity data as those reported previously, especially on the site occupancy refinement of O(10).

It can not be specified whether the neighboring site of Cl ion in O(10)B site is B or C sites which may be occupied by cations. The both cases may be possible. When the B cation neighbors Cl, the distance between them (2.793 Å) is too long to bond. If the

O(10)B is occupied by Cl ion and there is no hydrogen bond between O(10)B and O(10)A, the O(10)B site is coordinated only to cations at the Ca(3). Then, the O(10)B site lie above a square formed of four Ca(3). This form of fourfold coordination of Cl ion is quit peculiar. The existence of hydrogen around the two O(10) positions is not clear. This situation also suggest the existence of 4-coordinated B cation. However, whether the 4-coordination of B site actually exists or not is not clear. As regards the distribution of Cl ion, whether Cl interrupt an ordering of cations and whether disordered structure prefer Cl or not are remained to be discussed. This problem will be discussed in latter section.

Cu-bearing vesuvianite (Sauland)

The color of Sauland vesuvianite is deep-blue caused probably by presence of copper. In allusion to blue color, the byname "Cyprine" was given to this vesuvianite by Berzelius in the early nineteenth century. Paragenesis of Sauland vesuvianite is described by Neumann and Svinndal (1955). Cell parameter of Sauland vesuvianite is given in Ito and Arem (1970).

Sauland vesuvianite contains Cu ion in the B site. Furthermore, Sauland vesuvianite contains significant amounts of F although it contains very few Cl. In the electron density map (Fig. 14), the shape of O(10) implying the some positional disorder. However, the shape of O(10) in Sauland vesuvianite is rather normal than those of Cl-bearing vesuvianite.

Differing from Cl-bearing vesuvianite, Sauland Cu-bearing vesuvianite has different distribution of O(10) anion, i.e., hydrogen is bonded to O(10). Difference Fourier map of Sauland vesuvianite show double minima indicating hydrogen between adjacent O(10) atoms.

Lager et al. (1989) determined the hydrogen atom positions by neutron diffraction methods. They observed the H atom between the two O(10) atoms. They found a double minima between adjacent O(10) atoms along the four-fold rotation axis indicating

a statistical distribution of H(10) between two sites in difference Fourier maps. Because there is only room for one H between the two adjacent O(10) atoms, both sites cannot be occupied simultaneously. They concluded that the H atom lies solely between the two adjacent O(10) atoms occupying statistically one of these two H(10) sites. The H atom occupies a disordered off-center position being shared between two adjacent O(10) atoms. This configuration is in accordance with the well-known fact of the unsymmetrical hydrogen bonds. Their result also indicates that vesuvianite can have a maximum H content up to 9 atoms per formula unit.

Although the determination of the exact H atom positions by X-ray diffraction method is difficult, H atom was detected in difference Fourier maps only in the case of Sauland vesuvianite.

A difference Fourier map of Sauland vesuvianite is shown in Fig. 16. In the part of the structure, a fluctuation in O(10) under the influence of the surrounding cations should be present. The O(10)-O(10) interatomic distance of 2.772 Å is an appropriate distance for a linear hydrogen bond. The large electron density peaks in the difference Fourier map are probably correspond to the hydrogen atom. The height of electron density peak is approximately 0.6 e/A^3 and the distance from the O ion is about 1.07 Å. These values are also reasonable. In Figure 16, two peaks across a twofold rotation axis are recognized. The H atom statistically occupies one of these two positions.

In which case hydrogen atom bond to O(10) oxygen, i.e. one case B site is occupied and the other vacant? The fact is not yet clear. On the problem, Groat et al. (1992a, b) proposed that, in F-bearing vesuvianite, a hydrogen atom bonds to O(10) oxygen (bonded to B cation), and the other O(10) site (not bonded to B cation) is occupied by F (Fig. 17-a). However, the scheme is not established as a correct configuration. This configuration is in contradict to the previous proposal for low-symmetry vesuvianite (Giuseppetti and Mazzi, 1983 and Fitzgerald et al., 1986b) in which hydrogen bonds to O(10) oxygen (not bonded to B cation), and forms a hydrogen bond with the other O(10) oxygen (bonded to B cation) (Fig. 17-b).

In the present study, site occupancy refinement indicate that O(10) site contain F. That is, Sauland vesuvianite is occupied by nearly equal amounts of both O and F ions, although distinction between O and F is rather difficult.

Viewed from the standpoint of the bond-valence satisfaction, the configuration suggested by Groat et al. (1992a, b) is plausible. When the B site is occupied, the valence sum of O(10) is 1.21, and when the B site is vacant 0.88. These calculated values imply the bonding of hydrogen to O(10) oxygen and the latter bonds to B cation and forms hydrogen bond with the other O(10) fluorine. As described in the latter section, this problem is significant.

ii-2. Low-symmetry vesuvianites

(Ogose, Muslimbagh and Saueseter)

Site occupancies and cation-anion interatomic distances are also similar in these low-symmetry vesuvianites. The low-symmetry vesuvianites show that O(10) bonding to B cation shifts toward B from the average position of pseudo-symmetric two adjacent O(10) oxygen atoms, O(10a) and O(10b). The O(10a)-O(10b) distances of the three low-symmetry vesuvianites are 2.735 (Ogose), 2.612 (Muslimbagh) and 2.754 Å (Saueseter), respectively. The distance of Muslimbagh vesuvianite is slightly shorter than that of the others. This probably be interpreted as an overlapping of pseudo-symmetric O(10) atoms because the refinement is done in the space group $P4/n$ which is higher than the probable true symmetry of $P4$.

[When the refinement of low-symmetry vesuvianite is done in the space group $P4/nnc$ (higher than true symmetry), the shortening of O(10)-O(10) distance is occur. For example, when Saueseter vesuvianite is refined in the space group $P4/nnc$, the O(10)-O(10) distance is only 2.55 Å. This is because of the existence of symmetrical element (two-fold rotation symmetry) between two adjacent O(10) positions.]

Figure 18 shows the atomic arrangements along the fourfold rotation axis of Saueseter $P4nc$ vesuvianite. In Saueseter $P4$nc vesuvianite, the O(10a) anion shifts to

O(10b) anion against the perpendicular component of the attraction of Ca(3) cation. In addition, the O(10b) anion is almost coplanar with a square plane formed by four Ca(3) cations. This situation show an assumption that attractions on the O(10b) anion acting perpendicularly both sides of this squared plane are balanced each other. On a simplifying assumption, one is the sum of attraction of B cation and perpendicular component of repulsion of O(6b) anion, and the opposite is probably attraction of a hydrogen bond between O(10a) and O(10b) oxygens. Whether a hydrogen bond between O(10a) and O(10b) oxygens can provide the interacting force to satisfy the local bond balance is important. A rough estimation shows that this is possible. However, quantitative calculation of such atomic interactions is not able at present state.

Difference Fourier maps of the three low-symmetry vesuvianites show some electron density residuals between two adjacent O(10) positions. However hydrogen atom positions could not be decided exactly, because the difficulty of the decision of exact site occupancy of these sites.

According to previous consideration (in non-*P4/nnc* vesuvianite structures, Giuseppetti and Mazzi, 1983 and Fitzgerald et al., 1986b), hydrogen bonds to O(10) oxygen (not bonded to B cation) and forms a hydrogen bond with the other O(10) oxygen (bonded to B cation).

The bond-valence sums of O(10a) and O(10b) of Saueseter vesuvianite are 0.88 and 1.50, respectively. In appearance, these values seem to indicate a hydrogen bonding to O(10a) oxygen (not bonded to B cation) and forms hydrogen bond with O(10b) oxygen. However, the sum of bond-valences of O(10a) and O(10b) oxygens is 3.38 including a supply of hydrogen bond and the value is too small for two occupying oxygen sites. When both O(10) positions are occupied by oxygen, the incident bond-valence sums should be 4.0. This kind of shortage is already appeared in the previous works of non-*P4/nnc* vesuvianite (e.g. Giuseppetti and Mazzi, 1983 and Fitzgerald et al., 1986b). Groat et al. (1992b) stressed the significance of the problem.

As was Groat et al. (1992a, b) explained, this shortage are satisfied for the F-bearing vesuvianite in a way that H bonds to O(10) oxygen (bonded to B cation), and the other O(10) site (not bonded to B cation) is occupied by F. In this configuration, hydrogen bond exists between oxygen and fluorine atoms. Note that the proposal of Groat et al. (1992a, b) is in contradiction to the previous proposal. Because almost all low-symmetry vesuvianites contain few F, it is impossible to explain the shortage of low-symmetry vesuvianites based on the proposal of Groat et al. (1992a, b). Lager et al. (1989) determined the crystal structure in the space group *P4/nnc*, they did not clarified such local configuration which require lower-symmetry than *P4/nnc*. Therefore, local configuration and bond-valence satisfaction at the O(10) position are still remain to be solved. In the present state, more appropriate atomic configuration to explain this shortage is not possible. It may be concluded that O(10) sites of low-symmetry vesuvianites are almost occupied by oxygen and hydroxyl associated with hydrogen bonding.

6. Boron-bearing vesuvianite (Wilui River)

Boron is a major constituent in a certain group of vesuvianite. Groat et al. (1992a) showed that B is occurred more common in vesuvianite than hitherto recognition. Boron has a major effect on the overall compositional variation of vesuvianite.

The significant difference between boron-bearing and boron-free vesuvianite is observed in the optical properties. It is well-known that boron-bearing vesuvianite is optically positive, whereas boron-free vesuvianite is negative. Oftedal (1964) found that vesuvianites with less than 0.5 % B_2O_3 were optically negative whereas those with more than 1 % B_2O_3 were optically positive and the fact was also confirmed by Serdyuchenko et al. (1968).

The boron-bearing vesuvianite examined in this study is from Wilui River, Siberia. This is a typical locality of boron-bearing vesuvianite. The byname "Wiluite" was described in this locality. The specimen examined in this study is a typical specimen

having whole characters of boron-bearing vesuvianite. Color of the crystal is black with naked eye. The crystal contains small inclusions of birefringent grossular as described in Rock Forming Minerals (Deer et al., 1982).

In this study, the calculation of formula unit for boron-bearing vesuvianite is done based on 50 cations excluding B^{3+} (and H^{+}). However, Groat et al. (1992a) suggest that 50-cation normalization scheme for boron-bearing vesuvianite is not adequate, because details of the boron substitution in vesuvianite are not yet completely clarified. Moreover, the cation assignments in boron-bearing vesuvianite is significantly different from those of boron-free vesuvianite. The complete normalization scheme to determine the formula unit of boron-bearing vesuvianite is still remained to be established.

The chemical composition for boron-bearing vesuvianite shows that Mg content is larger than that of boron-free vesuvianite and that of Al is less than that of boron-free vesuvianite. The content of Mg and Al are 4.78 and 6.76 atom per formula unit, respectively. Boron content of vesuvianite also involves an increase in Mg and a decrease in Al. Groat et al. (1992a) examined the relationship between B and OH^{-} ($+F^{-}$) contents for both calculated and measured OH^{-} values, and found a negative correlation between B and OH^{-}, i.e. the ratio is approximately 1 (B) : 2 (H). They indicate that substitution (B^{3+} + Mg = 2H + Al) is the principal mechanism for the incorporation of B into vesuvianite. They also noticed that boron-bearing vesuvianite have less Si than the ideal value of 18.0 atom per formula unit observed in boron-free vesuvianite, and suggested that small amounts of substitution (B^{3+} + Al = 2H + Si) may occur.

The chemical analyses show that boron-bearing vesuvianite contain almost negligible Cl but a little amount of F. That is, in boron-bearing structure, there are no space for Cl to replace OH.

The present chemical analyses for boron-bearing vesuvianite completely follow the result of Groat et al. (1992a). In the present experiment, boron content is not determined. However, a chemical composition of vesuvianite from Wilui River is already given by

Groat et al. (1992a). Therefore, boron content of present Wilui River vesuvianite is estimated as that of Groat et al. (1992a) (see Table 1).

i. General Structure

The structural refinements of boron-bearing vesuvianites were already investigated by Groat et al. (1991). The cation assignments in boron-bearing vesuvianite must be significantly different from those in boron-free vesuvianite. As described by Groat et al. (1992a), boron-bearing vesuvianite has longer *a* and shorter *c* dimension than those of boron-free vesuvianite.

The difference Fourier maps of boron-bearing vesuvianite (Wilui River) show the existences of two additional cation sites (Bo(1) and Bo(2)) and an additional anion site (O(12)). The refinement was done assuming that Boron position is locate at centroid of the electron density peak in the Fourier map and O position is residual electron density. Finally, there are no prominent residual electron density in difference Fourier maps.

Bo(1) at the 8*h* position is tetrahedrally coordinated with two O(7) and two O(11), whereas anion coordination around Bo(2) is complex. Fig. 19 (left) shows atomic arrangement along the fourfold rotation axis of boron-bearing vesuvianite. There are 10 possible anion sites around the Bo(2) site (two O(10) and eight O(12) positions). These O(10) and O(12) are partly-occupancy sites. Two O(12) site are occupied in exchange for one O(10) site, and the O(12) site provides two of the three anions coordinating Bo(2). That is, Bo(2) at the 2*a* position is triangularly coordinated with one O(10) and two O(12) (Fig. 19; right). Bo(2)-O(10) distance is 1.419 Å and Bo(2)-O(12) is 1.265 Å. These assignments of atoms are correspond with the previous work by Groat et al. (1991).

If the Bo(2) site is fully occupied, the ideal occupancy ratio of O(10) and O(12) sites are 0.50 and 0.25, respectively. In the present refinement, the refined occupancy ratio suggest that the Bo(2) site is fully occupied by Boron. However, the refined occupancy ratio of O(10) and O(12) sites are 0.60 and 0.19, respectively. These discrepancies are interpreted as overlapping of electron densities of O(10) and O(12).

Groat et al. (1992a) indicated that the contents of boron is up to 4 atom per formula unit. Their calculation of the formula gives 2.57 boron per formula unit for their specimen from Wilui River. Their result shows that boron occupies a half of Bo(1) and Bo(2) sites of Wilui River vesuvianite. This value disagrees with the occupancies determined by the present structural analysis. That is, the analytically measured amounts of boron (Groat et al., 1992a) is not enough to fill up the capacity of Bo(1) and Bo(2) site. However, the refined occupancy ratio indicate that these sites are almost fully occupied by boron, i.e., the scattering power at these sites exceeds the expected values. This result suggests that some element other than boron should occupy in Boron positions.

Groat et al. (1992a) already noted such excess of the scattering power at the sites. They described that such excess indicates that the total number of cations (excluding B^{3+} and H^{+}) in boron-bearing vesuvianite exceeds 50 par formula unit. Consequently, a 50-cation normalization scheme for boron-bearing vesuvianite is not adequate.

Which of these sites is occupied by other element than boron? Bo(2) site can not be occupied by other element whereas Bo(1) site can be occupied by other element (probably Si or Al). If the adequate normalization scheme is adapted, therefore, the actual content of water should be less than that of calculated value based on 50 cation normarization.

Groat et al. (1991) observed a significant anion disorder around the Bo(1) site and also a split of O(7) site. In this study, a split of O(7) could not be recognized, although the temperature parameter of O(7) is greater than that of other oxygens. This result support that Bo(1) site is occupied by other cations than boron.

The valence sums for anions are calculated according to the method of Brown (1981). The value of bond strengths of O(1) through O(9) except O(7) of the Wilui River boron-bearing vesuvianite are almost 2.0 and indicate that these sites are occupied by oxygen ions. The selected valence sums are listed in Table 9. The valence sums of O(7) and O(11) oxygen which coordinate the Bo(1) site are 1.82 and 1.78, respectively. Although these values are slightly small for oxygen, but these sites are probably almost

occupied by oxygen. The valence sums of O(10) is exactly 2.00 when the B site is occupied indicating the coordination of O(10) to B cation. As considered above, the calculated value of bond-valence of O(10) site of vesuvianite is unusual. The valence sum of O(12) oxygen is 2.23. Taking into account of the uncertainty of O(12) position, the value can be accepted at the present state.

ii. Representation of polyhedra

Si(1), Si(2) and Si(3) tetrahedra

The measured amounts of SiO2 of boron-bearing vesuvianite is less than that of boron-free vesuvianites. The number of Si ion calculated with the 50 cation normalization scheme is less than ideal value of 18. It is not clear whether other cations substitute for Si ion at the Si sites, because the normalization scheme for boron-bearing vesuvianite is not clarified. If adequate normalization scheme are adopted to boron-bearing vesuvianite, this shortage will be solved. The volumes of tetrahedral sites of boron-bearing vesuvianite are almost same as that of boron-free vesuvianites.

Ca(1), Ca(2), Ca(3) and C polyhedra

The coordination polyhedra around Ca(1), Ca(2) and C are not so different from those of boron-free vesuvianite. The coordination polyhedron around Ca(2) is slightly larger than that of boron-free vesuvianite. The C-O(10) distance is 3.189 Å, and the value imply possible bonding of C cation to O(10).

Coordination polyhedron around Ca(3) cation in boron-bearing vesuvianite significantly differ from those of boron-free vesuvianite. The Ca(3)-O(7) distances are 2.450, 2.610 and 2.834 Å, and these values are longer than those of boron-free vesuvianites.

Additional O(12) produce a complex coordination for Ca(3) dodecahedron. Figure 20 shows the local configuration along the four-fold rotation axis of boron-bearing vesuvianite. It should be noted that two adjacent O(10) site are never occupied simultaneously, when the Bo(2) site is occupied. One O(10) is bond to four Ca(3). One

O(12) oxygen can bonded to three Ca(3) cation, and the respective bond distances are 2.250, 2.315 and 2.678 Å. As a result, two Ca(3) can bond to both O(10) and O(12), and the Ca(3) has ten-coordinate polyhedron. Ca(3)-O(10) distance is 2.616 Å and Ca(3)-O(12) distance is 2.678 Å. That is, the coordination polyhedron around Ca(3) have four possible types of forms (see Fig. 20 and Table 6). The Ca(3) polyhedra possibly has a flexibility to permit the complicated configuration of boron-bearing vesuvianite.

In a unit cell level, different configuration at O(10) and O(12) positions should be exist. Sixteen kinds of possible atomic arrangements exist in a unit cell. The ordering at O(10) and O(12) sites is also possible. If ordering at these sites occurs, the symmetry reduces towards lower than *P4/nnc*. However, Arem and Burnham (1969) reported that a evidence of lowering of symmetry than *P4/nnc* is not observed on the X-ray precession photograph of vesuvianite from Wilui River. This fact suggests that the ordering of O(12) positions is not occur even in short range. Therefore, the O(12) are statistically perfect random occupancy sites.

Although the configuration at O(12) positions must influence the local charge balances and atomic positions around O(12) positions, configuration at O(12) positions do not produce change of the configuration of O(12) positions of neighboring fourfold axis. That is, the indirect interaction led from scheme of occupancy at O(12) position is not communicated to long range. This is probably caused by the flexibility of Ca(3) polyhedron of vesuvianite.

B polyhedra

The B site cation is coordinated by four O(6) and one O(10). Because of long cation-anion distance of 3.185 Å, O(12) can not be bonded to B cation.

A and AlFe octahedra

The size of A site (mean inter-atomic distance is 1.932 Å) is greater than those of boron-free vesuvianite (Fig. 8). This fact indicate Mg occupancy at the A site. In

addition, the size of AlFe site (2.014 Å) is also greater than those of boron-free vesuvianite.

7. Chichibu vesuvianite

The reflection characteristics of Chichibu vesuvianite show certainly high-symmetry of the crystal. Whereas, the chemical composition of Chichibu vesuvianite is closely similar to the three low-symmetry vesuvianite, i.e., the specimen contains negligible amount of F and Cl.

In Chichibu vesuvianite, O(10) is occupied almost entirely by O because the chemical analyses show little F and Cl (Table 1). In the electron density maps, the shape of O(10) in Chichibu vesuvianite is less anomalous than those of the other high-symmetry vesuvianites. In the electron density map, a high electron density region between both O(10) positions is recognized. Another high density region is also recognized at 8*h* position. These locations of high density peaks are consist with boron position in boron-bearing vesuvianite. These positions are also situated near to hydrogen positions. However, the amount of electron density is far larger than that of hydrogen. It could not be considered that Chichibu vesuvianite contain considerable amount of boron.

The further refinement is done assuming that these positions are occupied by boron. Then, the *R* index is improved from 6.0% to 4.2%. The refined occupancy ratio shows that these two sites, Bo(1) and Bo(2), are 67% and 73% occupied by boron, respectively. In contrast with Wilui River boron-bearing vesuvianite, an electron density peak for O(12) position is not found, and refined occupancy ratio for O(10) site shows that the O(10) site is almost fully occupied by oxygen. These fact indicate an unthinkable situation that Bo(2) site is two coordinate.

Except for the existence of higher electron density regions, the crystal structure of Chichibu vesuvianite is almost similar to that of boron-free vesuvianite. In addition, *a* and *c* dimensions of Chichibu vesuvianite are also to those of boron-free vesuvianite, and contents of Mg is not so different from those of boron-free vesuvianite. Therefore, it is

difficult to consider that Chichibu vesuvianite is joined the sort of boron-bearing vesuvianite.

The detailed true character of the high electron densities located at Bo(1) and Bo(2) position is not clear. Because the O(10)-O(10) distance of 2.737 Å is suitable for hydrogen bond, only a hydrogen atom may present between two O(10) oxygens. Thus, indeed the high electron densities may be ascribed to some sort of 'ghost' resulted from an experimental uncertainties and remained to be clarified.

8. Role of O(10) for the cation ordering

A clear explanation for cation and vacancy ordering at B and C positions could not be obtained at the present state. However, cation and vacancy ordering will be considered based on a supposing model of Allen and Burnham (1992).

Allen and Burnham (1992) tried to clarify the detailed difference between high and low-symmetry vesuvianite. They explained that the ordering in low-symmetry vesuvianite presumably takes place during crystal growth rather than by an ordering transformation on cooling. Ordering of cation and vacancy sequences satisfies the local charge balance on the two adjacent O(10) positions, i.e. the charge distribution of two adjacent O(10) positions is the governing factor in the formation process of the cation ordering structure. How does charge balance of two adjacent O(10) oxygen pair effect on the sequence of B and C cation? If whole two adjacent O(10) positions are occupied only by one oxygen and one hydroxyl, the unsymmetrical charge distribution on the O(10) oxygen pair gives the impetus for the ordering of cations along the fourfold axis. This impetus in turn affects the next O(10) pair through B and C cations resulting regular ordered cation sequence along the fourfold axis.

The satisfaction of the local charge balance on O(10) ions requires alternate occupancy of oxygen and hydroxyl with an associated hydrogen bond and ordering sequences of cations. In high-symmetry vesuvianite, the local charge balance on the two O(10) pair will be broken because the sequences vary along the fourfold axis.

Considering the chemical composition of high-symmetry vesuvianite, Cl and F ions preferentially occupy the O(10) site. This kind of substitution is not found in low-symmetry vesuvianite. The Cl and F-bearing high-symmetry Obira vesuvianite shows that O(10)A anion is bonded to C cation, and the Cl ion in the other O(10)B position is not bonded to neither B nor C cation. Whichever the cations of B or C is the neighboring cation of the O(10) pair, the situation is possible. Thus, the sequence of ordered cations and vacancies along the fourfold axes are interrupted yielding the disorder.

The chemical compositions of high-symmetry vesuvianites are more variable than those of low-symmetry vesuvianites. Certain high-symmetry vesuvianites do not contain appreciable amounts of fluorine and chlorine ions. In high-symmetry vesuvianite containing very low F and Cl, the fact how the local charge balance of O(10) oxygen are satisfied will be important under the condition of varying string sequences along c. Further investigation on the local atomic configurations and local charge balances along the fourfold rotation axis of high-symmetry vesuvianite will give a significant further information.

IV. CONCLUSION

In this paper, some significant new data on the crystal chemistry and structure of vesuvianite were presented and possible structural variations in vesuvianite were described in detail. The following three chemical formulae were established for the investigated vesuvianite;

High-symmetry vesuvianite

$2[Ca_{19}(Al, Mg, Mn, Fe, Cu)(AL, Mg, Ti, Mn, Fe)_8Al_4(OH, F)_8(O, OH, F, Cl)_2(SiO_4)_{10}(Si_2O_7)_4]$.

Low-symmetry vesuvianite

$2[Ca_{19}(Al, Fe)(AL, Mg, Ti, Mn, Fe)_8Al_4(OH, F)_8(O, OH)_2(SiO_4)_{10}(Si_2O_7)_4]$.

Boron-bearing vesuvianite

$2[Ca_{19}(Al, Fe)(AL, Mg, Ti, Mn, Fe)_8Al_4(B, ?)_{1\text{-}5}(OH, F)_8O_3(SiO_4)_{10}(Si_2O_7)_4]$.

The symmetry of vesuvianite depends largely on the cation-vacancy ordering in B and C sites along the fourfold rotation axis. When long-range disorder of cation and vacancy in B and C sites is present, the crystal shows average symmetry of *P*4/*nnc*. However, short-range order does exist in a unit cell level, because the B and C sites are alternately occupied by cations. "Single crystal" of low-symmetry vesuvianite in nature always consists of domains having ordered structure. Such domain should be regarded as true single crystal, but it is almost impossible to isolate such small domain.

The ordering scheme of *P*4*nc* structure is firstly confirmed. Thus the two possible ordering schemes in vesuvianite are confirmed, i.e. one is *P*4*nc* and the other *P*4/*n*, and only the latter has been described in the previous literature. The local configuration along the fourfold rotation axis is almost identical between *P*4*nc* and *P*4/*n* structure. However, a problem are remained to be solved. That is the bond-valence of O(10) oxygens obtained in this study is not perfectly satisfied with atomic arrangement of present

interpretation. In relation to this, the governing factor of cation ordering is the attainment of local charge balance on the O(10). However, the adequate elucidation of the mechanism of cation-vacancy ordering and positional ordering around the four-fold rotation axis are also remained to be solved. These problems will not be solved until complete understanding of the vesuvianite structure.

Cl^- ion preferentially occupies the O(10) site in certain high-symmetry vesuvianite. This fact imply that the chemical composition is one of the possible factor of disordering of cation and vacancy. Indeed, chemical variation of the mineral with high-symmetry is rather variable as was described in this paper. Fluorine and/or chlorine in vesuvianite structure affect the atomic configuration especially along the fourfold rotation axis. Therefore, to clarify the role of these anions especially during crystal growth will be further problem. The disordering transformation from low-symmetry vesuvianite to high-symmetry vesuvianite has not been confirmed neither in nature nor in laboratory. As was already pointed out by Allen and Burnham (1992), heating experiments of long duration more than several months will give us significant information.

In boron-bearing vesuvianite, boron occupies the 2*a* and 8*h* position which are vacant in boron-free vesuvianite. In the former structure, two oxygens, O(12) are present instead of one O(10) oxygen. The atomic configuration of boron-bearing vesuvianite is quite different from that of boron-free vesuvianite. Therefore, boron-bearing vesuvianite should be treated separately from boron-free vesuvianite from the view point of crystal configuration. The investigation of crystal chemistry and structure of boron-bearing vesuvianite is now just started.

References

Allen, F.M. (1985) Structural and Chemical Variations in Vesuvianite. Ph.D. Thesis, Harvard Univ., Cambridge, Massachusetts.

Allen, F.M. and Burnham, C.W. (1983) Cation ordering in low-symmetry vesuvianite. *Geol. Soc. Am., Abstr. Programs*, **15**, 513.

Allen, F.M. and Burnham, C.W. (1992) A comprehensive structure-model for vesuvianite: Symmetry variations and crystal growth. *Can. Mineral.*, **30**, 1-18.

Arem, J.E. and Burnham, C.W. (1969) Structural variations in idocrase. *Am. Mineral.*, **54**, 1546-1550.

Barth, T.F.W. (1963) Contributions to the mineralogy of Norway. 22. Vesuvianite from Kristiansand; other occurrences in Norway; the general formula of vesuvianite. *Norsk Geol. Tidsskr.*, **43**, 457-472.

Brown, I.D. (1981) The bond-valence method: an empirical approach to chemical structure and bonding. *Structure and Bonding in Crystals*, Vol.II (M. O'Keeffe and A. Navrotsky, eds.). Academic Press, New York.

Coda, A., Della Giusta, A., Isetti, G. and Mazzi, F. (1970) On the crystal structure of vesuvianite. *Atti Accad. Sci. Torino*, **105**, 63-84.

Deer, W.A., Howie, R.A., and Zussman, J. (1982) *Rock-forming Minerals, orthosilicates*. Longman Group, London.

Finger, L.W. (1969) Determination of cation distribution by least-squares refinement of single-crystal X-ray data. *Carnegie Institution Year Book*, **67**, 216-217.

Fitzgerald, S., Leavens, P.B., Rheingold, A.L., and Nelen, J.A. (1987) Crystal structure of a REE-bearing vesuvianite from San Benito County, California. *Am. Mineral.*, **72**, 625-628.

Fitzgerald, S., Rheingold, A.L. and Leavens, P.B. (1986a) Crystal structure of a Cu-bearing vesuvianite. *Am. Mineral.*, **71**, 1011-1014.

Fitzgerald, S., Rheingold, A.L. and Leavens, P.B. (1986b) Crystal structure of a non-*P4/nnc* vesuvianite from Asbestos, Quebec. *Am. Mineral.*, **71**, 1483-1488.

Giuseppetti, G., and Mazzi, F. (1983) The crystal structure of a vesuvianite with *P4/n* symmetry. *Tschermaks Mineral. Petrogr. Mitt.*, **31**, 277-288.

Groat, L.A., Hawthorne, F.C. and Ercit, T.S. (1992a) The chemistry of vesuvianite. *Can. Mineral.*, **30**, 19-48.

Groat, L.A., Hawthorne, F.C. and Ercit, T.S. (1992b) The role of fluorine in vesuvianite: a crystal-structure study. *Can. Mineral.*, **30**, 1065-1075.

Groat, L.A., Hawthorne, F.C., Ercit, T.S. and Putnis, A. (1993) The symmetry of vesuvianite. *Can. Mineral.*, **31**, (in press).

Groat, L.A., Lager, G.A., Hawthorne, F.C., Rossman, G.R., and Schultz, A.J. (1991) Hydrogen in boron-bearing vesuvianite. *Eos Trans. AGU*, **72**, 143 (abstr.).

Hoisch, T.D. (1985) The solid solution chemistry of vesuvianite. *Contrib. Mineral. Petrol.*, **89**, 205-214.

Ibers, J.A., and Hamilton, W.C., Eds. (1974) *International Tables for X-ray Crystallography*, Vol. IV, P. 71-147. Kynoch Press, Birmingham, England.

Ito, J., and Arem, J.E. (1970) Idocrase: synthesis, phase relations and crystal chemistry. *Am. Mineral.*, **55**, 880-912.

Lager, G.A., Xie, Q., Ross, F.K., Rossman, G.R., Armbruster, T., Rotella, F.J. and Schultz, A.J. (1989) Crystal structure of a *P4/nnc* vesuvianite from Tanzania, Africa. *Geol. Soc. Am., Abstr. Programs*, **21**, A120.

Machatschki, F. (1932) Zur Formel des Vesuvian. *Z. Kristallogr.*, **81**, 148-152.

Maeda, H. (1987) Accurate bond length determination by EXAFS method. *J. Phys. Soc. Jpn.*, **56**, 2777-2787.

Neumann, H. and Svinndal, S. (1955) The cyprine-thulite deposit at Ovstebo near Kleppan in Sauland, Telemark. *Norsk Geol. Tidsskr.*, **34**, 139-156.

Oftedal, I. (1964) Contributions to the mineralogy of Norway. 29. Vesuvianite as a host mineral for boron. *Norsk Geol. Tidsskr.*, **44**, 377-383.

Ohkawa, M., Yoshiasa, A. and Takeno, S., (1992) Crystal chemistry of vesuvianite: Site preferences of square-pyramidal coordinated sites. *Am. Mineral.*, **77**, 945-953.

Rucklidge, J.C., Kocman, V., Whitlow, S.H. and Gabe, E.J. (1975) The crystal structures of three Canadian vesuvianites. *Can. Mineral.*, **13**, 15-21.

Serdyuchenko, D.P., Gubaydulin, F.G., Pavlov, V.A. and Sundakova, I.Y. (1968) Idocrases from skarns in central Asia and their chemical composition. *Doklady Akad. Sci. USSR, Earth Sci. Sect.*, **180**, 135-137.

Shannon, R.D. (1976) Revised effective ionic radii and systematic studies of interatomic distances in halides and chalcogenides. *Acta Crystallogr.*, **A32**, 751-767.

Teo, Boon-Keng and Lee, P.A. (1979) Ab initio calculations of amplitude and phase functions for extended X-ray absorption fine structure spectroscopy. *J. Am. Chem. Soc.*, **101**, 2815-2832.

Valley, J.W., Peacor, D.R., Bowman, J.R., Essene, E.J. and Allard, M.J. (1985) Crystal chemistry of a Mg-vesuvianite and implications of phase equilibria in the system CaO-MgO-Al_2O_3-SiO_2-H_2O-CO_2. *J. Metamorph. Geol.*, **3**, 137-153.

Veblen, D.R., and Wiechmann, M.J. (1991) Domain structure of low-symmetry vesuvianite from Crestmore, California. *Am. Mineral.*, **76**, 397-404.

Warren, B.E. and Modell, D.I. (1931) The structure of vesuvianite $Ca_{10}Al_4(Mg,Fe)_2Si_9O_{34}(OH)_4$. *Z. Kristallogr.*, **78**, 422-432.

Yoshiasa, A., and Matsumoto, T. (1986) The crystal structure of vesuvianite from Nakatatsu mine: Reinvestigation of the cation site-populations and of the hydroxyl groups. *Mineral. J.*, **13**, 1-12.

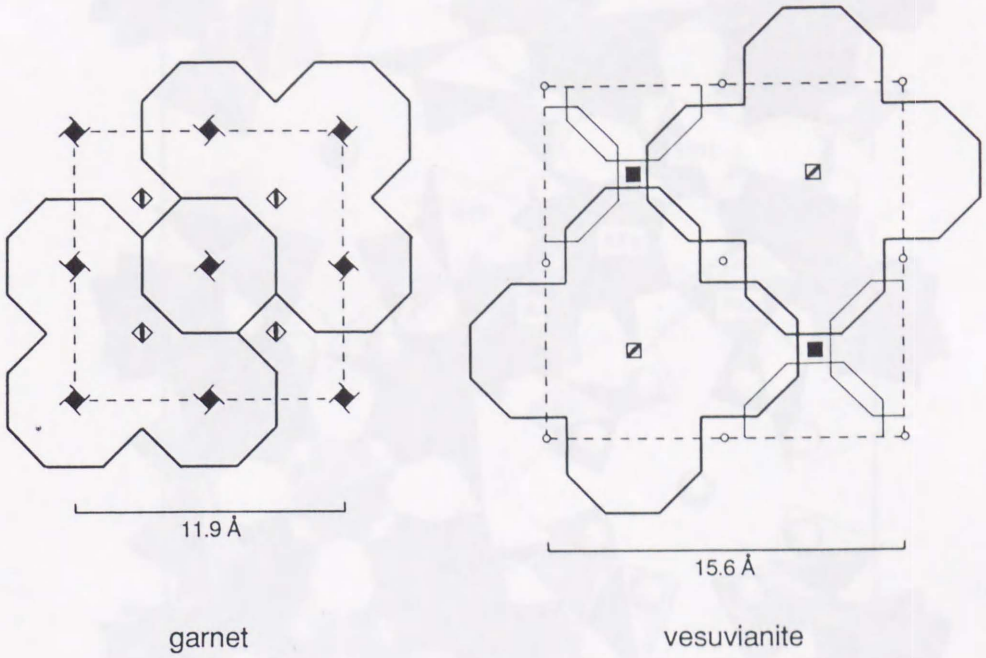

Fig. 1. Relation between the grossular garnet and vesuvianite structures (schematic). The columns perpendicular to this plane around four-fold inversion axis of the two minerals are identical.

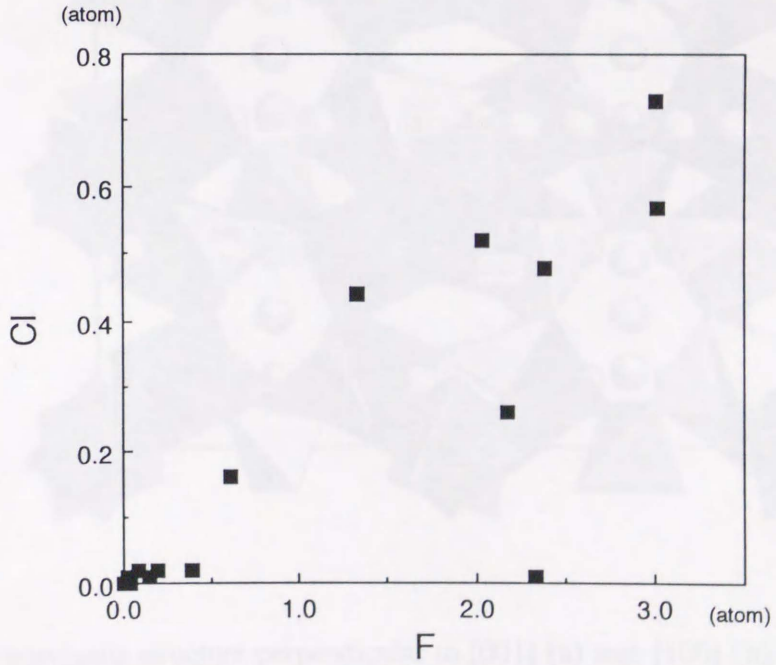

Fig. 2. Relation between F and Cl contents (atom per formula unit).

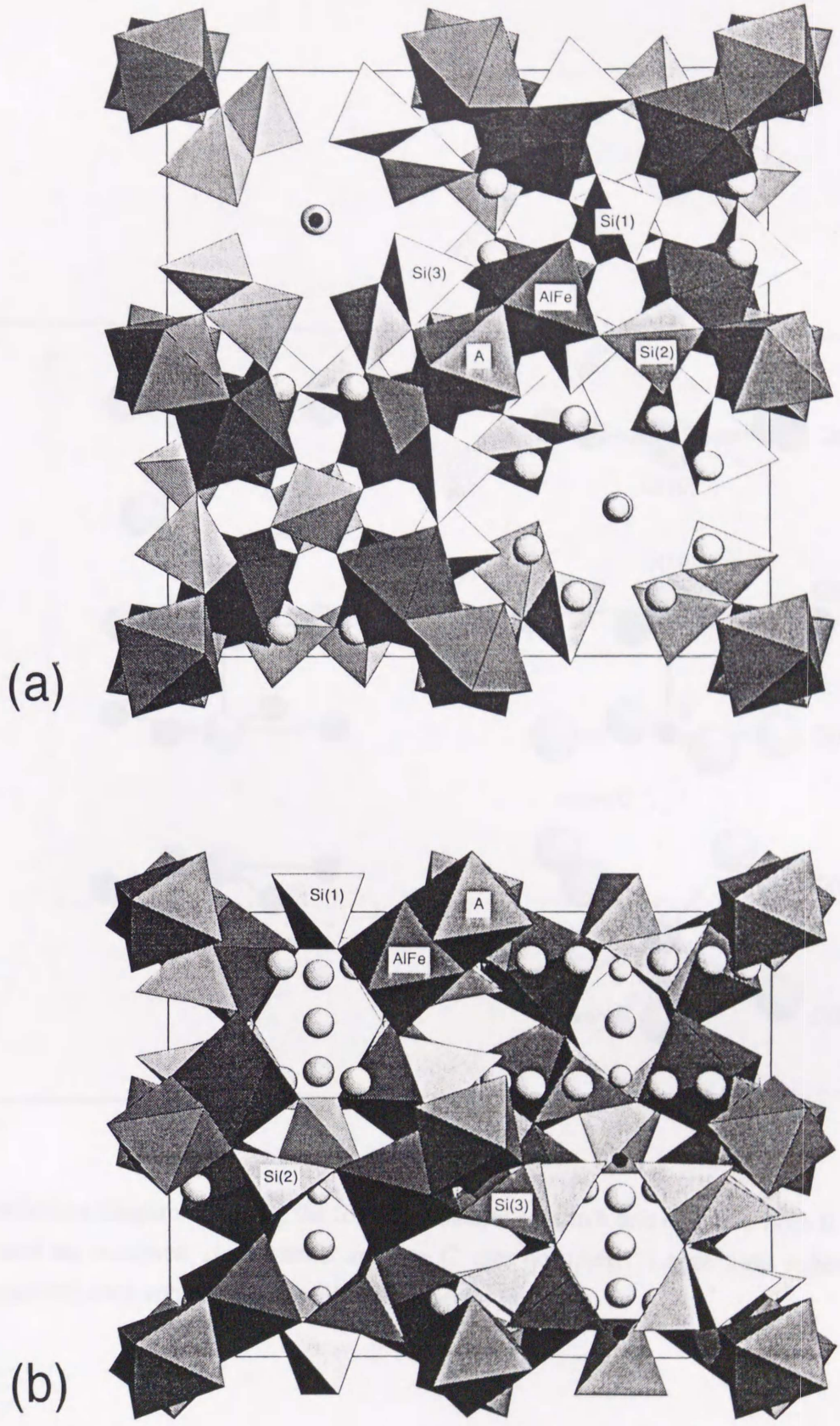

Fig. 3. Vesuvianite structure perpendicular to [001] (a) and [100] (b). The linkage of tetrahedra (light) and octahedra (dark) are illustrated. Large light spheres represent the Ca(1), Ca(2), Ca(3) and C cations. Medium light and small dark spheres represent the O(10) and B ions, respectively.

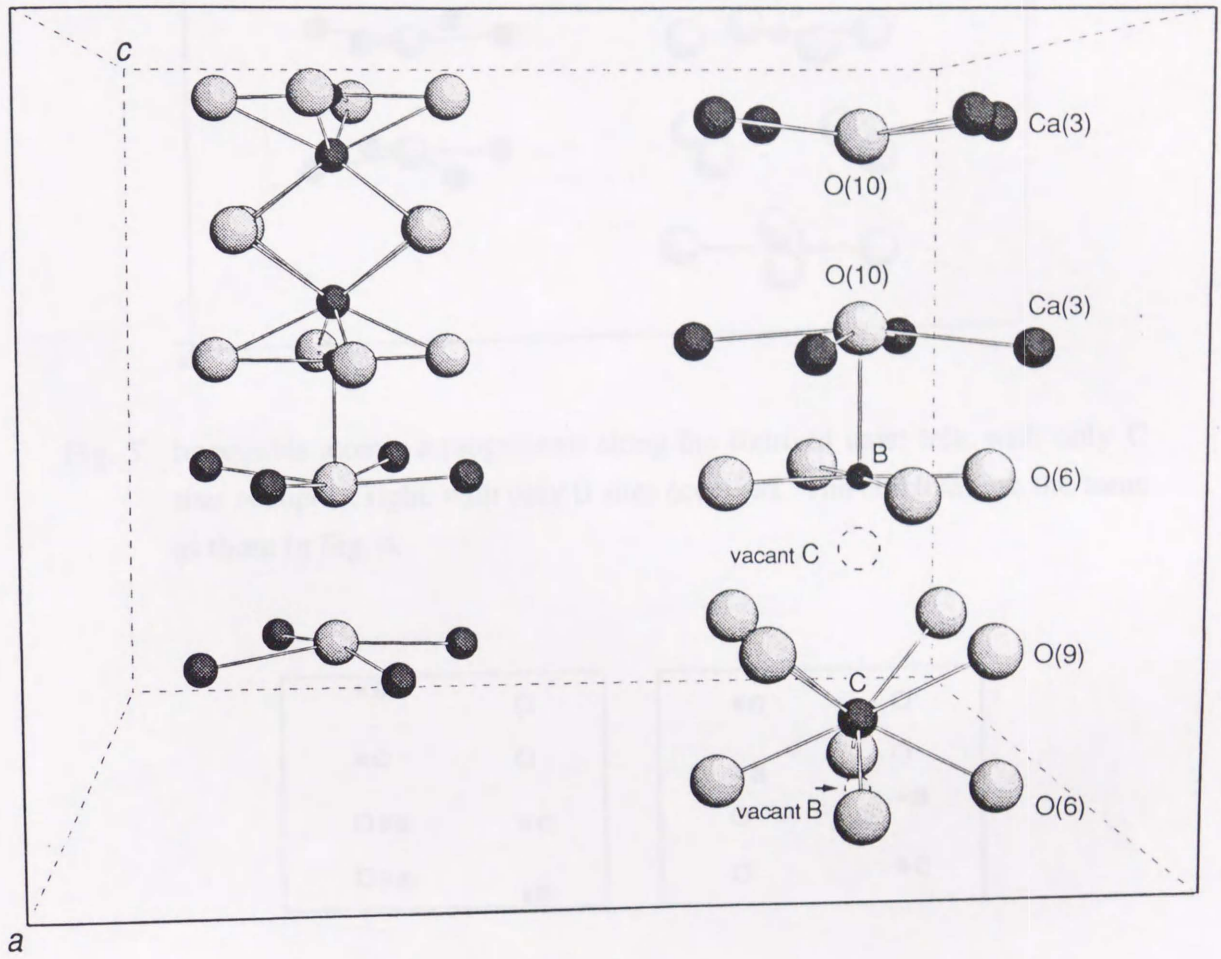

Fig. 4. Atomic arrangements along the fourfold rotation axes in a unit cell; left: both B and C sites are occupied; right: one B and one C sites occupied. Large light spheres: O, medium dark spheres: Ca, small dark spheres: Fe.

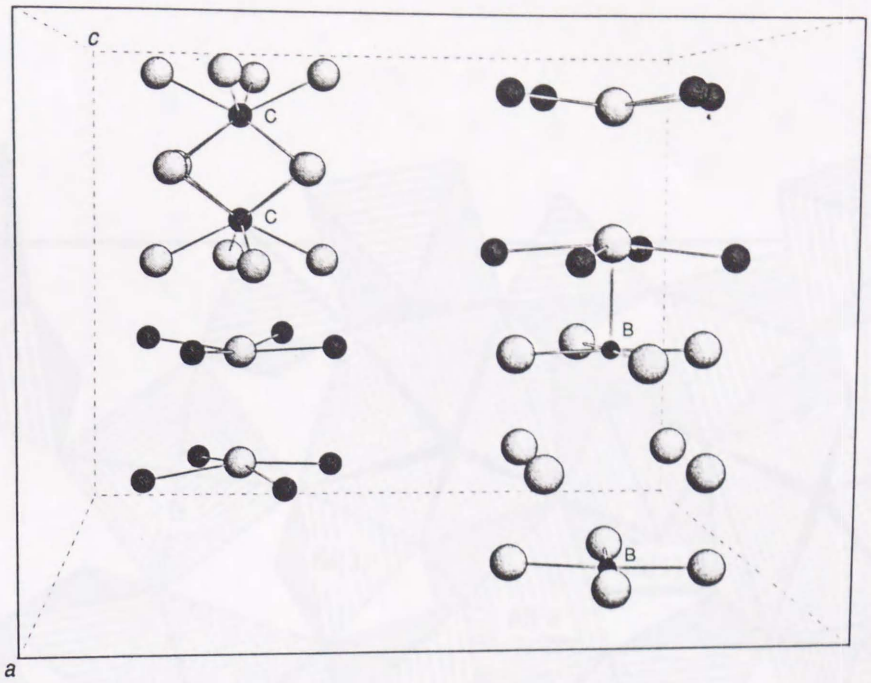

Fig. 5. Impossible atomic arrangements along the fourfold axis; left: with only C sites occupied; right: with only B sites occupied. The emblems are the same as those in Fig. 4.

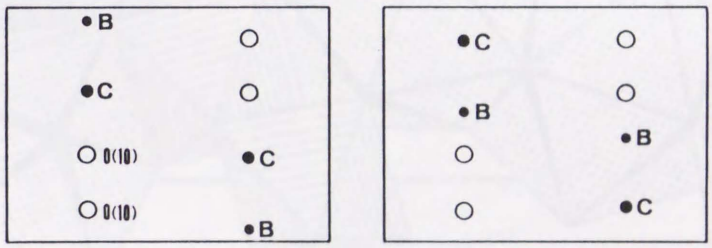

P4/n

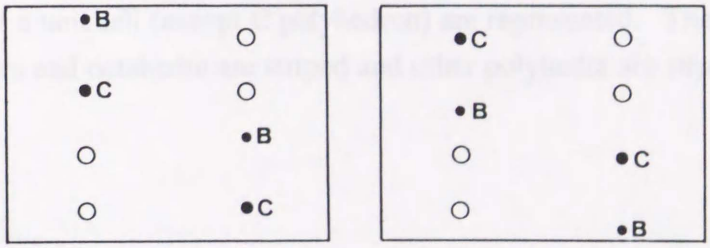

P4nc

Fig. 6. The four possible ordered arrangements of B and C sites along the four-fold rotation axes.

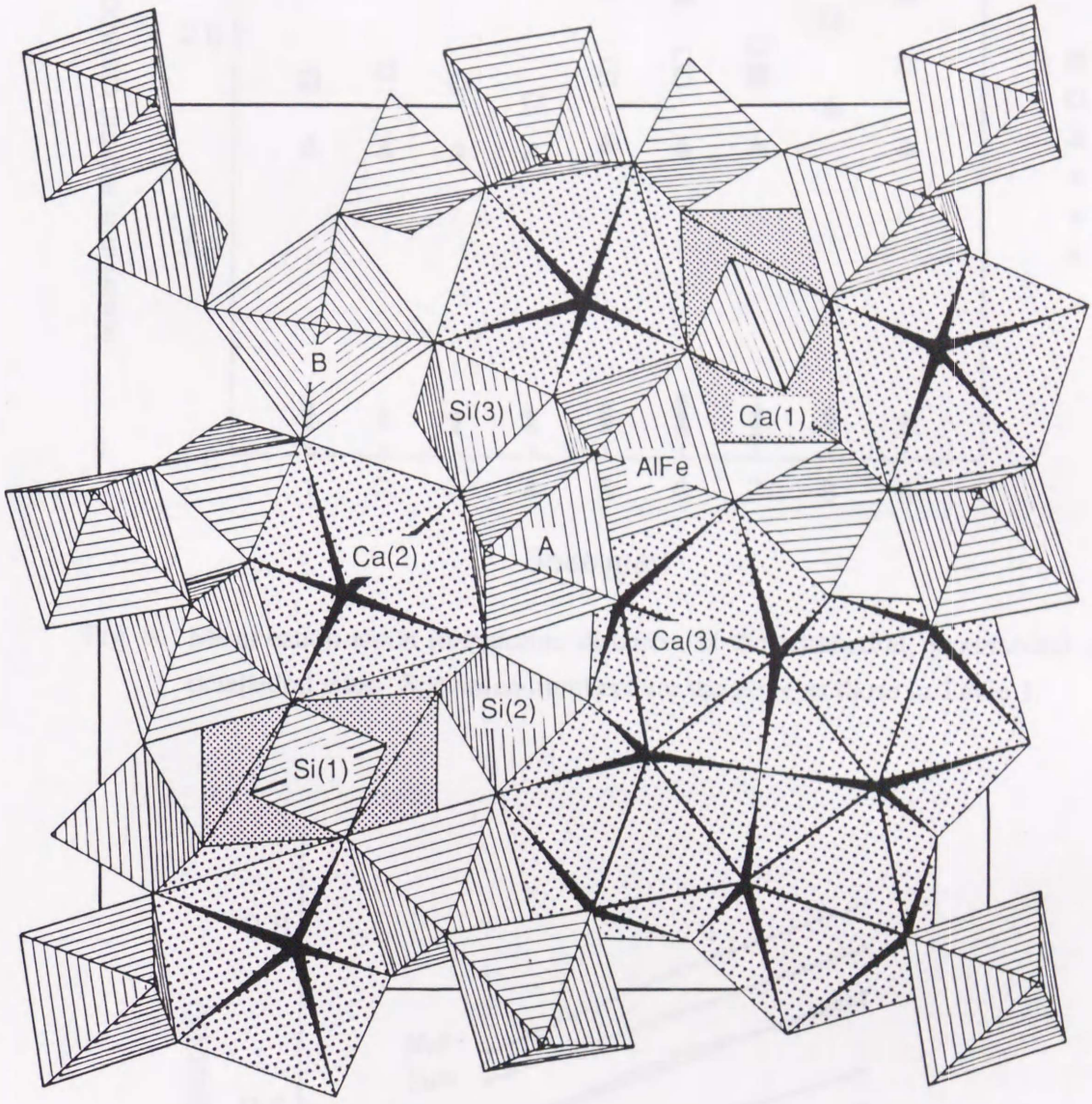

Fig. 7. A section of the vesuvianite structure perpendicular to [001]. Polyhedra in a quarter of a unit cell (except C polyhedron) are represented. The tetrahedra, pentahedra and octahedra are striped and other polyhedra are stippled.

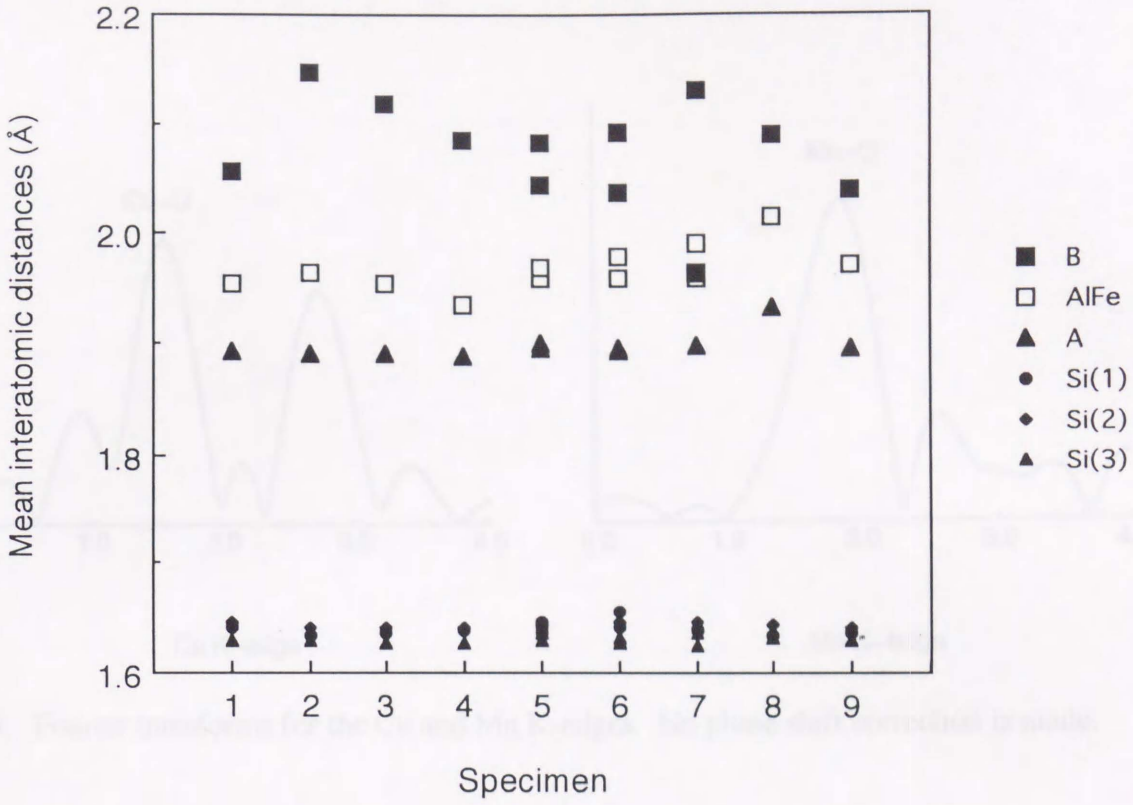

Fig. 8. Mean cation-anion interatomic distances of the tetrahedral, pentahedral and octahedral sites. Specimen numbers are the same as those in Table 1.

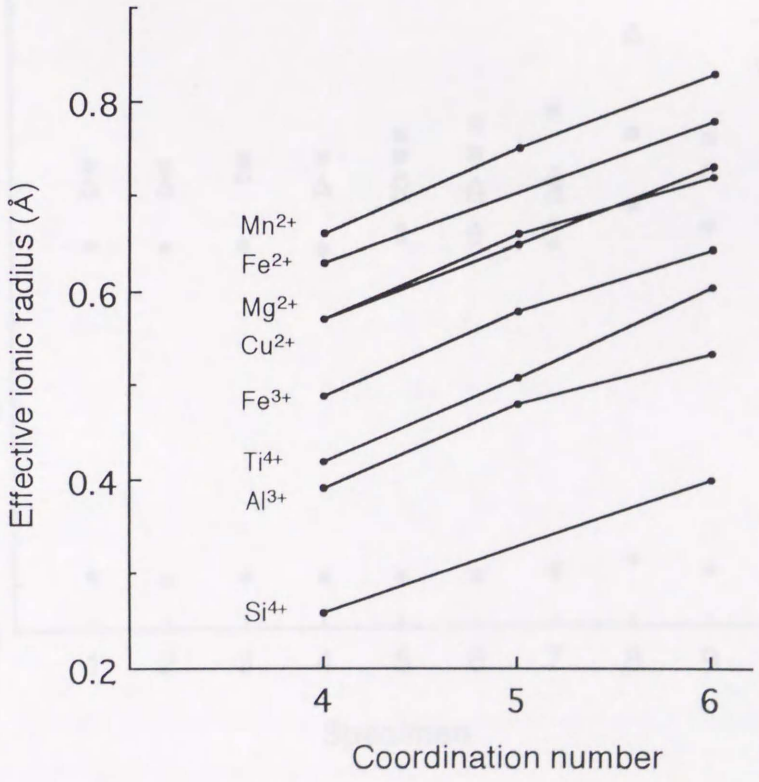

Fig. 9. Effective ionic radius (Shannon, 1976) versus coordination number.

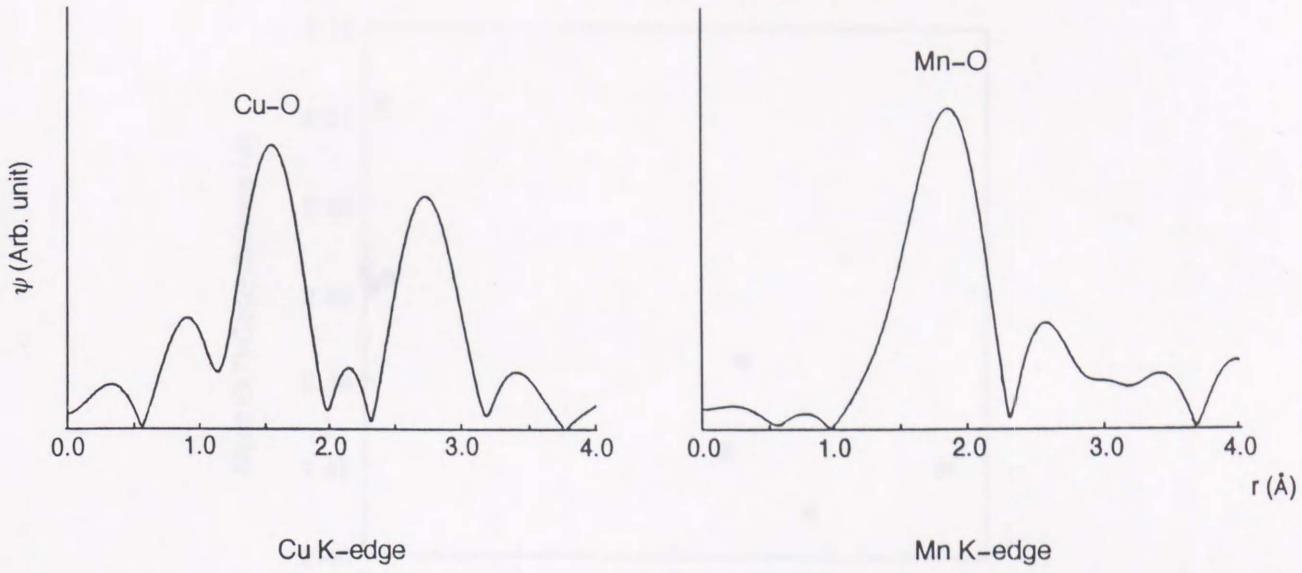

Fig. 10. Fourier transforms for the Cu and Mn K-edges. No phase shift correction is made.

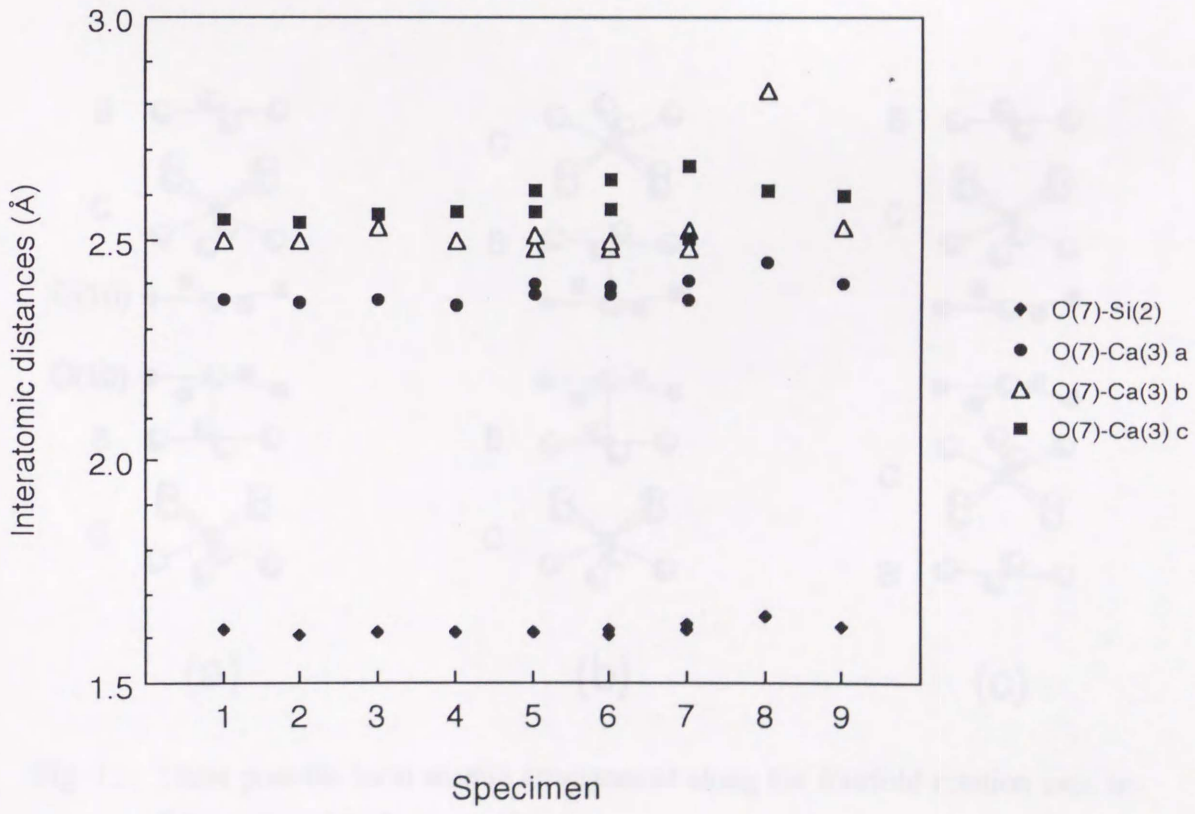

Fig. 11. Variation in O(7)-Si(2) and O(7)-Ca(3) bond lengths. Specimen numbers are the same as those in Table 1.

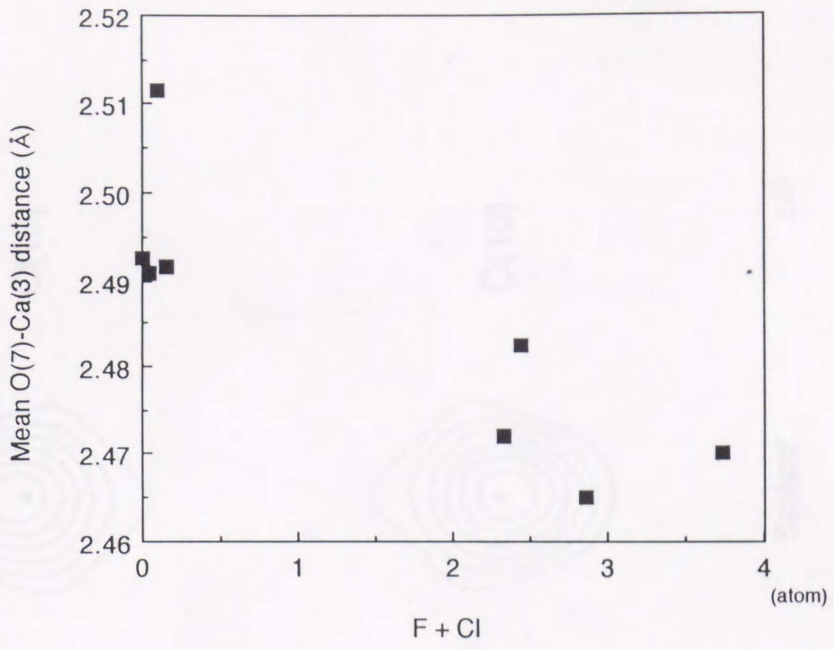

Fig. 12. Mean O(7)-Ca(3) interatomic distance versus F + Cl content (atom per formula unit). Specimen 8 is not shown.

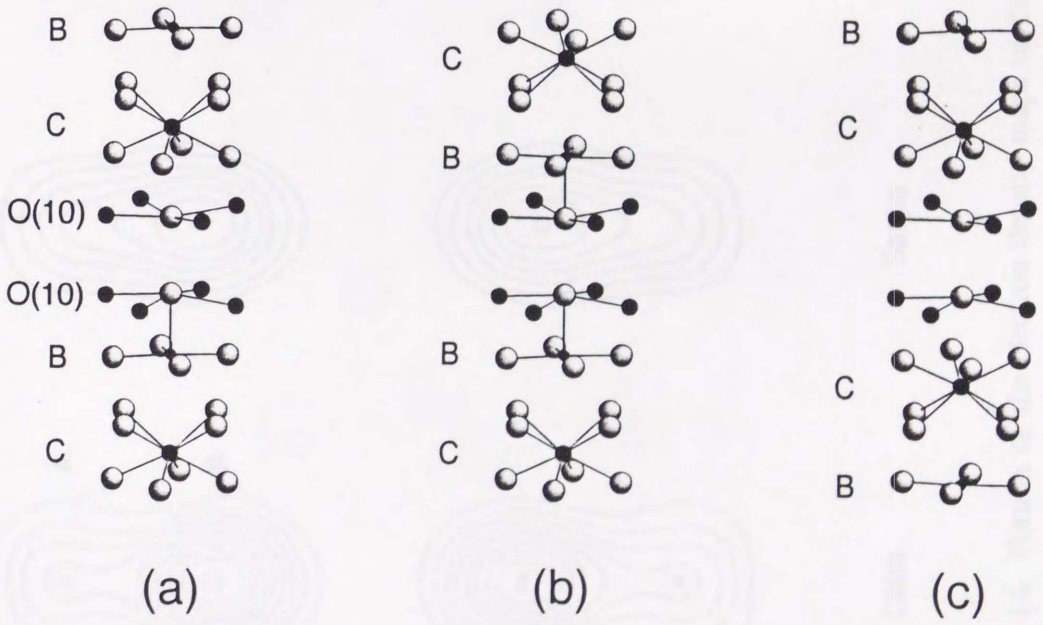

Fig. 13. Three possible local atomic arrangement along the fourfold rotation axis in P4/nnc disordered vesuvianite.

Fig. 14. Portion of the electron density maps of the four high-symmetry vesuvianites (Obira, Sanpo, Jinmu and Sauland) in the plane passing the O(10) ions. The refined positions of these sites are indicated by triangles. Contour starts from 2.5 $e/Å^3$ with interval of 2.5 $e/Å^3$.

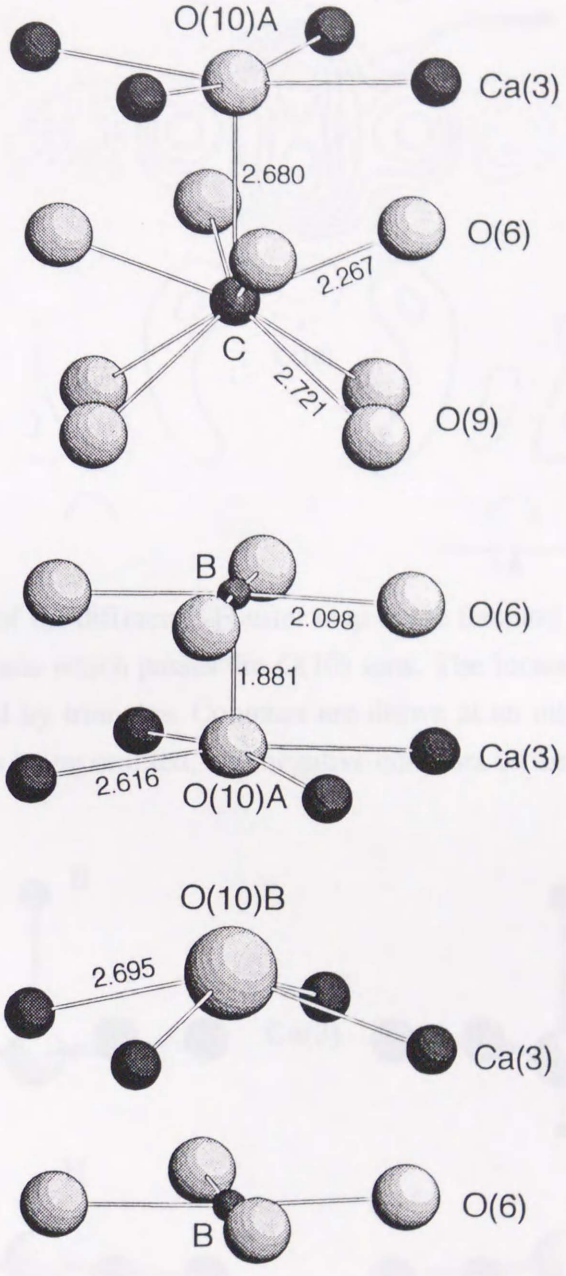

Fig. 15. Atomic arrangements along the fourfold rotation axes of Obira Cl-bearing vesuvianite together with bond lengths.

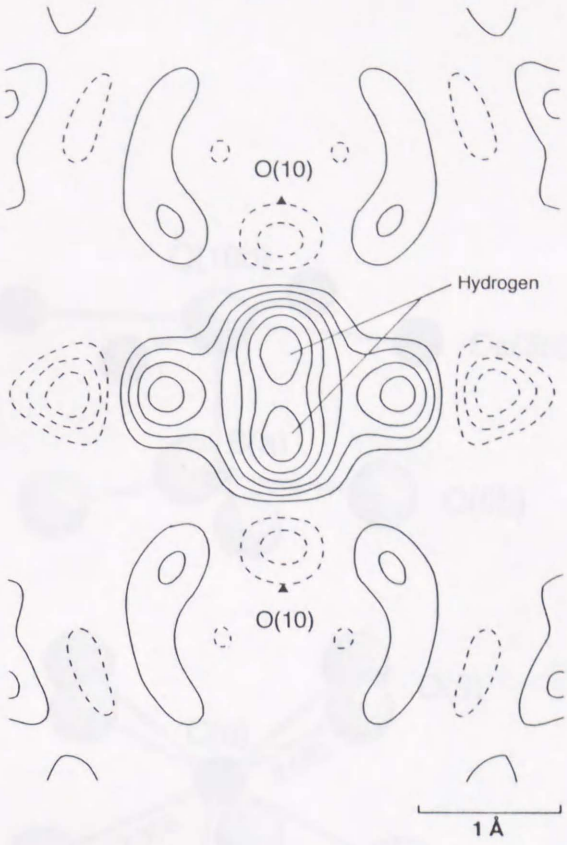

Fig. 16. Portion of the difference Fourier map of the Sauland Cu-bearing vesuvianite in the plane which passes the O(10) ions. The location of the O(10) sites is indicated by triangles. Contours are drawn at an interval of 0.1 $e/Å^3$, zero contours being omitted, and negative contours broken.

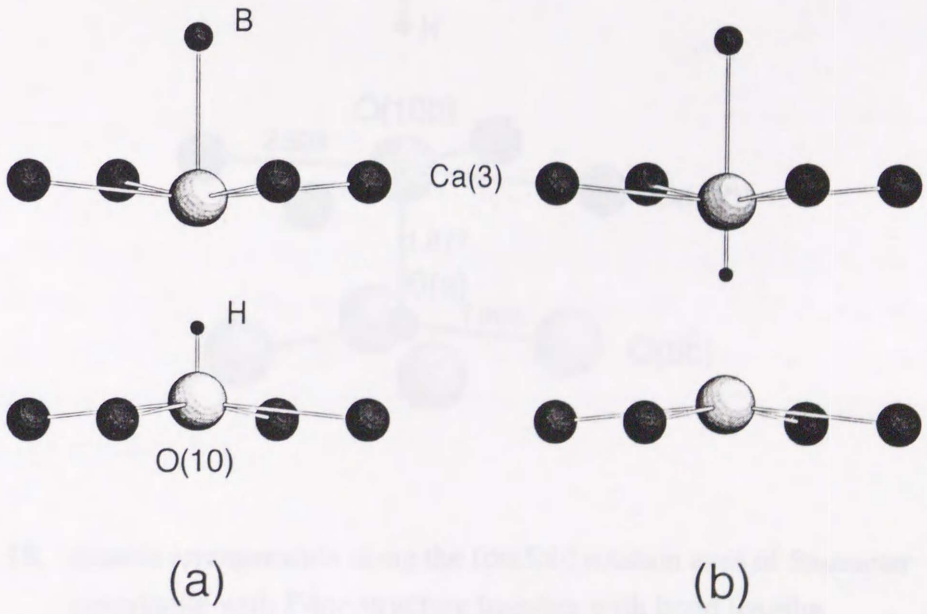

Fig. 17. Two possible local hydrogen configurations around O(10). (a) hydroxyl is not bonded to B site, and (b) hydroxyl is bonded to B site (see text).

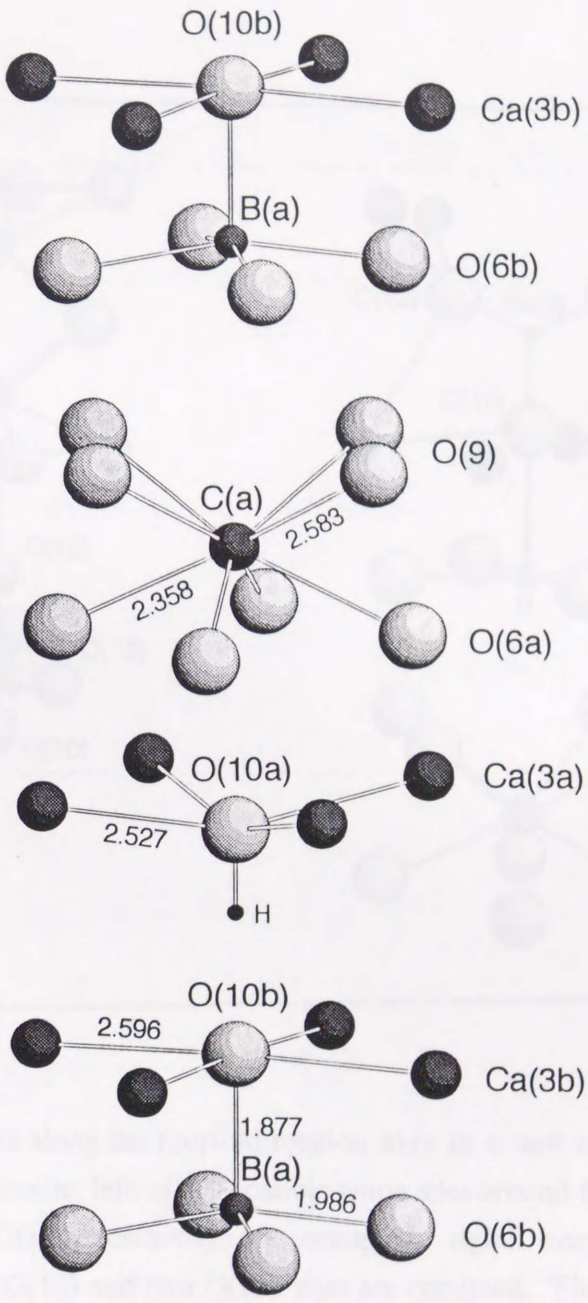

Fig. 18. Atomic arrangements along the fourfold rotation axes of Saueseter vesuvianite with *P4nc* structure together with bond lengths.

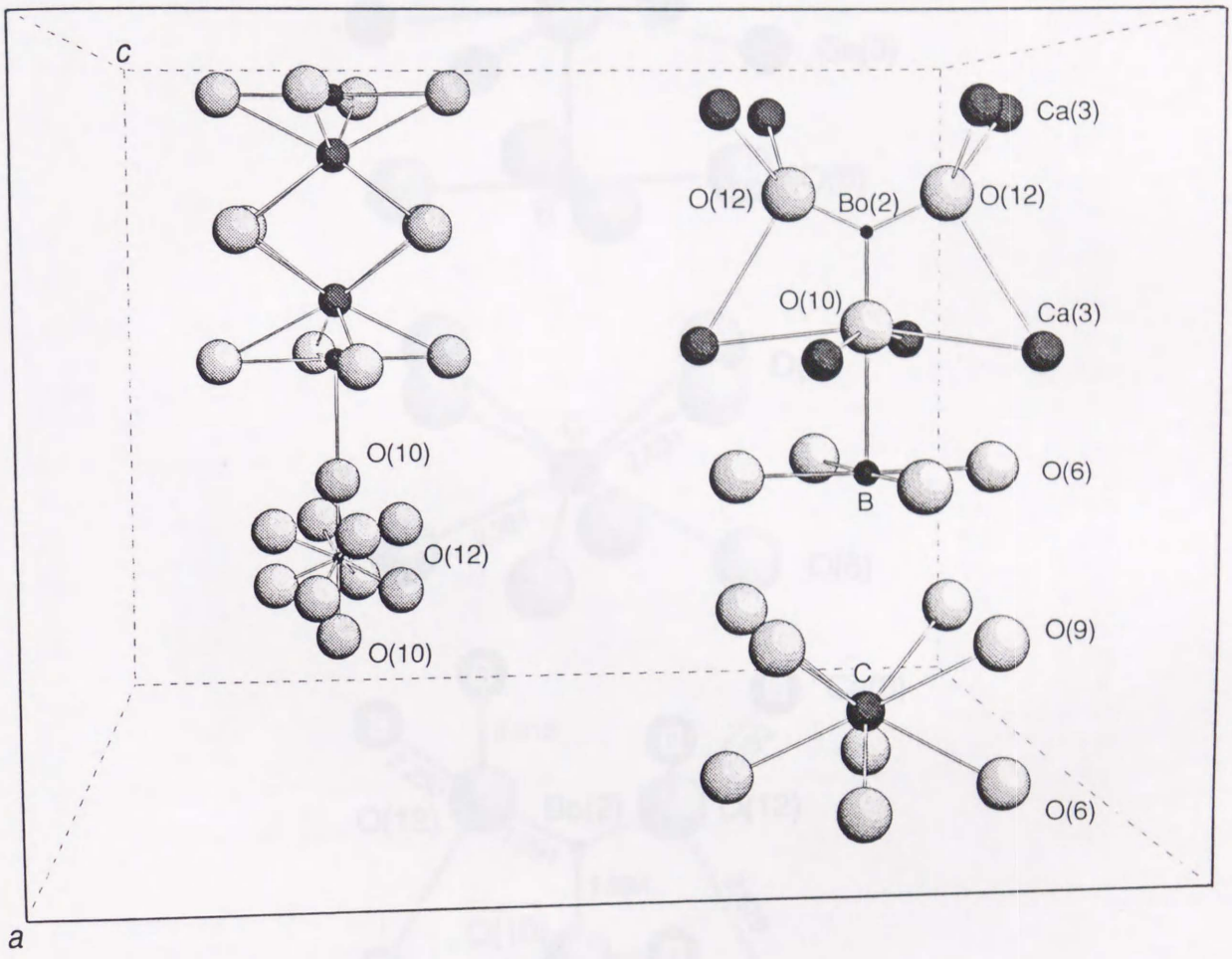

Fig. 19. Atomic arrangements along the fourfold rotation axes in a unit cell of Wilui River boron-bearing vesuvianite; left: all 10 possible anion sites around the Bo(2) site (two O(10) and eight O(12) positions) are occupied; right: one of the possible configurations, one O(10) and two O(12) sites are occupied. The emblems are the same as those in Fig. 4.

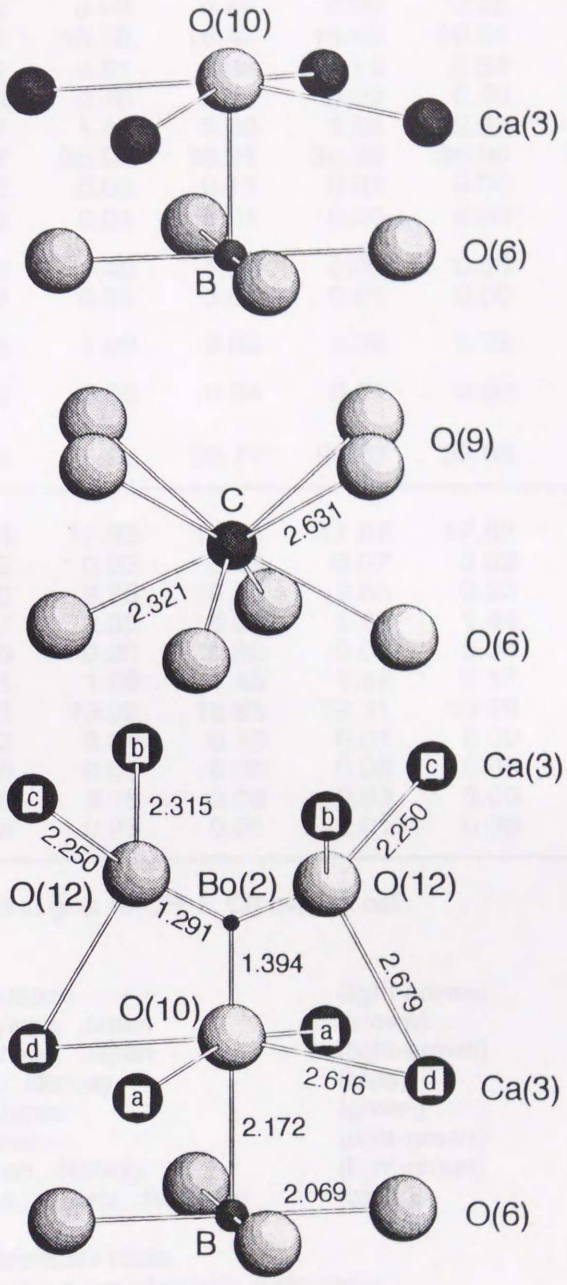

Fig. 20. Atomic arrangements along the fourfold rotation axes of Wilui River boron-bearing vesuvianite together with bond lengths. Letters in dark spheres (Ca(3)) such as a to d represent four different coordination of the sites (a to c are 9-fold, and d is 10-fold), respectively.

Table 1. Microprobe analyses for the vesuvianite samples

	1	2	3	4	5	6	7	8
SiO_2	36.20	35.96	36.14	37.04	36.67	36.52	36.35	35.50
TiO_2	0.37	2.22	0.08	0.24	0.20	0.05	0.48	1.39
Al_2O_3	16.52	15.21	16.78	18.47	16.62	16.04	15.42	11.65
FeO	5.66	4.01	4.91	0.86	3.14	3.52	3.36	3.24
MnO	0.15	0.20	0.48	0.73	0.09	0.10	0.01	0.05
MgO	1.05	1.77	1.48	2.00	2.58	2.99	3.15	6.52
CaO	35.51	35.97	35.98	36.31	36.98	36.90	36.61	36.20
Na_2O	0.01	0.02	0.05	0.11	0.01	0.00	0.00	0.01
K_2O	0.00	0.01	0.01	0.01	0.00	0.00	0.01	0.00
F	1.90	1.53	1.40	1.52	0.02	0.00	0.09	0.25
Cl	0.87	0.57	0.31	0.01	0.01	0.00	0.01	0.03
H_2O	1.59	1.85	1.99	2.04	2.76	2.76	2.70	0.61#
-O=F,Cl	1.00	0.76	0.66	0.64	0.01	0.00	0.04	0.11
Total	98.83	98.56	98.95	99.71*	99.07	98.88	98.64**	98.36#
Si	18.02	17.93	17.83	17.95	17.87	17.82	17.82	17.48
Ti	0.14	0.83	0.03	0.09	0.07	0.02	0.18	0.51
Al	9.69	8.93	9.75	10.55	9.55	9.22	8.91	6.76
Fe	2.36	1.67	2.02	0.35	1.28	1.44	1.38	1.34
Mn	0.06	0.09	0.20	0.30	0.04	0.04	0.01	0.02
Mg	0.78	1.31	1.09	1.45	1.87	2.17	2.30	4.78
Ca	18.94	19.21	19.02	18.85	19.31	19.29	19.23	19.10
Na	0.01	0.02	0.04	0.10	0.01	0.00	0.00	0.01
K	0.00	0.00	0.00	0.00	0.00	0.00	0.00	0.00
F	3.00	2.38	2.18	2.33	0.03	0.00	0.14	0.39
Cl	0.73	0.48	0.26	0.01	0.01	0.00	0.01	0.02

Water was calculated to give 18(OH, F, Cl) per unit cell

1. Obira mine, Oita, Japan (light-brown)
2. Sanpo mine, Okayama, Japan (brown)
3. Jinmu mine, Hiroshima, Japan (light-brown)
4. Sauland, Telemark, Norway (blue)
5. Ogose, Saitama, Japan (green)
6. Muslimbagh, Pakistan (light-green)
7. Saueseter, Drammen, Norway (light-green)
8. Wilui River, Yakutia, Siberia, Russian (black)

1-4, 8 : Metamorphic calc-silicate rocks
5-7 : Rodingites and veins associated with mafic rocks and serpentinites

* CuO 1.01wt.% (0.37 atom per formula unit)
** SO_3 0.49wt.% (0.18 atom per formula unit)

\# Total values of specimen 8 (98.36) contains H_2O and B_2O_3 (3.02wt.%) contents taken from that of Groat et al. (1992a).

Table 1. (cont.)

	9	10	11	12	13	14	15	16
SiO_2	36.74	35.89	36.71	36.58	35.83	36.16	36.48	36.81
TiO_2	0.35	1.13	0.55	0.03	2.66	1.43	3.57	0.19
Al_2O_3	17.17	17.14	15.86	17.84	13.45	16.21	13.45	18.91
FeO	2.88	2.72	3.42	2.08	5.12	3.03	4.69	0.91
MnO	0.02	0.80	0.09	0.01	0.09	0.21	0.12	0.07
MgO	3.45	2.27	3.25	3.64	2.69	2.40	1.42	2.31
CaO	36.85	36.28	36.67	36.94	35.96	36.09	35.87	37.19
Na_2O	0.01	0.02	0.01	0.01	0.02	0.00	0.10	0.01
K_2O	0.00	0.00	0.00	0.01	0.00	0.00	0.00	0.01
F	0.05	1.94	0.40	0.12	1.29	0.85	0.02	0.02
Cl	0.03	0.69	0.19	0.02	0.61	0.52	0.00	0.01
H_2O	2.78	1.66	2.54	2.75	1.95	2.20	2.68	2.78
-O=F,Cl	0.03	0.97	0.21	0.06	0.68	0.48	0.01	0.01
Total	100.3	99.57	99.48	99.97	98.99	98.62	98.39	99.21
Si	17.61	17.56	17.84	17.52	17.81	17.85	18.31	17.80
Ti	0.13	0.42	0.20	0.01	0.99	0.53	1.35	0.07
Al	9.70	9.88	9.08	10.07	7.88	9.43	7.86	10.78
Fe	1.16	1.11	1.39	0.83	2.13	1.25	1.97	0.37
Mn	0.01	0.33	0.04	0.00	0.04	0.09	0.05	0.03
Mg	2.47	1.65	2.35	2.60	1.99	1.77	1.06	1.66
Ca	18.93	19.02	19.09	18.95	19.15	19.09	19.29	19.27
Na	0.01	0.02	0.01	0.01	0.02	0.00	0.10	0.01
K	0.00	0.00	0.00	0.00	0.00	0.00	0.00	0.00
F	0.08	3.01	0.61	0.19	2.03	1.33	0.04	0.03
Cl	0.02	0.57	0.16	0.02	0.52	0.44	0.00	0.00

Water was calculated to give 18(OH, F, Cl) per unit cell

9. Chichibu mine, Saitama, Japan (green)
10. Nakatatsu mine, Fukui, Japan (light-brown)
11. Tetta, Okayama, Japan (dark-brown)
12. Tojyo, Hiroshima, Japan (green)
13. Kiura mine, Oita, Japan (dark-brown)
14. Houei mine, Oita, Japan (dark-brown)
15. Yawatahama, Ehime, Japan (pink)
16. Jeffrey mine, Asbestos, Quebec, Canada (lilac)

9–14 : Metamorphic calc-silicate rocks
15, 16 : Rodingites and veins associated with mafic rocks and serpentinites

Table 2. Experimental data and information

	Obira	Sanpo	Jinmu	Sauland
a (Å)	15.568(2)	15.559(3)	15.528(3)	15.472(2)
c	11.790(1)	11.797(2)	11.755(2)	11.754(1)
V (Å^3)	2857.5	2855.7	2834.1	2813.7
Space group	*P4/nnc*	*P4/nnc*	*P4/nnc*	*P4/nnc*
D_{calc} (g/cm^3)	3.44	3.43	3.44	3.40
Radiation used	MoKα (0.71069Å)			
Monochromator	graphite			
Crystal size (mm)	0.15 (dia.)	0.18 (dia.)	0.16×0.13×0.11	0.16 (dia.)
μ(MoKα) (cm^{-1})	30.09	29.43	29.52	25.73
Diffractometer	RIGAKU AFC-5 FOS			
Scan type	ω–2θ	ω	ω	ω
2θ range (°)	1 – 60	1 – 55	1 – 55	1 – 55
Observed reflections	3456	2785	2474	2629
Independent reflections with $Fo>3\sigma(Fo)$	1821	1493	1357	1415
R (%)	3.8	3.1	4.0	3.2
R_w (%)	4.7	3.4	3.8	3.5

	Ogose	Muslimbagh	Saueseter	Wilui River	Chichibu
a (Å)	15.564(2)	15.559(3)	15.572(2)	15.759(1)	15.563(2)
c	11.841(1)	11.826(2)	11.833(2)	11.727(1)	11.818(1)
V (Å^3)	2868.3	2862.9	2869.4	2912.2	2862.5
Space group	*P4/n*	*P4/n*	*P4nc*	*P4/nnc*	*P4/nnc*
D_{calc} (g/cm^3)	3.36	3.37	3.37	3.33	3.36
Radiation used	MoKα (0.71069Å)				
Monochromator	graphite				
Crystal size (mm)	0.15 (dia.)	0.22 (dia.)	0.20 (dia.)	0.17 (dia.)	0.23 (dia.)
μ(MoKα) (cm^{-1})	27.17	27.5	27.4	27.12	26.67
Diffractometer	RIGAKU AFC-5 FOS				
Scan type	ω<30°<ω–2θ	ω–2θ	ω–2θ	ω–2θ	ω–2θ
2θ range (°)	5 – 60	2 – 60	2 – 60	1 – 60	2 – 60
Observed reflections	3145	3995	3821	3198	3486
Independent reflections with $Fo>3\sigma(Fo)$	3024	3743	2053	1745	1873
R (%)	6.3	8.2	3.8	3.9	4.2
R_w (%)	6.3	11.0	4.9	3.7	4.1

Table 3. Refined occupancy factors

Obira					Total
C	Ca	0.5			0.5
B	Fe	0.5			0.5
AlFe	Al	0.88(1)	Fe	0.12	1.0
O(10)	F	0.5	Cl	0.5	1.0
O(11)	O	0.42	F	0.58(5)	1.0
Sanpo					
C	Ca	0.5			0.5
B	Fe	0.5			0.5
AlFe	Al	0.80(1)	Fe	0.20	1.0
O(10)	O	0.69(2)	Cl	0.31	1.0
O(11)	O	0.57	F	0.43(4)	1.0
Jinmu					
C	Ca	0.5			0.5
B	Fe	0.5			0.5
AlFe	Al	0.87(1)	Fe	0.13	1.0
O(10)	O	0.82(2)	Cl	0.18	1.0
O(11)	O	0.47	F	0.53(6)	1.0
Sauland					
C	Ca	0.5			0.5
B	Cu	0.25(1)	Al	0.25	0.5
AlFe	Al	0.87(11)	Mg	0.13	1.0
O(10)	O	0.43	F	0.57(10)	1.0
O(11)	O	0.47	F	0.53(4)	1.0
Ogose					
C(a)	Ca	0.63			0.63
C(b)	Ca	0.37			0.37
B(a)	Fe	0.47(2)	Al	0.16	0.63
B(b)	Fe	0.34(1)	Al	0.03	0.37
AlFe(a)	Al	0.98(1)	Fe	0.02	1.0
AlFe(b)	Al	0.95(1)	Fe	0.05	1.0

Table 3. (cont.)

Muslimbagh					Total
C(a)	Ca	0.62			0.62
C(b)	Ca	0.38			0.38
B(a)	Fe	0.61(2)	Al	0.01	0.62
B(b)	Fe	0.31(2)	Al	0.07	0.38
AlFe(a)	Al	0.96(1)	Fe	0.04	1.0
AlFe(b)	Al	0.97(1)	Fe	0.03	1.0
Saueseter					
C(a)	Ca	0.92			0.92
C(b)	Ca	0.08			0.08
B(a)	Fe	0.76(2)	Al	0.16	0.92
B(b)	Fe	0.08			0.08
AlFe(a)	Al	0.92(1)	Fe	0.08	1.0
AlFe(b)	Al	0.93(1)	Fe	0.07	1.0
Wilui River					
C	Ca	0.5			0.5
B	Mg	0.30(1)	Fe	0.20	0.5
AlFe	Al	0.90(1)	Fe	0.10	1.0
Bo(1)	B	0.95(2)			0.95
Bo(2)	B	1.01(5)			1.01
O(10)	O	0.60(2)			0.60
O(12)	O	0.19(1)			0.19
O(11)	O	1.0			1.0
Chichibu					
C	Ca	0.5			0.5
B	Al	0.25(1)	Fe	0.25	0.5
AlFe	Al	0.98(1)	Fe	0.02	1.0
Bo(1)	B	0.67(2)			0.67
Bo(2)	B	0.73(5)			0.73
O(10)	O	0.97(2)			1.0
O(11)	O	1.0			1.0

Table 4. Atomic positions for vesuvianites

Obira

Atom	Position	*x*	*y*	*z*
Ca(1)	4*c*	3/4	1/4	1/4
Ca(2)	16*k*	0.8111(1)	0.0433(1)	0.3795(1)
Ca(3)	16*k*	0.0985(1)	0.1787(1)	0.1137(1)
C	4*e*	1/4	1/4	0.6328(4)
B	4*e*	1/4	1/4	0.5650(3)
AlFe	16*k*	0.8870(1)	0.1210(1)	0.1264(1)
A	8*f*	0	0	0
Si(1)	4*d*	3/4	1/4	0
Si(2)	16*k*	0.8192(1)	0.0406(1)	0.8714(1)
Si(3)	16*k*	0.0823(1)	0.1506(1)	0.6354(1)
O(1)	16*k*	0.7800(2)	0.1725(2)	0.0857(2)
O(2)	16*k*	0.8831(2)	0.1599(2)	0.2792(2)
O(3)	16*k*	0.9510(2)	0.2218(2)	0.0760(2)
O(4)	16*k*	0.9383(2)	0.1060(2)	0.4699(2)
O(5)	16*k*	0.8301(2)	0.0152(2)	0.1790(2)
O(6)	16*k*	0.1169(2)	0.2710(2)	0.9402(2)
O(7)	16*k*	0.0561(2)	0.1744(2)	0.3219(2)
O(8)	16*k*	0.0609(2)	0.0902(2)	0.9343(2)
O(9)	8*h*	0.1435(2)	0.1435	3/4
O(10)A	4*e*	1/4	1/4	0.0945(12)
O(10)B	4*e*	1/4	1/4	0.1719(6)
O(11)	16*k*	0.9957(2)	0.0621(2)	0.1359(2)

Sanpo

Atom	Position	*x*	*y*	*z*
Ca(1)	4*c*	3/4	1/4	1/4
Ca(2)	16*k*	0.8110(1)	0.0437(1)	0.3795(1)
Ca(3)	16*k*	0.0986(1)	0.1785(1)	0.1145(1)
C	4*e*	1/4	1/4	0.6356(3)
B	4*e*	1/4	1/4	0.5567(3)
AlFe	16*k*	0.8882(1)	0.1205(1)	0.1270(1)
A	8*f*	0	0	0
Si(1)	4*d*	3/4	1/4	0
Si(2)	16*k*	0.8193(1)	0.0402(1)	0.8715(1)
Si(3)	16*k*	0.0830(1)	0.1507(1)	0.6357(1)
O(1)	16*k*	0.7793(1)	0.1727(1)	0.0855(2)
O(2)	16*k*	0.8831(1)	0.1602(1)	0.2800(2)
O(3)	16*k*	0.9513(1)	0.2223(1)	0.0755(2)
O(4)	16*k*	0.9386(1)	0.1060(1)	0.4699(2)
O(5)	16*k*	0.8295(1)	0.0146(1)	0.1794(2)
O(6)	16*k*	0.1180(1)	0.2712(1)	0.9401(2)
O(7)	16*k*	0.0561(1)	0.1745(1)	0.3221(2)
O(8)	16*k*	0.0609(1)	0.0905(1)	0.9335(2)
O(9)	8*h*	0.1443(1)	0.1443	3/4
O(10)	4*e*	1/4	1/4	0.1475(6)
O(11)	16*k*	0.9961(1)	0.0618(1)	0.1357(2)

Table 4. (cont. 1)

Jinmu

Atom	Position	*x*	*y*	*z*
Ca(1)	4*c*	3/4	1/4	1/4
Ca(2)	16*k*	0.8108(1)	0.0441(1)	0.3795(1)
Ca(3)	16*k*	0.1003(1)	0.1796(1)	0.1116(1)
C	4*e*	1/4	1/4	0.6410(4)
B	4*e*	1/4	1/4	0.5556(4)
AlFe	16*k*	0.8877(1)	0.1209(1)	0.1266(1)
A	8*f*	0	0	0
Si(1)	4*d*	3/4	1/4	0
Si(2)	16*k*	0.8194(1)	0.0407(1)	0.8711(1)
Si(3)	16*k*	0.0827(1)	0.1506(1)	0.6355(1)
O(1)	16*k*	0.7800(2)	0.1728(2)	0.0862(3)
O(2)	16*k*	0.8825(2)	0.1598(2)	0.2792(2)
O(3)	16*k*	0.9519(2)	0.2219(2)	0.0763(3)
O(4)	16*k*	0.9381(2)	0.1064(2)	0.4699(2)
O(5)	16*k*	0.8298(2)	0.0150(2)	0.1794(3)
O(6)	16*k*	0.1179(2)	0.2720(2)	0.9417(3)
O(7)	16*k*	0.0557(2)	0.1726(2)	0.3206(3)
O(8)	16*k*	0.0608(2)	0.0906(2)	0.9337(2)
O(9)	8*h*	0.1447(2)	0.1447	3/4
O(10)	4*e*	1/4	1/4	0.1375(8)
O(11)	16*k*	0.9965(2)	0.0616(2)	0.1361(2)

Sauland

Atom	Position	*x*	*y*	*z*
Ca(1)	4*c*	3/4	1/4	1/4
Ca(2)	16*k*	0.8109(1)	0.0443(1)	0.3795(1)
Ca(3)	16*k*	0.1015(1)	0.1802(1)	0.1118(1)
C	4*e*	1/4	1/4	0.6428(2)
B	4*e*	1/4	1/4	0.5543(2)
AlFe	16*k*	0.8876(1)	0.1211(1)	0.1265(1)
A	8*f*	0	0	0
Si(1)	4*d*	3/4	1/4	0
Si(2)	16*k*	0.8190(1)	0.0406(1)	0.8709(1)
Si(3)	16*k*	0.0831(1)	0.1508(1)	0.6352(1)
O(1)	16*k*	0.7811(1)	0.1726(1)	0.0858(2)
O(2)	16*k*	0.8832(1)	0.1593(1)	0.2784(2)
O(3)	16*k*	0.9511(1)	0.2215(1)	0.0767(2)
O(4)	16*k*	0.9381(1)	0.1065(1)	0.4707(2)
O(5)	16*k*	0.8299(1)	0.0154(1)	0.1780(2)
O(6)	16*k*	0.1188(2)	0.2716(1)	0.9414(2)
O(7)	16*k*	0.0561(1)	0.1733(1)	0.3212(2)
O(8)	16*k*	0.0606(1)	0.0908(1)	0.9337(2)
O(9)	8*h*	0.1447(1)	0.1447	3/4
O(10)	4*e*	1/4	1/4	0.1324(4)
O(11)	16*k*	0.9955(1)	0.0625(1)	0.1362(2)

Table 4. (cont. 2)

Ogose

Atom	Position	*x*	*y*	*z*
Ca(1)	4*f*	3/4	1/4	0.2497(2)
Ca(2a)	8*g*	0.8108(1)	0.0446(1)	0.3799(1)
Ca(2b)	8*g*	0.0439(1)	0.8107(1)	0.1204(1)
Ca(3a)	8*g*	0.1020(1)	0.1828(1)	0.1097(1)
Ca(3b)	8*g*	0.1811(1)	0.1008(1)	0.3849(1)
C(a)	2*c*	1/4	1/4	0.8501(4)
C(b)	2*c*	1/4	1/4	0.6501(6)
B(a)	2*c*	1/4	1/4	0.5331(3)
B(b)	2*c*	1/4	1/4	0.9660(5)
AlFe(a)	8*g*	0.8881(1)	0.1217(1)	0.1261(2)
AlFe(b)	8*g*	0.1211(1)	0.8877(1)	0.3734(2)
A(a)	4*d*	0	0	0
A(b)	4*e*	0	0	1/2
Si(1a)	2*a*	3/4	1/4	0
Si(1b)	2*b*	1/4	3/4	1/2
Si(2a)	8*g*	0.8195(1)	0.0410(1)	0.8720(2)
Si(2b)	8*g*	0.0405(1)	0.8193(1)	0.6292(2)
Si(3a)	8*g*	0.0843(1)	0.1508(1)	0.6353(2)
Si(3b)	8*g*	0.1505(1)	0.0827(1)	0.8641(2)
O(1a)	8*g*	0.7803(3)	0.1732(3)	0.0857(4)
O(1b)	8*g*	0.1723(3)	0.7797(3)	0.4143(4)
O(2a)	8*g*	0.8829(3)	0.1604(3)	0.2787(4)
O(2b)	8*g*	0.1596(3)	0.8824(3)	0.2200(4)
O(3a)	8*g*	0.9515(3)	0.2217(3)	0.0758(4)
O(3b)	8*g*	0.2232(3)	0.9523(3)	0.4237(4)
O(4a)	8*g*	0.9388(3)	0.1065(3)	0.4695(4)
O(4b)	8*g*	0.1065(3)	0.9374(3)	0.0299(4)
O(5a)	8*g*	0.8303(3)	0.0151(3)	0.1792(4)
O(5b)	8*g*	0.0133(3)	0.8285(3)	0.3215(4)
O(6a)	8*g*	0.1188(3)	0.2722(3)	0.9394(5)
O(6b)	8*g*	0.2711(3)	0.1204(3)	0.5589(4)
O(7a)	8*g*	0.0559(3)	0.1737(3)	0.3215(4)
O(7b)	8*g*	0.1719(3)	0.0551(3)	0.1774(4)
O(8a)	8*g*	0.0608(3)	0.0909(3)	0.9322(4)
O(8b)	8*g*	0.0909(3)	0.0609(3)	0.5653(4)
O(9)	8*g*	0.1446(3)	0.1452(3)	0.7508(4)
O(10a)	2*c*	1/4	1/4	0.1373(10)
O(10b)	2*c*	1/4	1/4	0.3683(10)
O(11a)	8*g*	0.9966(3)	0.0613(3)	0.1357(4)
O(11b)	8*g*	0.0617(3)	0.9950(3)	0.3642(4)

Table 4. (cont. 3)

Muslimbagh

Atom	Position	*x*	*y*	*z*
Ca(1)	4*f*	3/4	1/4	0.2498(2)
Ca(2a)	8*g*	0.8111(1)	0.0447(1)	0.3804(1)
Ca(2b)	8*g*	0.0437(1)	0.8104(1)	0.1212(1)
Ca(3a)	8*g*	0.1025(1)	0.1832(1)	0.1081(1)
Ca(3b)	8*g*	0.1811(1)	0.1004(1)	0.3847(1)
C(a)	2*c*	1/4	1/4	0.8513(4)
C(b)	2*c*	1/4	1/4	0.6467(8)
B(a)	2*c*	1/4	1/4	0.5351(3)
B(b)	2*c*	1/4	1/4	0.9623(6)
AlFe(a)	8*g*	0.8884(1)	0.1217(1)	0.1265(2)
AlFe(b)	8*g*	0.1208(1)	0.8871(1)	0.3731(2)
A(a)	4*d*	0	0	0
A(b)	4*e*	0	0	1/2
Si(1a)	2*a*	3/4	1/4	0
Si(1b)	2*b*	1/4	3/4	1/2
Si(2a)	8*g*	0.8198(1)	0.0411(1)	0.8726(2)
Si(2b)	8*g*	0.0403(1)	0.8194(1)	0.6290(2)
Si(3a)	8*g*	0.0850(1)	0.1510(1)	0.6351(2)
Si(3b)	8*g*	0.1506(1)	0.0826(1)	0.8635(2)
O(1a)	8*g*	0.7796(3)	0.1710(3)	0.0853(4)
O(1b)	8*g*	0.1724(3)	0.7782(3)	0.4135(4)
O(2a)	8*g*	0.8825(3)	0.1598(3)	0.2783(4)
O(2b)	8*g*	0.1594(3)	0.8814(3)	0.2198(4)
O(3a)	8*g*	0.9523(3)	0.2226(3)	0.0751(4)
O(3b)	8*g*	0.2221(3)	0.9528(3)	0.4244(4)
O(4a)	8*g*	0.9386(3)	0.1054(3)	0.4684(5)
O(4b)	8*g*	0.1060(3)	0.9376(3)	0.0295(4)
O(5a)	8*g*	0.8298(4)	0.0148(4)	0.1803(4)
O(5b)	8*g*	0.0119(3)	0.8282(3)	0.3210(5)
O(6a)	8*g*	0.1190(4)	0.2715(4)	0.9390(5)
O(6b)	8*g*	0.2717(4)	0.1221(4)	0.5583(5)
O(7a)	8*g*	0.0555(3)	0.1736(3)	0.3217(5)
O(7b)	8*g*	0.1722(4)	0.0559(3)	0.1759(5)
O(8a)	8*g*	0.0608(3)	0.0906(3)	0.9319(5)
O(8b)	8*g*	0.0920(3)	0.0613(3)	0.5652(4)
O(9)	8*g*	0.1459(3)	0.1440(3)	0.7501(4)
O(10a)	2*c*	1/4	1/4	0.1419(11)
O(10b)	2*c*	1/4	1/4	0.3629(12)
O(11a)	8*g*	0.9964(3)	0.0615(3)	0.1355(4)
O(11b)	8*g*	0.0604(4)	0.9959(4)	0.3644(4)

Table 4. (cont. 4)

Saueseter

Atom	Position	*x*	*y*	*z*
Ca(1)	4*b*	0	1/2	0.2475(3)
Ca(2a)	8*c*	0.0606(1)	0.2953(1)	0.3771(2)
Ca(2b)	8*c*	0.2934(1)	0.0611(1)	0.1185(2)
Ca(3a)	8*c*	0.1455(1)	0.0652(1)	0.8954(2)
Ca(3b)	8*c*	0.0709(1)	0.1508(1)	0.6183(2)
C(a)	2*a*	0	0	0.1463(3)
C(b)	2*a*	0	0	0.3377(34)
B(a)	2*a*	0	0	0.4645(3)
B(b)	2*a*	0	0	0.0377(25)
AlFe(a)	8*c*	0.1372(1)	0.3731(1)	0.1237(2)
AlFe(b)	8*c*	0.3697(1)	0.1386(1)	0.3710(2)
A	8*c*	0.2482(2)	0.2497(2)	0.4968(3)
Si(1)	4*b*	0	1/2	0.4979(4)
Si(2a)	8*c*	0.0689(1)	0.2910(1)	0.8701(2)
Si(2b)	8*c*	0.2901(1)	0.0696(1)	0.6269(2)
Si(3a)	8*c*	0.1626(1)	0.0991(1)	0.3625(2)
Si(3b)	8*c*	0.0995(1)	0.1697(1)	0.1329(3)
O(1a)	8*c*	0.0298(4)	0.4225(4)	0.0837(5)
O(1b)	8*c*	0.4226(4)	0.0300(4)	0.4134(5)
O(2a)	8*c*	0.1334(4)	0.4122(4)	0.2772(5)
O(2b)	8*c*	0.4084(4)	0.1334(4)	0.2175(6)
O(3a)	8*c*	0.2026(4)	0.4723(4)	0.0730(6)
O(3b)	8*c*	0.4724(4)	0.2036(4)	0.4217(5)
O(4a)	8*c*	0.1874(4)	0.3562(4)	0.4672(5)
O(4b)	8*c*	0.3559(4)	0.1905(4)	0.0286(5)
O(5a)	8*c*	0.0807(4)	0.2667(4)	0.1772(5)
O(5b)	8*c*	0.2594(4)	0.0777(4)	0.3191(6)
O(6a)	8*c*	0.0221(4)	0.1339(4)	0.0577(5)
O(6b)	8*c*	0.1242(4)	0.0224(4)	0.4399(5)
O(7a)	8*c*	0.3067(4)	0.4207(4)	0.3221(6)
O(7b)	8*c*	0.4249(4)	0.3058(4)	0.1799(5)
O(8a)	8*c*	0.1893(4)	0.1609(4)	0.0656(5)
O(8b)	8*c*	0.1562(4)	0.1886(4)	0.4326(5)
O(9)	8*c*	0.1031(4)	0.1059(4)	0.2455(5)
O(10a)	2*a*	0	0	0.8559(13)
O(10b)	2*a*	0	0	0.6231(11)
O(11a)	8*c*	0.2460(3)	0.3133(3)	0.1317(4)
O(11b)	8*c*	0.3079(3)	0.2475(3)	0.3582(5)

Table 4. (cont. 5)

Wilui River

Atom	Position	x	y	z
Ca(1)	4c	3/4	1/4	1/4
Ca(2)	16k	0.8093(1)	0.0451(1)	0.3800(1)
Ca(3)	16k	0.1012(1)	0.1793(1)	0.1033(1)
C	4e	1/4	1/4	0.6430(2)
B	4e	1/4	1/4	0.5541(3)
AlFe	16k	0.8888(1)	0.1201(1)	0.1283(1)
A	8f	0	0	0
Si(1)	4d	3/4	1/4	0
Si(2)	16k	0.8218(1)	0.0436(1)	0.8724(1)
Si(3)	16k	0.0841(1)	0.1501(1)	0.6353(1)
Bo(1)	8h	0.0533(3)	0.0533	1/4
Bo(2)	2a	1/4	1/4	1/4
O(1)	16k	0.7802(1)	0.1731(1)	0.0843(2)
O(2)	16k	0.8789(2)	0.1606(1)	0.2834(2)
O(3)	16k	0.9579(2)	0.2254(1)	0.0782(2)
O(4)	16k	0.9381(1)	0.1044(1)	0.4715(2)
O(5)	16k	0.8282(1)	0.0112(1)	0.1795(2)
O(6)	16k	0.1215(2)	0.2768(2)	0.9467(2)
O(7)	16k	0.0495(2)	0.1601(3)	0.3131(3)
O(8)	16k	0.0607(1)	0.0924(1)	0.9330(2)
O(9)	8h	0.1462(1)	0.1462	3/4
O(10)	4e	1/4	1/4	0.1311(9)
O(11)	16k	0.9984(2)	0.0578(2)	0.1464(2)
O(12)	16k	0.2275(10)	0.1790(11)	0.2042(15)

Chichibu

Atom	Position	x	y	z
Ca(1)	4c	3/4	1/4	1/4
Ca(2)	16k	0.8107(1)	0.0448(1)	0.3793(1)
Ca(3)	16k	0.1013(1)	0.1821(1)	0.1095(1)
C	4e	1/4	1/4	0.6497(2)
B	4e	1/4	1/4	0.5358(2)
AlFe	16k	0.8875(1)	0.1212(1)	0.1257(1)
A	8f	0	0	0
Si(1)	4d	3/4	1/4	0
Si(2)	16k	0.8194(1)	0.0416(1)	0.8715(1)
Si(3)	16k	0.0840(1)	0.1507(1)	0.6354(1)
Bo(1)	8h	0.0557(4)	0.0557	1/4
Bo(2)	2a	1/4	1/4	1/4
O(1)	16k	0.7800(1)	0.1727(1)	0.0849(2)
O(2)	16k	0.8824(1)	0.1599(1)	0.2796(2)
O(3)	16k	0.9531(1)	0.2226(1)	0.0757(2)
O(4)	16k	0.9385(1)	0.1059(1)	0.4693(2)
O(5)	16k	0.8289(1)	0.0133(2)	0.1782(2)
O(6)	16k	0.1215(2)	0.2733(2)	0.9415(2)
O(7)	16k	0.0551(2)	0.1714(2)	0.3207(2)
O(8)	16k	0.0605(1)	0.0916(1)	0.9327(2)
O(9)	8h	0.1453(1)	0.1453	3/4
O(10)	4e	1/4	1/4	0.1326(5)
O(11)	16k	0.9960(1)	0.0611(1)	0.1356(2)

Table 5. Anisotropic temperature factors ($\times 10^5$) for vesuvianites

Obira

Atom	β_{11}	β_{22}	β_{33}	β_{12}	β_{13}	β_{23}
Ca(1)	110(6)	62(5)	57(9)	0	0	0
Ca(2)	58(3)	84(3)	88(5)	6(2)	−6(3)	5(3)
Ca(3)	101(3)	91(3)	204(5)	29(2)	−42(3)	−25(3)
C	82(9)	82	455(31)	0	0	0
B	70(6)	70	464(23)	0	0	0
AlFe	45(4)	43(4)	53(6)	0(3)	6(4)	−2(4)
A	49(5)	45(5)	106(9)	8(5)	−2(6)	−6(6)
Si(1)	66(4)	66	47(12)	0	0	0
Si(2)	49(4)	56(4)	79(6)	1(3)	−3(4)	9(4)
Si(3)	96(4)	45(4)	68(6)	−1(3)	0(4)	−1(4)
O(1)	99(10)	65(9)	99(17)	−2(8)	2(11)	−7(11)
O(2)	78(10)	75(10)	130(18)	−1(8)	−31(11)	15(11)
O(3)	76(10)	58(9)	92(17)	2(8)	3(10)	−6(10)
O(4)	77(10)	67(10)	108(18)	2(8)	−18(10)	4(11)
O(5)	86(10)	118(11)	119(18)	36(9)	7(11)	−7(12)
O(6)	214(13)	96(11)	130(18)	37(9)	49(13)	53(12)
O(7)	69(10)	104(10)	153(18)	11(8)	1(11)	−0(11)
O(8)	62(9)	69(10)	115(17)	6(8)	29(10)	16(11)
O(9)	120(9)	120	108(23)	−21(13)	−23(12)	23
O(10)A	306(40)	306	401(95)	0	0	0
O(10)B	142(11)	142	914(56)	0	0	0
O(11)	111(11)	135(11)	125(17)	−8(8)	−3(10)	−20(10)

Sanpo

Atom	β_{11}	β_{22}	β_{33}	β_{12}	β_{13}	β_{23}
Ca(1)	116(4)	66(4)	98(7)	0	0	0
Ca(2)	57(2)	83(2)	127(4)	7(2)	−7(2)	1(2)
Ca(3)	93(2)	85(2)	275(5)	20(2)	−47(2)	−21(3)
C	95(7)	95	372(21)	0	0	0
B	62(5)	62	829(25)	0	0	0
AlFe	73(3)	58(3)	108(5)	−8(2)	17(3)	−6(3)
A	44(4)	33(4)	120(7)	6(3)	2(5)	5(5)
Si(1)	55(3)	55	92(10)	0	0	0
Si(2)	47(3)	55(3)	115(5)	1(2)	−4(3)	7(3)
Si(3)	95(3)	45(3)	102(5)	−3(2)	5(3)	−4(3)
O(1)	104(8)	62(7)	126(13)	7(6)	−3(8)	11(8)
O(2)	80(7)	72(8)	171(14)	−5(6)	−32(8)	−3(8)
O(3)	83(7)	54(7)	136(13)	−4(6)	−2(8)	−5(8)
O(4)	81(8)	58(7)	138(14)	1(6)	−8(8)	9(8)
O(5)	71(7)	119(8)	154(14)	36(6)	16(8)	−9(9)
O(6)	216(10)	78(8)	182(15)	41(7)	25(10)	43(9)
O(7)	66(7)	106(8)	177(14)	7(6)	−1(8)	12(9)
O(8)	56(7)	69(7)	161(14)	4(6)	23(8)	9(8)
O(9)	118(7)	118	115(18)	−28(10)	−6(9)	6
O(10)	91(11)	91	2554(88)	0	0	0
O(11)	95(8)	123(9)	163(15)	−11(6)	−5(8)	−9(8)

Table 5. (cont. 1)

Jinmu

Atom	β_{11}	β_{22}	β_{33}	β_{12}	β_{13}	β_{23}
Ca(1)	119(7)	76(6)	122(11)	0	0	0
Ca(2)	63(3)	84(3)	122(6)	5(2)	−9(4)	3(4)
Ca(3)	91(3)	86(3)	286(7)	15(3)	−41(4)	−27(4)
C	91(9)	91	328(30)	0	0	0
B	74(7)	74	850(36)	0	0	0
AlFe	62(4)	63(4)	106(8)	−1(3)	5(5)	2(4)
A	49(6)	63(6)	141(11)	2(6)	−8(7)	6(8)
Si(1)	64(5)	64	118(15)	0	0	0
Si(2)	57(4)	62(4)	109(8)	0(3)	−3(5)	4(5)
Si(3)	94(4)	45(4)	112(7)	1(4)	5(5)	1(5)
O(1)	121(11)	61(10)	119(19)	−6(10)	−2(13)	−3(13)
O(2)	85(11)	88(11)	150(21)	1(9)	−21(13)	12(13)
O(3)	83(11)	64(10)	150(20)	11(9)	4(13)	13(13)
O(4)	89(11)	58(11)	139(21)	7(9)	−7(13)	3(13)
O(5)	73(11)	102(12)	209(22)	25(10)	5(13)	−11(14)
O(6)	203(13)	88(12)	159(21)	23(10)	24(15)	35(13)
O(7)	78(11)	153(13)	225(22)	32(10)	28(14)	54(15)
O(8)	49(10)	74(11)	177(21)	−2(9)	19(12)	3(13)
O(9)	119(10)	119	126(26)	−26(15)	−6(15)	6
O(10)	159(22)	159	1572(107)	0	0	0
O(11)	120(12)	114(12)	191(22)	−16(9)	5(13)	−25(12)

Sauland

Atom	β_{11}	β_{22}	β_{33}	β_{12}	β_{13}	β_{23}
Ca(1)	134(5)	98(5)	156(9)	0	0	0
Ca(2)	60(2)	85(2)	104(4)	9(2)	−5(3)	0(3)
Ca(3)	85(3)	79(3)	259(5)	14(2)	−42(3)	−24(3)
C	73(6)	73	225(21)	0	0	0
B	54(7)	54	489(28)	0	0	0
AlFe	51(6)	58(6)	88(11)	−4(3)	9(4)	−2(4)
A	59(5)	49(5)	145(8)	−2(4)	3(5)	12(5)
Si(1)	55(4)	55	96(11)	0	0	0
Si(2)	48(3)	57(3)	91(6)	3(2)	−3(3)	5(3)
Si(3)	99(3)	51(3)	84(6)	1(3)	4(3)	−2(3)
O(1)	90(9)	62(8)	99(14)	1(7)	7(9)	6(9)
O(2)	73(8)	73(8)	151(16)	−3(7)	−40(9)	9(9)
O(3)	81(8)	57(8)	98(14)	6(7)	−10(9)	−1(9)
O(4)	78(9)	62(8)	108(15)	7(7)	−6(9)	7(9)
O(5)	77(9)	117(9)	147(16)	36(7)	15(10)	11(10)
O(6)	228(11)	85(9)	156(16)	32(8)	17(11)	35(10)
O(7)	83(9)	131(10)	161(15)	18(7)	17(10)	25(10)
O(8)	68(8)	72(8)	138(15)	7(7)	23(9)	9(9)
O(9)	98(7)	98	106(19)	−15(10)	−5(10)	5
O(10)	155(15)	155	460(42)	0	0	0
O(11)	106(9)	102(9)	147(16)	−3(7)	−11(9)	−3(8)

Table 5. (cont. 2)

Ogose

Atom	β_{11}	β_{22}	β_{33}	β_{12}	β_{13}	β_{23}
Ca(1)	82(6)	49(6)	77(10)	-3(5)	0	0
Ca(2a)	56(4)	72(4)	102(8)	5(3)	-0(5)	4(5)
Ca(2b)	66(4)	59(4)	107(8)	4(3)	-1(5)	3(5)
Ca(3a)	90(5)	111(5)	353(12)	29(4)	-88(6)	-75(6)
Ca(3b)	102(5)	81(5)	387(12)	31(4)	82(6)	82(6)
C(a)	79(9)	79	202(30)	0	0	0
C(b)	12(13)	12	218(49)	0	0	0
B(a)	40(8)	40	226(22)	0	0	0
B(b)	40	40	226	0	0	0
AlFe(a)	40(7)	35(7)	112(14)	-2(5)	9(7)	12(7)
AlFe(b)	51(7)	46(7)	55(13)	9(5)	7(7)	-17(7)
A(a)	45(9)	53(9)	87(17)	-4(8)	11(10)	16(10)
A(b)	36(9)	47(9)	113(17)	20(8)	6(10)	0(10)
Si(1a)	69(8)	69	31(21)	0	0	0
Si(1b)	58(8)	58	88(22)	0	0	0
Si(2a)	52(6)	48(6)	110(11)	5(5)	-7(7)	4(7)
Si(2b)	53(6)	39(6)	73(10)	2(5)	-18(7)	2(7)
Si(3a)	85(6)	47(6)	51(10)	10(5)	-7(7)	-2(6)
Si(3b)	25(6)	83(6)	102(11)	-7(5)	2(6)	3(7)
O(1a)	96(17)	71(16)	82(29)	9(14)	-31(18)	-21(18)
O(1b)	62(16)	75(16)	53(27)	5(13)	-17(17)	-11(17)
O(2a)	78(16)	59(16)	88(28)	-7(13)	-14(18)	-7(17)
O(2b)	96(17)	61(16)	128(30)	-15(13)	-1(18)	46(18)
O(3a)	58(16)	40(15)	101(29)	-10(13)	-7(17)	10(17)
O(3b)	66(16)	84(17)	41(27)	15(14)	15(17)	-1(17)
O(4a)	60(16)	73(16)	143(32)	16(13)	1(18)	5(19)
O(4b)	54(16)	99(17)	87(29)	-0(13)	-22(18)	1(18)
O(5a)	76(17)	102(18)	154(32)	26(14)	14(19)	-25(20)
O(5b)	122(19)	84(17)	93(30)	43(14)	14(19)	-50(19)
O(6a)	189(21)	71(18)	206(36)	38(15)	58(22)	55(20)
O(6b)	94(18)	152(20)	124(32)	22(15)	-11(19)	-26(20)
O(7a)	65(17)	91(18)	217(33)	5(14)	46(19)	-5(20)
O(7b)	95(18)	44(16)	202(32)	3(13)	12(20)	-13(19)
O(8a)	64(16)	45(16)	231(35)	17(13)	31(19)	25(19)
O(8b)	100(18)	32(15)	178(33)	23(14)	4(19)	-55(18)
O(9)	126(18)	106(17)	70(26)	-39(15)	13(20)	2(19)
O(10a)	53(20)	53	370(80)	0	0	0
O(10b)	172(26)	172	203(72)	0	0	0
O(11a)	76(16)	103(17)	90(29)	-4(14)	-9(19)	-30(19)
O(11b)	98(17)	52(15)	109(29)	8(13)	25(18)	17(18)

Table 5. (cont. 3)

Muslimbagh

Atom	β_{11}	β_{22}	β_{33}	β_{12}	β_{13}	β_{23}
Ca(1)	106(7)	85(7)	113(12)	2(6)	0	0
Ca(2a)	78(5)	87(5)	142(9)	8(4)	1(5)	11(5)
Ca(2b)	97(6)	78(5)	124(9)	4(4)	−10(5)	4(5)
Ca(3a)	111(6)	116(6)	293(11)	16(5)	−90(7)	−63(7)
Ca(3b)	117(6)	100(6)	307(11)	18(5)	67(7)	60(6)
C(a)	65(10)	65	186(30)	0	0	0
C(b)	70(17)	70	283(57)	0	0	0
B(a)	74(10)	74	286(29)	0	0	0
B(b)	33(17)	33	369(56)	0	0	0
AlFe(a)	55(8)	59(8)	91(15)	−14(6)	11(8)	13(8)
AlFe(b)	60(8)	47(8)	92(15)	−12(6)	9(8)	−13(7)
A(a)	46(11)	63(11)	127(20)	10(9)	−16(12)	−10(12)
A(b)	42(11)	60(11)	126(20)	18(9)	20(11)	14(12)
Si(1a)	104(10)	104	132(27)	0	0	0
Si(1b)	72(9)	72	57(23)	0	0	0
Si(2a)	70(7)	67(7)	104(13)	−0(6)	5(7)	14(7)
Si(2b)	64(7)	68(7)	85(12)	−3(6)	−10(7)	9(7)
Si(3a)	118(8)	44(7)	110(12)	6(6)	20(8)	18(7)
Si(3b)	44(7)	106(8)	114(12)	6(6)	−4(7)	1(8)
O(1a)	109(20)	86(19)	70(32)	−13(16)	−16(20)	−17(20)
O(1b)	72(19)	125(21)	76(32)	1(16)	10(20)	11(20)
O(2a)	70(19)	99(19)	127(33)	−28(16)	8(20)	18(21)
O(2b)	116(21)	73(19)	152(34)	−49(16)	−7(21)	−26(21)
O(3a)	99(20)	82(19)	64(32)	2(16)	13(20)	18(20)
O(3b)	101(20)	99(20)	73(32)	5(16)	−17(20)	22(20)
O(4a)	90(20)	73(19)	202(36)	0(16)	−49(22)	−1(22)
O(4b)	65(19)	118(21)	94(32)	18(16)	7(20)	35(21)
O(5a)	146(22)	145(22)	54(31)	53(18)	−28(22)	−51(22)
O(5b)	110(21)	100(20)	152(34)	41(16)	37(22)	35(22)
O(6a)	188(24)	101(21)	151(36)	4(18)	−14(24)	84(22)
O(6b)	130(22)	163(23)	165(37)	34(18)	−38(23)	−21(24)
O(7a)	68(19)	123(22)	226(37)	1(16)	33(22)	−36(23)
O(7b)	133(22)	85(20)	211(37)	2(17)	−2(23)	6(22)
O(8a)	59(19)	70(19)	306(40)	37(15)	72(23)	−41(22)
O(8b)	110(20)	52(18)	135(34)	−1(15)	44(21)	−46(20)
O(9)	119(20)	111(20)	89(29)	−22(17)	3(21)	7(22)
O(10a)	167(31)	167	364(93)	0	0	0
O(10b)	169(32)	169	489(108)	0	0	0
O(11a)	90(20)	105(21)	97(33)	3(16)	2(20)	−47(20)
O(11b)	147(23)	120(21)	108(34)	−1(18)	51(22)	55(22)

Table 5. (cont. 4)

Saueseter

Atom	β_{11}	β_{22}	β_{33}	β_{12}	β_{13}	β_{23}
Ca(1)	105(6)	56(5)	87(9)	5(11)	0	0
Ca(2a)	60(6)	85(6)	117(10)	9(5)	-4(7)	-4(7)
Ca(2b)	72(6)	64(6)	109(9)	3(5)	-10(7)	11(8)
Ca(3a)	95(6)	81(6)	233(12)	10(5)	-64(7)	-10(7)
Ca(3b)	89(6)	73(6)	252(11)	8(5)	17(7)	23(8)
C(a)	65(6)	65	139(21)	0	0	0
C(b)	65	65	139	0	0	0
B(a)	75(6)	75	150(16)	0	0	0
B(b)	75	75	150	0	0	0
AlFe(a)	42(7)	46(7)	67(12)	3(5)	7(8)	-8(8)
AlFe(b)	43(7)	52(7)	97(12)	-13(5)	-9(7)	-49(8)
A	44(6)	54(6)	91(10)	7(5)	5(6)	1(6)
Si(1)	74(12)	38(11)	68(13)	-14(15)	0	0
Si(2a)	60(7)	54(7)	75(11)	-2(5)	-5(8)	14(8)
Si(2b)	66(7)	40(6)	122(12)	0(5)	-9(8)	-3(8)
Si(3a)	70(7)	46(7)	75(11)	0(5)	-9(8)	-8(8)
Si(3b)	47(8)	61(8)	92(12)	0(6)	1(9)	-1(9)
O(1a)	80(22)	71(24)	95(32)	17(18)	-2(25)	10(24)
O(1b)	41(23)	108(24)	131(35)	5(18)	-10(24)	-9(27)
O(2a)	54(22)	78(21)	141(37)	-7(18)	-7(24)	25(25)
O(2b)	66(21)	69(22)	200(40)	-14(19)	-28(26)	61(25)
O(3a)	100(26)	42(21)	197(39)	2(19)	-24(25)	-13(25)
O(3b)	49(21)	70(24)	114(36)	10(18)	14(24)	-6(23)
O(4a)	108(23)	64(21)	134(37)	3(19)	-40(26)	1(25)
O(4b)	46(21)	75(21)	149(38)	-9(18)	7(24)	-37(24)
O(5a)	62(21)	68(21)	52(33)	27(17)	28(22)	20(22)
O(5b)	117(24)	72(23)	160(40)	6(18)	18(25)	5(25)
O(6a)	61(21)	127(23)	123(36)	-23(17)	-17(23)	62(23)
O(6b)	121(23)	101(23)	154(38)	-7(19)	14(25)	62(25)
O(7a)	57(22)	129(25)	215(42)	28(19)	14(25)	-11(26)
O(7b)	106(24)	64(22)	165(39)	-11(19)	9(25)	8(24)
O(8a)	46(20)	43(20)	180(38)	-3(17)	26(23)	-4(24)
O(8b)	79(22)	71(22)	155(37)	20(18)	-49(24)	-30(24)
O(9)	155(32)	60(27)	61(25)	-12(13)	-12(24)	42(22)
O(10a)	73(26)	73	480(104)	0	0	0
O(10b)	119(27)	119	110(63)	0	0	0
O(11a)	66(17)	66(17)	93(30)	-20(14)	6(21)	19(20)
O(11b)	117(20)	110(20)	167(35)	6(16)	47(23)	15(23)

Table 5. (cont. 5)

Wilui River

Atom	β_{11}	β_{22}	β_{33}	β_{12}	β_{13}	β_{23}
Ca(1)	122(5)	80(4)	109(8)	0	0	0
Ca(2)	86(2)	106(2)	139(4)	14(2)	−8(2)	−2(3)
Ca(3)	106(2)	126(3)	341(5)	−3(2)	−50(3)	−30(3)
C	81(6)	81	231(20)	0	0	0
B	77(9)	77	429(31)	0	0	0
AlFe	86(3)	85(4)	131(6)	4(2)	11(3)	2(3)
A	51(4)	51(4)	159(8)	3(4)	−1(5)	1(5)
Si(1)	79(4)	79	98(11)	0	0	0
Si(2)	95(3)	135(3)	139(6)	15(3)	1(4)	25(4)
Si(3)	89(3)	65(3)	123(5)	10(2)	3(3)	1(3)
Bo(1)	182(18)	182	216(42)	−53(20)	−67(19)	67
Bo(2)	169(36)	169	338(96)	0	0	0
O(1)	138(9)	97(8)	139(15)	−5(7)	−17(9)	10(9)
O(2)	138(9)	97(9)	194(16)	−0(7)	−60(10)	30(9)
O(3)	164(10)	124(9)	151(16)	36(8)	35(10)	25(10)
O(4)	125(9)	84(8)	168(16)	7(7)	−15(9)	0(9)
O(5)	115(9)	115(9)	163(16)	37(7)	12(9)	−31(10)
O(6)	156(9)	119(9)	234(17)	18(7)	28(11)	61(10)
O(7)	241(13)	649(22)	304(22)	230(14)	91(14)	244(17)
O(8)	81(8)	80(8)	196(15)	9(7)	21(9)	−6(9)
O(9)	121(7)	121	162(20)	−10(10)	−26(10)	26
O(10)	274(35)	274	432(84)	0	0	0
O(11)	111(9)	149(9)	362(20)	−10(8)	38(11)	−91(11)
O(12)	171(65)	401(92)	775(176)	82(61)	−128(78)	−467(99)

Chichibu

Atom	β_{11}	β_{22}	β_{33}	β_{12}	β_{13}	β_{23}
Ca(1)	101(5)	72(5)	104(8)	0	0	0
Ca(2)	72(2)	93(2)	130(4)	7(2)	−1(3)	1(3)
Ca(3)	110(3)	134(3)	520(7)	26(2)	−90(3)	−108(4)
C	69(6)	69	226(18)	0	0	0
B	76(8)	76	340(23)	0	0	0
AlFe	68(4)	71(4)	120(7)	5(3)	8(4)	−1(4)
A	73(5)	62(5)	111(8)	6(4)	2(5)	−6(5)
Si(1)	64(4)	64	90(11)	0	0	0
Si(2)	58(3)	74(3)	110(6)	1(3)	−3(4)	13(4)
Si(3)	114(4)	58(3)	120(6)	6(3)	−5(4)	−3(4)
Bo(1)	104(22)	104	249(59)	7(24)	3(25)	−3
Bo(2)	148(53)	148	945(259)	0	0	0
O(1)	115(9)	83(8)	109(15)	4(7)	−8(10)	4(9)
O(2)	85(9)	88(9)	164(16)	−5(7)	−20(10)	3(10)
O(3)	94(9)	88(8)	141(15)	11(7)	−6(10)	−6(10)
O(4)	97(9)	68(8)	183(17)	−3(7)	−20(10)	15(10)
O(5)	95(9)	156(10)	151(16)	41(8)	12(10)	−5(11)
O(6)	222(11)	111(10)	202(17)	22(8)	48(12)	38(10)
O(7)	93(9)	173(10)	208(17)	36(8)	10(10)	20(11)
O(8)	85(8)	87(9)	163(16)	9(7)	27(9)	10(10)
O(9)	131(8)	131	109(20)	−29(11)	−19(10)	19
O(10)	153(16)	153	484(54)	0	0	0
O(11)	90(9)	115(9)	147(15)	−9(8)	−14(10)	−32(10)

Table 6. Interatomic distances (Å) in cation coordination polyhedra

Obira

Ca(1)	– O(1) ×4	2.330(3)	C	– O(6) ×4	2.267(4)	Si(1)	– O(1) ×4	1.642(3)
	– O(2) ×4	2.525(3)		– O(9) ×4	2.721(3)			
				– O(10)A	2.680(15)	Si(2)	– O(2)	1.643(3)
	mean	2.427					– O(3)	1.644(3)
				mean	[8O] 2.494		– O(4)	1.677(3)
Ca(2)	– O(1)	2.495(3)			[9O] 2.515		– O(7)	1.618(3)
	– O(2)	2.439(3)						
	– O(3)	2.375(3)	B	– O(6) ×4	2.098(3)		mean	1.646
	– O(4)	2.452(3)		– O(10)A	1.881(14)			
	– O(5)	2.344(3)				Si(3)	– O(5)	1.631(3)
	– O(5)	2.421(3)		mean	2.055		– O(6)	1.604(3)
	– O(6)	2.892(3)					– O(8)	1.625(3)
	– O(8)	2.326(3)	AlFe	– O(1)	1.910(3)		– O(9)	1.657(2)
				– O(2)	1.901(3)			
	mean	2.468		– O(3)	1.953(3)		mean	1.629
				– O(4)	2.066(3)			
Ca(3)	– O(3)	2.434(3)		– O(5)	1.969(3)			
	– O(6)	2.516(3)		– O(11)	1.927(3)			
	– O(6)	3.039(3)						
	– O(7)	2.369(3)		mean	1.954			
	– O(7)	2.498(3)						
	– O(7)	2.543(3)	A	– O(4) ×2	1.942(3)			
	– O(8)	2.593(3)		– O(8) ×2	1.863(3)			
	– O(10)A	2.616(1)		– O(11)×2	1.873(2)			
	– O(10)B	2.695(2)						
	– O(11)	2.435(3)		mean	1.893			
	mean	[A] 2.560						
		[B] 2.569						

Sanpo

Ca(1)	– O(1) ×4	2.328(2)	C	– O(6) ×4	2.264(3)	Si(1)	– O(1) ×4	1.634(2)
	– O(2) ×4	2.523(2)		– O(9) ×4	2.689(2)			
						Si(2)	– O(2)	1.641(2)
	mean	2.426		mean	2.477		– O(3)	1.639(2)
							– O(4)	1.676(2)
Ca(2)	– O(1)	2.485(2)	B	– O(6) ×4	2.081(2)		– O(7)	1.610(2)
	– O(2)	2.434(2)		– O(10)	2.409(7)			
	– O(3)	2.371(2)					mean	1.641
	– O(4)	2.453(2)		mean	2.147			
	– O(5)	2.338(2)				Si(3)	– O(5)	1.632(2)
	– O(5)	2.421(2)	AlFe	– O(1)	1.941(2)		– O(6)	1.603(2)
	– O(6)	2.912(2)		– O(2)	1.910(2)		– O(8)	1.622(2)
	– O(8)	2.324(2)		– O(3)	1.961(2)		– O(9)	1.655(1)
				– O(4)	2.071(2)			
	mean	2.467		– O(5)	1.983(2)		mean	1.628
				– O(11)	1.913(2)			
Ca(3)	– O(3)	2.434(2)						
	– O(6)	2.531(2)		mean	1.963			
	– O(6)	3.037(2)						
	– O(7)	2.362(2)	A	– O(4) ×2	1.938(2)			
	– O(7)	2.496(2)		– O(8) ×2	1.869(2)			
	– O(7)	2.537(2)		– O(11)×2	1.868(2)			
	– O(8)	2.605(2)						
	– O(10)	2.635(1)		mean	1.892			
	– O(11)	2.430(2)						
	mean	2.563						

Table 6. Interatomic distances (Å) in cation coordination polyhedra

Obira

Ca(1)	– O(1) ×4	2.330(3)	C	– O(6) ×4	2.267(4)	Si(1)	– O(1) ×4	1.642(3)
	– O(2) ×4	2.525(3)		– O(9) ×4	2.721(3)			
				– O(10)A	2.680(15)	Si(2)	– O(2)	1.643(3)
	mean	2.427					– O(3)	1.644(3)
				mean	[8O] 2.494		– O(4)	1.677(3)
Ca(2)	– O(1)	2.495(3)			[9O] 2.515		– O(7)	1.618(3)
	– O(2)	2.439(3)						
	– O(3)	2.375(3)	B	– O(6) ×4	2.098(3)		mean	1.646
	– O(4)	2.452(3)		– O(10)A	1.881(14)			
	– O(5)	2.344(3)				Si(3)	– O(5)	1.631(3)
	– O(5)	2.421(3)		mean	2.055		– O(6)	1.604(3)
	– O(6)	2.892(3)					– O(8)	1.625(3)
	– O(8)	2.326(3)	AlFe	– O(1)	1.910(3)		– O(9)	1.657(2)
				– O(2)	1.901(3)			
	mean	2.468		– O(3)	1.953(3)		mean	1.629
				– O(4)	2.066(3)			
Ca(3)	– O(3)	2.434(3)		– O(5)	1.969(3)			
	– O(6)	2.516(3)		– O(11)	1.927(3)			
	– O(6)	3.039(3)						
	– O(7)	2.369(3)		mean	1.954			
	– O(7)	2.498(3)						
	– O(7)	2.543(3)	A	– O(4) ×2	1.942(3)			
	– O(8)	2.593(3)		– O(8) ×2	1.863(3)			
	– O(10)A	2.616(1)		– O(11)×2	1.873(2)			
	– O(10)B	2.695(2)						
	– O(11)	2.435(3)		mean	1.893			
	mean	[A] 2.560						
		[B] 2.569						

Sanpo

Ca(1)	– O(1) ×4	2.328(2)	C	– O(6) ×4	2.264(3)	Si(1)	– O(1) ×4	1.634(2)
	– O(2) ×4	2.523(2)		– O(9) ×4	2.689(2)			
						Si(2)	– O(2)	1.641(2)
	mean	2.426		mean	2.477		– O(3)	1.639(2)
							– O(4)	1.676(2)
Ca(2)	– O(1)	2.485(2)	B	– O(6) ×4	2.081(2)		– O(7)	1.610(2)
	– O(2)	2.434(2)		– O(10)	2.409(7)			
	– O(3)	2.371(2)					mean	1.641
	– O(4)	2.453(2)		mean	2.147			
	– O(5)	2.338(2)				Si(3)	– O(5)	1.632(2)
	– O(5)	2.421(2)	AlFe	– O(1)	1.941(2)		– O(6)	1.603(2)
	– O(6)	2.912(2)		– O(2)	1.910(2)		– O(8)	1.622(2)
	– O(8)	2.324(2)		– O(3)	1.961(2)		– O(9)	1.655(1)
				– O(4)	2.071(2)			
	mean	2.467		– O(5)	1.983(2)		mean	1.628
				– O(11)	1.913(2)			
Ca(3)	– O(3)	2.434(2)						
	– O(6)	2.531(2)		mean	1.963			
	– O(6)	3.037(2)						
	– O(7)	2.362(2)	A	– O(4) ×2	1.938(2)			
	– O(7)	2.496(2)		– O(8) ×2	1.869(2)			
	– O(7)	2.537(2)		– O(11)×2	1.868(2)			
	– O(8)	2.605(2)						
	– O(10)	2.635(1)		mean	1.892			
	– O(11)	2.430(2)						
	mean	2.563						

Table 6. (cont. 1)

Jinmu

Ca(1)	– O(1) ×4	2.316(3)	C	– O(6) ×4	2.295(4)	Si(1)	– O(1) ×4	1.637(3)
	– O(2) ×4	2.512(3)		– O(9) ×4	2.644(3)			
						Si(2)	– O(2)	1.642(3)
	mean	2.414		mean	2.469		– O(3)	1.639(3)
							– O(4)	1.670(3)
Ca(2)	– O(1)	2.479(3)	B	– O(6) ×4	2.079(3)		– O(7)	1.614(3)
	– O(2)	2.420(3)		– O(10)	2.270(10)			
	– O(3)	2.369(3)					mean	1.641
	– O(4)	2.444(3)		mean	2.117			
	– O(5)	2.333(3)				Si(3)	– O(5)	1.631(3)
	– O(5)	2.412(3)	AlFe	– O(1)	1.916(3)		– O(6)	1.602(3)
	– O(6)	2.919(3)		– O(2)	1.894(3)		– O(8)	1.619(3)
	– O(8)	2.325(3)		– O(3)	1.950(3)		– O(9)	1.657(2)
				– O(4)	2.059(3)			
	mean	2.463		– O(5)	1.974(3)		mean	1.627
				– O(11)	1.928(3)			
Ca(3)	– O(3)	2.433(3)						
	– O(6)	2.474(3)		mean	1.954			
	– O(6)	2.972(3)						
	– O(7)	2.366(3)	A	– O(4) ×2	1.944(3)			
	– O(7)	2.526(3)		– O(8) ×2	1.865(3)			
	– O(7)	2.555(3)		– O(11)×2	1.864(3)			
	– O(8)	2.581(3)						
	– O(10)	2.586(1)		mean	1.891			
	– O(11)	2.458(3)						
	mean	2.550						

Sauland

Ca(1)	– O(1) ×4	2.322(2)	C	– O(6) ×4	2.282(3)	Si(1)	– O(1) ×4	1.638(2)
	– O(2) ×4	2.516(2)		– O(9) ×4	2.626(2)			
						Si(2)	– O(2)	1.638(2)
	mean	2.419		mean	2.454		– O(3)	1.635(2)
							– O(4)	1.677(2)
Ca(2)	– O(1)	2.477(2)	B	– O(6) ×4	2.057(3)		– O(7)	1.611(2)
	– O(2)	2.415(2)		– O(10)	2.194(6)			
	– O(3)	2.373(2)					mean	1.640
	– O(4)	2.439(2)		mean	2.085			
	– O(5)	2.325(2)				Si(3)	– O(5)	1.632(2)
	– O(5)	2.428(2)	AlFe	– O(1)	1.891(2)		– O(6)	1.600(2)
	– O(6)	2.920(3)		– O(2)	1.881(2)		– O(8)	1.616(2)
	– O(8)	2.314(2)		– O(3)	1.929(2)		– O(9)	1.655(2)
				– O(4)	2.050(2)			
	mean	2.461		– O(5)	1.959(2)		mean	1.626
				– O(11)	1.903(2)			
Ca(3)	– O(3)	2.448(2)						
	– O(6)	2.467(2)		mean	1.935			
	– O(6)	2.962(2)						
	– O(7)	2.354(2)	A	– O(4) ×2	1.936(2)			
	– O(7)	2.500(2)		– O(8) ×2	1.860(2)			
	– O(7)	2.562(2)		– O(11)×2	1.871(2)			
	– O(8)	2.588(2)						
	– O(10)	2.550(1)		mean	1.889			
	– O(11)	2.468(2)						
	mean	2.544						

Table 6. (cont. 2)

Ogose

Ca(1)	– O(1a) ×2	2.328(5)				AlFe(a)	– O(1a)	1.920(5)	AlFe(b) – O(1b) 1.922(5)
	– O(1b) ×2	2.339(5)					– O(2a)	1.907(5)	– O(2b) 1.915(5)
	– O(2a) ×2	2.518(4)					– O(3a)	1.937(5)	– O(3b) 1.972(5)
	– O(2b) ×2	2.520(5)					– O(4b)	2.065(5)	– O(4a) 2.083(5)
							– O(5a)	1.989(5)	– O(5b) 2.010(5)
	mean	2.426					– O(11a)	1.937(5)	– O(11b) 1.912(5)
Ca(2a)	– O(1b)	2.470(5)	Ca(2b)	– O(1a)	2.495(5)		mean	1.959	mean 1.969
	– O(2a)	2.438(5)		– O(2b)	2.426(5)				
	– O(3b)	2.386(5)		– O(3a)	2.378(5)	A(a)	– O(4b) ×2	1.955(4)	A(b) – O(4a) ×2 1.946(5)
	– O(4a)	2.455(5)		– O(4b)	2.446(5)		– O(8a) ×2	1.881(5)	– O(8b) ×2 1.870(5)
	– O(5b)	2.326(5)		– O(5a)	2.345(5)		– O(11a)×2	1.869(5)	– O(11b)×2 1.874(5)
	– O(5a)	2.439(5)		– O(5b)	2.444(5)				
	– O(6b)	2.956(5)		– O(6a)	2.928(5)		mean	1.902	mean 1.897
	– O(8b)	2.337(5)		– O(8a)	2.321(5)				
						Si(1a)	– O(1a) ×4	1.637(5)	Si(1b) – O(1b) ×4 1.645(4)
	mean	2.476		mean	2.473				
						Si(2a)	– O(2b)	1.647(5)	Si(2b) – O(2a) 1.647(5)
Ca(3a)	– O(3a)	2.451(5)	Ca(3b)	– O(3b)	2.446(5)		– O(3a)	1.646(5)	– O(3b) 1.625(5)
	– O(6a)	2.463(5)		– O(6b)	2.510(5)		– O(4b)	1.671(5)	– O(4a) 1.674(5)
	– O(6a)	2.982(5)		– O(6b)	3.018(5)		– O(7b)	1.612(5)	– O(7a) 1.613(5)
	– O(7b)	2.404(5)		– O(7a)	2.376(5)				
	– O(7b)	2.507(5)		– O(7a)	2.483(5)		mean	1.644	mean 1.640
	– O(7a)	2.613(5)		– O(7b)	2.562(5)				
	– O(8a)	2.622(5)		– O(8b)	2.630(5)	Si(3a)	– O(5b)	1.635(5)	Si(3b) – O(5a) 1.633(5)
	– O(10a)	2.551(2)		– O(10b)	2.565(2)		– O(6b)	1.616(5)	– O(6a) 1.600(5)
	– O(11a)	2.523(5)		– O(11b)	2.495(5)		– O(8b)	1.629(5)	– O(8a) 1.618(5)
							– O(9)	1.661(5)	– O(9) 1.661(5)
	mean	2.568		mean	2.565				
							mean	1.635	mean 1.628
C(a)	– O(6a) ×4	2.325(6)	C(b)	– O(6b) ×4	2.312(6)				
	– O(9) ×4	2.595(5)		– O(9) ×4	2.603(6)				
	mean	2.460		mean	2.457				
B(a)	– O(6b) ×4	2.067(5)	B(b)	– O(6a) ×4	2.094(5)				
	– O(10b)	1.952(12)		– O(10a)	2.028(13)				
	mean	2.044		mean	2.081				

Table 6. (cont. 3)

Muslimbagh

Ca(1)	– O(1a) ×2	2.346(5)				AlFe(a)	– O(1a)	1.922(6)	AlFe(b)	– O(1b)	1.936(6)
	– O(1b) ×2	2.323(5)					– O(2a)	1.893(5)		– O(2b)	1.913(6)
	– O(2a) ×2	2.517(5)					– O(3a)	1.956(6)		– O(3b)	1.973(6)
	– O(2b) ×2	2.509(5)					– O(4b)	2.065(5)		– O(4a)	2.093(6)
							– O(5a)	2.001(6)		– O(5b)	2.023(6)
	mean	2.424					– O(11a)	1.926(6)		– O(11b)	1.938(6)
Ca(2a)	– O(1b)	2.456(5)	Ca(2b)	– O(1a)	2.463(5)		mean	1.960		mean	1.979
	– O(2a)	2.429(5)		– O(2b)	2.412(6)						
	– O(3b)	2.365(5)		– O(3a)	2.378(5)	A(a)	– O(4b) ×2	1.945(5)	A(b)	– O(4a) ×2	1.935(5)
	– O(4a)	2.431(5)		– O(4b)	2.455(5)		– O(8a) ×2	1.879(5)		– O(8b) ×2	1.885(5)
	– O(5b)	2.334(6)		– O(5a)	2.336(6)		– O(11a)×2	1.867(5)		– O(11b)×2	1.860(5)
	– O(5a)	2.429(5)		– O(5b)	2.430(6)						
	– O(6b)	2.986(6)		– O(6a)	2.923(6)		mean	1.897		mean	1.893
	– O(8b)	2.325(5)		– O(8a)	2.326(5)						
						Si(1a)	– O(1a) ×4	1.655(5)	Si(1b)	– O(1b) ×4	1.642(5)
	mean	2.470		mean	2.465						
Ca(3a)	– O(3a)	2.447(5)	Ca(3b)	– O(3b)	2.430(5)	Si(2a)	– O(2b)	1.658(6)	Si(2b)	– O(2a)	1.658(5)
	– O(6a)	2.440(6)		– O(6b)	2.513(6)		– O(3a)	1.638(5)		– O(3b)	1.644(6)
	– O(6a)	2.974(6)		– O(6b)	3.003(6)		– O(4b)	1.669(5)		– O(4a)	1.675(6)
	– O(7b)	2.396(6)		– O(7a)	2.381(6)		– O(7b)	1.620(6)		– O(7a)	1.605(6)
	– O(7b)	2.496(6)		– O(7a)	2.480(6)						
	– O(7a)	2.634(6)		– O(7b)	2.568(6)		mean	1.646		mean	1.645
	– O(8a)	2.614(6)		– O(8b)	2.618(5)						
	– O(10a)	2.552(3)		– O(10b)	2.575(2)	Si(3a)	– O(5b)	1.627(6)	Si(3b)	– O(5a)	1.629(6)
	– O(11a)	2.532(6)		– O(11b)	2.496(6)		– O(6b)	1.614(6)		– O(6a)	1.609(6)
							– O(8b)	1.626(5)		– O(8a)	1.619(6)
	mean	2.565		mean	2.563		– O(9)	1.662(6)		– O(9)	1.648(6)
C(a)	– O(6a) ×4	2.311(6)	C(b)	– O(6b) ×4	2.273(7)		mean	1.632		mean	1.626
	– O(9) ×4	2.602(6)		– O(9) ×4	2.615(7)						
	mean	2.457		mean	2.444						
B(a)	– O(6b) ×4	2.037(6)	B(b)	– O(6a) ×4	2.084(6)						
	– O(10b)	2.037(15)		– O(10a)	2.125(15)						
	mean	2.037		mean	2.092						

Table 6. (cont. 4)

Saueseter

Ca(1)	– O(1a) ×2	2.330(7)				AlFe(a)	– O(1a)	1.900(6)	AlFe(b)	– O(1b)	1.947(6)
	– O(1b) ×2	2.351(7)					– O(2a)	1.917(7)		– O(2b)	1.916(7)
	– O(2a) ×2	2.512(6)					– O(3a)	1.946(6)		– O(3b)	1.985(6)
	– O(2b) ×2	2.545(6)					– O(4a)	2.080(7)		– O(4b)	2.089(6)
							– O(5a)	1.979(6)		– O(5b)	2.056(6)
	mean	2.434					– O(11a)	1.935(5)		– O(11b)	1.956(5)
Ca(2a)	– O(1b)	2.471(6)	Ca(2b)	– O(1a)	2.493(6)		mean	1.960		mean	1.991
	– O(2a)	2.448(6)		– O(2b)	2.418(6)						
	– O(3a)	2.374(7)		– O(3b)	2.388(7)	A	– O(4a)	1.941(7)			
	– O(4a)	2.435(6)		– O(4b)	2.478(6)		– O(4b)	1.939(6)			
	– O(5b)	2.329(6)		– O(5a)	2.352(6)		– O(8a)	1.889(7)			
	– O(5a)	2.428(6)		– O(5b)	2.445(7)		– O(8b)	1.881(7)			
	– O(6b)	3.054(7)		– O(6a)	2.893(7)		– O(11a)	1.862(6)			
	– O(8b)	2.325(6)		– O(8a)	2.331(6)		– O(11b)	1.886(7)			
	mean	2.483		mean	2.475		mean	1.900			
Ca(3a)	– O(3b)	2.441(6)	Ca(3b)	– O(3a)	2.440(6)	Si(1)	– O(1a) ×2	1.645(7)			
	– O(6a)	2.360(7)		– O(6b)	2.596(7)		– O(1b) ×2	1.633(7)			
	– O(6a)	2.919(7)		– O(6b)	3.023(7)						
	– O(7a)	2.408(6)		– O(7b)	2.368(6)		mean	1.639			
	– O(7a)	2.523(7)		– O(7b)	2.481(6)						
	– O(7b)	2.665(7)		– O(7a)	2.505(7)	Si(2a)	– O(2a)	1.637(6)	Si(2b)	– O(2b)	1.639(7)
	– O(8a)	2.597(6)		– O(8b)	2.633(7)		– O(3b)	1.624(6)		– O(3a)	1.648(6)
	– O(10a)	2.527(3)		– O(10b)	2.596(2)		– O(4a)	1.672(6)		– O(4b)	1.671(6)
	– O(11b)	2.622(5)		– O(11a)	2.421(5)		– O(7a)	1.632(6)		– O(7b)	1.622(6)
	mean	2.562		mean	2.562		mean	1.641		mean	1.645
C(a)	– O(6a) ×4	2.358(7)	C(b)	– O(6b) ×4	2.307(22)	Si(3a)	– O(5b)	1.627(6)	Si(3b)	– O(5a)	1.625(6)
	– O(9) ×4	2.583(7)		– O(9) ×4	2.547(19)		– O(6b)	1.620(7)		– O(6a)	1.599(7)
							– O(8b)	1.625(7)		– O(8a)	1.616(6)
	mean	2.471		mean	2.427		– O(9)	1.670(7)		– O(9)	1.662(7)
B(a)	– O(6b) ×4	1.986(6)	B(b)	– O(6a) ×4	2.126(7)		mean	1.635		mean	1.625
	– O(10b)	1.877(13)		– O(10a)	2.151(34)						
	mean	1.964		mean	2.131						

Table 6. (cont. 5)

Wilui River

Ca(1)	– O(1) ×4	2.340(2)	C	– O(6) ×4	2.321(3)	Si(1)	– O(1) ×4	1.634(2)
	– O(2) ×4	2.504(2)		– O(9) ×4	2.631(2)			
						Si(2)	– O(2)	1.630(3)
	mean	2.422		mean	2.476		– O(3)	1.625(3)
							– O(4)	1.670(2)
Ca(2)	– O(1)	2.497(2)	B	– O(6) ×4	2.069(2)		– O(7)	1.649(3)
	– O(2)	2.408(2)		– O(10)	2.172(11)			
	– O(3)	2.389(2)					mean	1.643
	– O(4)	2.479(2)		mean	2.089			
	– O(5)	2.337(2)				Si(3)	– O(5)	1.625(3)
	– O(5)	2.429(2)	AlFe	– O(1)	1.974(2)		– O(6)	1.613(3)
	– O(6)	3.056(3)		– O(2)	1.935(2)		– O(8)	1.626(2)
	– O(8)	2.360(2)		– O(3)	2.069(3)		– O(9)	1.665(2)
				– O(4)	2.056(2)			
	mean	2.494		– O(5)	2.054(2)		mean	1.632
				– O(11)	1.998(3)			
Ca(3)	– O(3)	2.391(2)				Bo(1)	– O(7) ×2	1.839(6)
	– O(6)	2.415(3)		mean	2.014		– O(11)×2	1.493(4)
	– O(6)	2.811(3)						
	– O(7)	2.451(3)	A	– O(4) ×2	1.942(2)		mean	1.666
	– O(7)	2.834(4)		– O(8) ×2	1.911(2)			
	– O(7)	2.609(3)		– O(11)×2	1.943(3)	Bo(2)	– O(10)	1.394(11)
	– O(8)	2.505(2)					– O(12)×2	1.291(18)
	– O(10)	2.616(2) (a, d)		mean	1.932			
	– O(11)	2.559(3)					mean	1.325
	– O(12)	2.315(16) (b)						
	– O(12)	2.250(17) (c)						
	– O(12)	2.679(18) (d)						
	mean	(a) 2.577						
		(b) 2.543						
		(c) 2.536						
		(d) 2.587						

Chichibu

Ca(1)	– O(1) ×4	2.340(2)	C	– O(6) ×4	2.301(3)	Si(1)	– O(1) ×4	1.635(2)
	– O(2) ×4	2.517(2)		– O(9) ×4	2.591(2)			
						Si(2)	– O(2)	1.638(2)
	mean	2.429		mean	2.446		– O(3)	1.633(2)
							– O(4)	1.668(2)
Ca(2)	– O(1)	2.476(2)	B	– O(6) ×4	2.050(3)		– O(7)	1.627(3)
	– O(2)	2.416(2)		– O(10)	1.990(7)			
	– O(3)	2.378(2)					mean	1.641
	– O(4)	2.447(2)		mean	2.038			
	– O(5)	2.329(2)				Si(3)	– O(5)	1.628(3)
	– O(5)	2.443(2)	AlFe	– O(1)	1.917(2)		– O(6)	1.602(3)
	– O(6)	2.993(3)		– O(2)	1.918(2)		– O(8)	1.622(2)
	– O(8)	2.323(2)		– O(3)	1.970(2)		– O(9)	1.659(2)
				– O(4)	2.071(2)			
	mean	2.476		– O(5)	2.010(3)		mean	1.628
				– O(11)	1.933(2)			
Ca(3)	– O(3)	2.424(2)				Bo(1)	– O(7) ×2	1.984(6)
	– O(6)	2.461(3)		mean	1.970		– O(11)×2	1.643(4)
	– O(6)	2.938(3)						
	– O(7)	2.403(3)	A	– O(4) ×2	1.941(2)		mean	1.814
	– O(7)	2.530(3)		– O(8) ×2	1.885(2)			
	– O(7)	2.602(3)		– O(11)×2	1.865(2)	Bo(2)	– O(10)	1.388(6)
	– O(8)	2.598(2)						
	– O(10)	2.559(1)		mean	1.897			
	– O(11)	2.515(2)						
	mean	2.559						

Table 7. The length of edges of polyhedra

Obira

< B >		< A >		< Si(2) >	
O(6) – O(6) ×4	2.966(4)	O(4) – O(8) ×2	2.669(4)	O(2) – O(3)	2.726(4)
O(6) – O(10)A×4	2.777(10)	O(4) – O(8) ×2	2.713(4)	O(2) – O(4)	2.549(4)
O(6) – O(10)B×4	3.444(6)	O(4) – O(11) ×2	2.868(4)	O(2) – O(7)	2.750(4)
		O(4) – O(11) ×2	2.517(4)	O(3) – O(4)	2.743(4)
< AlFe >		O(8) – O(11) ×2	2.622(4)	O(3) – O(7)	2.596(4)
		O(8) – O(11) ×2	2.661(4)	O(4) – O(7)	2.746(4)
O(1) – O(2)	2.796(4)				
O(1) – O(3)	2.773(4)	< Si(1) >		< Si(3) >	
O(1) – O(4)	2.827(4)				
O(1) – O(5)	2.795(4)	O(1) – O(1) ×2	2.588(5)	O(5) – O(6)	2.656(4)
O(2) – O(3)	2.790(4)	O(1) – O(1) ×4	2.726(5)	O(5) – O(8)	2.712(4)
O(2) – O(5)	2.673(4)			O(5) – O(9)	2.642(4)
O(2) – O(11)	2.871(4)			O(6) – O(8)	2.651(4)
O(3) – O(4)	2.926(4)			O(6) – O(9)	2.640(3)
O(3) – O(11)	2.676(4)			O(8) – O(9)	2.658(3)
O(4) – O(5)	2.756(4)				
O(4) – O(11)	2.517(4)				
O(5) – O(11)	2.727(4)				

Sanpo

< B >		< A >		< Si(2) >	
O(6) – O(6) ×4	2.942(3)	O(4) – O(8) ×2	2.670(3)	O(2) – O(3)	2.715(3)
O(6) – O(10) ×4	3.212(5)	O(4) – O(8) ×2	2.715(3)	O(2) – O(4)	2.545(3)
		O(4) – O(11) ×2	2.854(3)	O(2) – O(7)	2.745(3)
< AlFe >		O(4) – O(11) ×2	2.519(3)	O(3) – O(4)	2.733(3)
		O(8) – O(11) ×2	2.628(3)	O(3) – O(7)	2.588(3)
O(1) – O(2)	2.813(3)	O(8) – O(11) ×2	2.657(3)	O(4) – O(7)	2.742(3)
O(1) – O(3)	2.788(3)				
O(1) – O(4)	2.837(3)	< Si(1) >		< Si(3) >	
O(1) – O(5)	2.809(3)				
O(2) – O(3)	2.807(3)	O(1) – O(1) ×2	2.572(4)	O(5) – O(6)	2.657(3)
O(2) – O(5)	2.691(3)	O(1) – O(1) ×4	2.716(4)	O(5) – O(8)	2.711(3)
O(2) – O(11)	2.886(3)			O(5) – O(9)	2.640(3)
O(3) – O(4)	2.935(3)			O(6) – O(8)	2.648(3)
O(3) – O(11)	2.687(3)			O(6) – O(9)	2.632(2)
O(4) – O(5)	2.766(3)			O(8) – O(9)	2.659(2)
O(4) – O(11)	2.519(3)				
O(5) – O(11)	2.743(3)				

Table 7. (cont. 1)

Jinmu

< B >		< A >		< Si(2) >	
O(6) – O(6) ×4	2.940(5)	O(4) – O(8) ×2	2.667(4)	O(2) – O(3)	2.724(4)
O(6) – O(10) ×4	3.101(7)	O(4) – O(8) ×2	2.719(4)	O(2) – O(4)	2.541(4)
		O(4) – O(11) ×2	2.852(4)	O(2) – O(7)	2.740(4)
< AlFe >		O(4) – O(11) ×2	2.524(4)	O(3) – O(4)	2.729(4)
		O(8) – O(11) ×2	2.619(4)	O(3) – O(7)	2.598(4)
O(1) – O(2)	2.779(4)	O(8) – O(11) ×2	2.654(4)	O(4) – O(7)	2.733(4)
O(1) – O(3)	2.777(4)				
O(1) – O(4)	2.818(4)	< Si(1) >		< Si(3) >	
O(1) – O(5)	2.794(4)				
O(2) – O(3)	2.789(4)	O(1) – O(1) ×2	2.572(5)	O(5) – O(6)	2.663(4)
O(2) – O(5)	2.665(4)	O(1) – O(1) ×4	2.722(5)	O(5) – O(8)	2.710(4)
O(2) – O(11)	2.880(4)			O(5) – O(9)	2.644(4)
O(3) – O(4)	2.924(4)			O(6) – O(8)	2.633(4)
O(3) – O(11)	2.679(4)			O(6) – O(9)	2.632(3)
O(4) – O(5)	2.753(4)			O(8) – O(9)	2.658(3)
O(4) – O(11)	2.524(4)				
O(5) – O(11)	2.737(4)				

Sauland

< B >		< A >		< Si(2) >	
O(6) – O(6) ×4	2.908(4)	O(4) – O(8) ×2	2.659(3)	O(2) – O(3)	2.721(3)
O(6) – O(10) ×4	3.045(4)	O(4) – O(8) ×2	2.710(3)	O(2) – O(4)	2.549(3)
		O(4) – O(11) ×2	2.869(3)	O(2) – O(7)	2.730(3)
< AlFe >		O(4) – O(11) ×2	2.504(3)	O(3) – O(4)	2.727(3)
		O(8) – O(11) ×2	2.622(3)	O(3) – O(7)	2.594(3)
O(1) – O(2)	2.768(3)	O(8) – O(11) ×2	2.655(3)	O(4) – O(7)	2.737(3)
O(1) – O(3)	2.738(3)				
O(1) – O(4)	2.790(3)	< Si(1) >		< Si(3) >	
O(1) – O(5)	2.768(3)				
O(2) – O(3)	2.765(3)	O(1) – O(1) ×2	2.582(4)	O(5) – O(6)	2.664(3)
O(2) – O(5)	2.651(3)	O(1) – O(1) ×4	2.721(4)	O(5) – O(8)	2.699(3)
O(2) – O(11)	2.837(3)			O(5) – O(9)	2.646(3)
O(3) – O(4)	2.905(3)			O(6) – O(8)	2.634(3)
O(3) – O(11)	2.648(3)			O(6) – O(9)	2.627(3)
O(4) – O(5)	2.725(3)			O(8) – O(9)	2.655(2)
O(4) – O(11)	2.504(3)				
O(5) – O(11)	2.708(3)				

Table 7. (cont. 2)

Ogose			
< B(a) >		< B(b) >	
O(6b) – O(6b)	×4 2.891(7)	O(6a) – O(6a)	×4 2.928(8)
O(6b) – O(10b)	×4 3.045(10)	O(6a) – O(10a)	×4 3.126(10)
< AlFe(a) >		< AlFe(b) >	
O(1a) – O(2a)	2.795(7)	O(1b) – O(2b)	2.808(6)
O(1a) – O(3a)	2.773(6)	O(1b) – O(3b)	2.802(6)
O(1a) – O(4b)	2.819(6)	O(1b) – O(4a)	2.833(6)
O(1a) – O(5a)	2.809(7)	O(1b) – O(5b)	2.812(7)
O(2a) – O(3a)	2.797(6)	O(2b) – O(3b)	2.824(6)
O(2a) – O(5a)	2.678(7)	O(2b) – O(5b)	2.708(7)
O(2a) – O(11a)	2.895(6)	O(2b) – O(11b)	2.883(6)
O(3a) – O(4b)	2.918(6)	O(3b) – O(4a)	2.966(6)
O(3a) – O(11a)	2.689(6)	O(3b) – O(11b)	2.693(6)
O(4b) – O(5a)	2.765(7)	O(4a) – O(5b)	2.776(7)
O(4b) – O(11a)	2.533(6)	O(4a) – O(11b)	2.525(6)
O(5a) – O(11a)	2.734(6)	O(5b) – O(11b)	2.746(6)
< A(a) >		< A(b) >	
O(4b) – O(8a)	×2 2.677(6)	O(4a) – O(8b)	×2 2.679(6)
O(4b) – O(8a)	×2 2.748(6)	O(4a) – O(8b)	×2 2.718(7)
O(4b) – O(11a)	×2 2.865(6)	O(4a) – O(11b)	×2 2.867(6)
O(4b) – O(11a)	×2 2.533(6)	O(4a) – O(11b)	×2 2.525(6)
O(8a) – O(11a)	×2 2.649(7)	O(8b) – O(11b)	×2 2.633(7)
O(8a) – O(11a)	×2 2.655(7)	O(8b) – O(11b)	×2 2.663(7)
< Si(1a) >		< Si(1b) >	
O(1a) – O(1a)	×2 2.569(9)	O(1b) – O(1b)	×2 2.588(9)
O(1a) – O(1a)	×4 2.724(8)	O(1b) – O(1b)	×4 2.734(8)
< Si(2a) >		< Si(2b) >	
O(2b) – O(3a)	2.735(6)	O(2a) – O(3b)	2.720(6)
O(2b) – O(4b)	2.546(7)	O(2a) – O(4a)	2.562(6)
O(2b) – O(7b)	2.741(6)	O(2a) – O(7a)	2.748(6)
O(3a) – O(4b)	2.737(6)	O(3b) – O(4a)	2.714(6)
O(3a) – O(11a)	2.689(6)	O(3b) – O(7a)	2.577(7)
O(4b) – O(7b)	2.729(7)	O(4a) – O(7a)	2.735(7)
< Si(3a) >		< Si(3b) >	
O(5b) – O(6b)	2.671(7)	O(5a) – O(6a)	2.672(7)
O(5b) – O(8b)	2.718(7)	O(5a) – O(8a)	2.708(7)
O(5b) – O(9)	2.634(7)	O(5a) – O(9)	2.658(7)
O(6b) – O(8b)	2.655(7)	O(6a) – O(8a)	2.638(7)
O(6b) – O(9)	2.646(7)	O(6a) – O(9)	2.615(7)
O(8b) – O(9)	2.691(7)	O(8a) – O(9)	2.652(7)

Table 7. (cont. 3)

Muslimbagh			
< B(a) >		< B(b) >	
O(6b) – O(6b) ×4	2.855(8)	O(6a) – O(6a) ×4	2.921(8)
O(6b) – O(10b) ×4	3.069(12)	O(6a) – O(10a) ×4	3.167(11)
< AlFe(a) >		< AlFe(b) >	
O(1a) – O(2a)	2.794(7)	O(1b) – O(2b)	2.806(7)
O(1a) – O(3a)	2.807(7)	O(1b) – O(3b)	2.827(7)
O(1a) – O(4b)	2.806(7)	O(1b) – O(4a)	2.866(7)
O(1a) – O(5a)	2.790(8)	O(1b) – O(5b)	2.836(7)
O(2a) – O(3a)	2.813(7)	O(2b) – O(3b)	2.835(7)
O(2a) – O(5a)	2.666(8)	O(2b) – O(5b)	2.718(8)
O(2a) – O(11a)	2.887(7)	O(2b) – O(11b)	2.910(8)
O(3a) – O(4b)	2.927(7)	O(3b) – O(4a)	2.945(7)
O(3a) – O(11a)	2.695(7)	O(3b) – O(11b)	2.698(8)
O(4b) – O(5a)	2.776(7)	O(4a) – O(5b)	2.804(8)
O(4b) – O(11a)	2.518(7)	O(4a) – O(11b)	2.528(8)
O(5a) – O(11a)	2.743(8)	O(5b) – O(11b)	2.764(8)
< A(a) >		< A(b) >	
O(4b) – O(8a) ×2	2.670(7)	O(4a) – O(8b) ×2	2.667(7)
O(4b) – O(8a) ×2	2.737(7)	O(4a) – O(8b) ×2	2.735(7)
O(4b) – O(11a) ×2	2.862(7)	O(4a) – O(11b) ×2	2.831(8)
O(4b) – O(11a) ×2	2.518(7)	O(4a) – O(11b) ×2	2.528(8)
O(8a) – O(11a) ×2	2.646(8)	O(8b) – O(11b) ×2	2.630(7)
O(8a) – O(11a) ×2	2.651(7)	O(8b) – O(11b) ×2	2.666(8)
< Si(1a) >		< Si(1b) >	
O(1a) – O(1a) ×2	2.624(10)	O(1b) – O(1b) ×2	2.568(10)
O(1a) – O(1a) ×4	2.742(9)	O(1b) – O(1b) ×4	2.736(9)
< Si(2a) >		< Si(2b) >	
O(2b) – O(3a)	2.741(7)	O(2a) – O(3b)	2.749(7)
O(2b) – O(4b)	2.553(7)	O(2a) – O(4a)	2.556(7)
O(2b) – O(7b)	2.771(7)	O(2a) – O(7a)	2.749(7)
O(3a) – O(4b)	2.731(7)	O(3b) – O(4a)	2.743(7)
O(3a) – O(7b)	2.588(7)	O(3b) – O(7a)	2.582(7)
O(4b) – O(7b)	2.729(8)	O(4a) – O(7a)	2.730(8)
< Si(3a) >		< Si(3b) >	
O(5b) – O(6b)	2.675(8)	O(5a) – O(6a)	2.673(8)
O(5b) – O(8b)	2.717(7)	O(5a) – O(8a)	2.711(8)
O(5b) – O(9)	2.631(8)	O(5a) – O(9)	2.631(8)
O(6b) – O(8b)	2.642(8)	O(6a) – O(8a)	2.648(8)
O(6b) – O(9)	2.647(8)	O(6a) – O(9)	2.606(8)
O(8b) – O(9)	2.673(7)	O(8a) – O(9)	2.659(8)

Table 7. (cont. 4)

Saueseter

< B(a) >		< B(b) >	
O(6b) – O(6b)	×4 2.778(9)	O(6a) – O(6a)	×4 2.988(9)
O(6b) – O(10b)	×4 2.926(11)	O(6a) – O(10a)	×4 3.188(13)
< AlFe(a) >		< AlFe(b) >	
O(1a) – O(2a)	2.805(9)	O(1b) – O(2b)	2.832(9)
O(1a) – O(3a)	2.804(9)	O(1b) – O(3b)	2.814(8)
O(1a) – O(4a)	2.825(9)	O(1b) – O(4b)	2.850(8)
O(1a) – O(5a)	2.782(8)	O(1b) – O(5b)	2.873(8)
O(2a) – O(3a)	2.807(9)	O(2b) – O(3b)	2.833(9)
O(2a) – O(5a)	2.685(8)	O(2b) – O(5b)	2.753(9)
O(2a) – O(11a)	2.900(8)	O(2b) – O(11b)	2.895(8)
O(3a) – O(4a)	2.931(9)	O(3b) – O(4b)	2.982(8)
O(3a) – O(11a)	2.659(8)	O(3b) – O(11b)	2.755(8)
O(4a) – O(5a)	2.766(9)	O(4b) – O(5b)	2.797(9)
O(4a) – O(11a)	2.514(8)	O(4b) – O(11b)	2.580(8)
O(5a) – O(11a)	2.727(7)	O(5b) – O(11b)	2.789(8)
< A >		< Si(1) >	
O(4a) – O(8b)	2.686(8)	O(1a) – O(1a)	2.587(12)
O(4a) – O(8a)	2.727(8)	O(1a) – O(1b)	2.719(9)
O(4a) – O(11a)	2.514(8)	O(1a) – O(1b)	2.723(9)
O(4a) – O(11b)	2.837(8)	O(1b) – O(1b)	2.584(12)
O(4b) – O(8a)	2.670(8)		
O(4b) – O(8b)	2.733(8)		
O(4b) – O(11a)	2.842(7)		
O(4b) – O(11b)	2.580(8)		
O(8a) – O(11a)	2.649(7)		
O(8a) – O(11b)	2.689(8)		
O(8b) – O(11a)	2.611(8)		
O(8b) – O(11b)	2.684(8)		
< Si(2a) >		< Si(2b) >	
O(2a) – O(3b)	2.711(9)	O(2b) – O(3a)	2.745(9)
O(2a) – O(4a)	2.554(9)	O(2b) – O(4b)	2.541(9)
O(2a) – O(7a)	2.754(8)	O(2b) – O(7b)	2.734(8)
O(3b) – O(4a)	2.735(8)	O(3a) – O(4b)	2.733(8)
O(3b) – O(7a)	2.595(9)	O(3a) – O(7b)	2.597(9)
O(4a) – O(7a)	2.722(9)	O(4b) – O(7b)	2.754(9)
< Si(3a) >		< Si(3b) >	
O(5b) – O(6b)	2.687(9)	O(5a) – O(6a)	2.666(9)
O(5b) – O(8b)	2.715(9)	O(5a) – O(8a)	2.704(8)
O(5b) – O(9)	2.623(9)	O(5a) – O(9)	2.653(9)
O(6b) – O(8b)	2.636(9)	O(6a) – O(8a)	2.639(9)
O(6b) – O(9)	2.664(9)	O(6a) – O(9)	2.592(9)
O(8b) – O(9)	2.691(9)	O(8a) – O(9)	2.658(9)

Table 7. (cont. 5)

Wilui River

< B >		< A >		< Si(3) >	
O(6) – O(6) ×4	2.925(3)	O(4) – O(8) ×2	2.685(3)	O(5) – O(6)	2.687(3)
O(6) – O(10) ×4	2.993(8)	O(4) – O(8) ×2	2.764(3)	O(5) – O(8)	2.733(3)
O(6) – O(12)	3.153(18)	O(4) – O(11) ×2	2.874(3)	O(5) – O(9)	2.646(3)
		O(4) – O(11) ×2	2.614(3)	O(6) – O(8)	2.607(3)
< AlFe >		O(8) – O(11) ×2	2.743(3)	O(6) – O(9)	2.636(3)
		O(8) – O(11) ×2	2.707(3)	O(8) – O(9)	2.672(3)
O(1) – O(2)	2.814(3)				
O(1) – O(3)	2.919(3)	< Si(1) >		< Bo(1) >	
O(1) – O(4)	2.850(3)				
O(1) – O(5)	2.886(3)	O(1) – O(1) ×2	2.604(4)	O(7) – O(7)	2.874(7)
O(2) – O(3)	2.895(3)	O(1) – O(1) ×4	2.701(4)	O(7) – O(11)	2.659(4)
O(2) – O(5)	2.769(3)			O(7) – O(11)	2.595(5)
O(2) – O(11)	2.958(3)	< Si(2) >			
O(3) – O(4)	3.027(3)			< Bo(2) >	
O(3) – O(11)	2.833(3)	O(2) – O(3)	2.722(3)		
O(4) – O(5)	2.778(3)	O(2) – O(4)	2.553(3)	O(10) – O(12)	2.260(20)
O(4) – O(11)	2.614(3)	O(2) – O(7)	2.710(4)	O(12) – O(12)	2.347(35)
O(5) – O(11)	2.808(3)	O(3) – O(4)	2.762(3)		
		O(3) – O(7)	2.640(4)		
		O(4) – O(7)	2.703(4)		

Chichibu

< B >		< A >		< Si(3) >	
O(6) – O(6) ×4	2.874(4)	O(4) – O(8) ×2	2.668(3)	O(5) – O(6)	2.674(3)
O(6) – O(10) ×4	3.038(5)	O(4) – O(8) ×2	2.742(3)	O(5) – O(8)	2.710(3)
		O(4) – O(11) ×2	2.848(3)	O(5) – O(9)	2.641(3)
< AlFe >		O(4) – O(11) ×2	2.525(3)	O(6) – O(8)	2.629(3)
		O(8) – O(11) ×2	2.643(3)	O(6) – O(9)	2.620(3)
O(1) – O(2)	2.807(3)	O(8) – O(11) ×2	2.659(3)	O(8) – O(9)	2.665(3)
O(1) – O(3)	2.806(3)				
O(1) – O(4)	2.830(3)	< Si(1) >		< Bo(1) >	
O(1) – O(5)	2.819(3)				
O(2) – O(3)	2.824(3)	O(1) – O(1) ×2	2.582(4)	O(7) – O(7)	3.056(5)
O(2) – O(5)	2.708(3)	O(1) – O(1) ×4	2.712(4)	O(7) – O(11)	2.928(3)
O(2) – O(11)	2.895(3)			O(7) – O(11)	2.780(3)
O(3) – O(4)	2.951(3)	< Si(2) >			
O(3) – O(11)	2.695(3)				
O(4) – O(5)	2.773(3)	O(2) – O(3)	2.735(3)		
O(4) – O(11)	2.525(3)	O(2) – O(4)	2.547(3)		
O(5) – O(11)	2.751(3)	O(2) – O(7)	2.737(3)		
		O(3) – O(4)	2.730(3)		
		O(3) – O(7)	2.597(3)		
		O(4) – O(7)	2.723(3)		

Table 8. Interatomic distances determined by EXAFS (Å)

	Sauland		Nakatatsu	
1 shell (5-fold)	Cu-O	1.98(1)	Mn-O	2.10(1)

X-ray diffraction

	Sauland	Nakatatsu
B-O(6)	2.057(3)	2.077(2)*
B-O(10)	2.194(6)	2.33(7)*

* (Yoshiasa and Matsumoto, 1986)

Effective ionic radius (Shannon, 1976)

$0.75(^{V}Mn^{2+}) + 1.38(^{IV}O^{2-}) = 2.13$

$0.65(^{V}Cu^{2+}) + 1.38(^{IV}O^{2-}) = 2.03$

Table 9. The selected bond-valence sums

Obira			Sauland		Saueseter				Wilui River	
< O(7) >			< O(7) >		< O(7a) >		< O(7b) >		< O(7) >	
Ca(3)	0.21		Ca(3)	0.20	Ca(3b)	0.23	Ca(3a)	0.17	Ca(3)	0.12
Ca(3)	0.23		Ca(3)	0.23	Ca(3a)	0.22	Ca(3b)	0.24	Ca(3)	0.19
Ca(3)	0.31		Ca(3)	0.32	Ca(3a)	0.29	Ca(3b)	0.31	Ca(3)	0.26
Si(2)	1.03		Si(2)	1.05	Si(2a)	0.99	Si(2b)	1.02	Si(2)	0.95
									Bo(1)	0.31
Total	1.79		Total	1.81	Total	1.73		1.75	Total	1.82
< O(10)A >	(O)	(F)	< O(10) >		< O(10a) >		< O(10b) >		< O(10) >	
Ca(3) ×4	0.18	0.14	Ca(3) ×4	0.21	Ca(3a) ×4	0.22	Ca(3b) ×4	0.19	Ca(3) ×4	0.18
C	0.16	0.12	B	0.25			B(a)	0.74	B	0.32
B	0.73	0.56							Bo(2)	0.95
Total	0.89	0.69	Total	0.84	Total	0.88		1.50	Total	1.68
	1.46	1.12		1.08						2.00
< O(11) >			< O(11) >		< O(11a) >		< O(11b) >		< O(11) >	
Ca(3)	0.27		Ca(3)	0.25	Ca(3b)	0.28	Ca(3a)	0.18	Ca(3)	0.21
AlFe	0.47		AlFe	0.51	AlFe(a)	0.47	AlFe(b)	0.44	AlFe	0.39
A	0.55		A	0.55	A	0.56	A	0.53	A	0.46
									Bo(1)	0.72
Total	1.29		Total	1.31	Total	1.31		1.15	Total	1.78
									< O(12) >	
									Ca(3)	0.35
									Ca(3)	0.41
									Ca(3)	0.16
									Bo(2)	1.31
									Total	2.23

参　考　論　文

1. **Crystal chemistry of vesuvianite: Site preferences of square-pyramidal coordinated sites.**

   American Mineralogist, Vol. 77, 945-953. (1992)

2. **Structural investigation of high- and low-symmetry vesuvianite.**

   Accepted for publication in "*Mineralogical Journal*, Vol. 17, No. 2 (1994)"